The climatic implications of lake level expansion in the Mackenzie Bison Sanctuary, Fort Providence, Northwest Territories

by

Peter André deMontigny

A thesis submitted to the Faculty of Graduate and Post Doctoral Affairs in partial fulfillment of the requirements for the degree of

Master of Science

in

Geography

Carleton University
Ottawa, Ontario

ABSTRACT

Remotely sensed data indicates that lake expansion north of Fort Providence, Northwest Territories, is statistically significant, potentially contributing to wood bison (*Bison bison athabascae*) migrating beyond the Mackenzie Bison Sanctuary. The Mackenzie herd is one of the few remaining populations not infected by bovine brucellosis (*Brucella abortus*) and tuberculosis (*Mycobacterium bovis*). Interaction with nearby infected herds could introduce widespread infection.

Lake expansion is often driven by changes in climate, however climate records for this region are lacking. Dendrochronology can be used to examine longer-term climate. Climate was reconstructed using nine white spruce (*Picea glauca*) chronologies. Correlations were highest between the chronologies and the Palmer Drought Severity Index, which show climate variability has increased within the study area since 1915. Remote sensing results correlate with positive phases of the July-October Pacific North American pattern, however the freezing date of the active layer may provide a better understanding of water level fluctuations.

ACKNOWLEDGEMENTS

I would like to thank my supervisor Michael Pisaric for not only the feedback, guidance, and help in the field, but for taking me on as an undergraduate student. The experiences I gained from my time as a research assistant were invaluable, providing me opportunities to view such amazing parts of our country that I would likely never get to appreciate in person otherwise. Additionally, thanks to my second supervisor, Murray Richardson, for accepting the unexpected role without hesitation and providing great feedback.

To Terry Armstrong and Environment and Natural Resources, Government of the Northwest Territories, for allowing me to be a part of this project and providing financial and field assistance. Outstanding field assistance was also provided by Phil Muise, Sam Elleze, and Steve Kokelj.

I would also like to thank the DGES academic and technical staff at Carleton University, especially Natalie Pressburger and Quang Ngo, for making sure everything runs smoothly in the department.

A special thanks to the community of Fort Providence and the North Slave and Dehcho regions for the hospitality and approval of this research.

To Trevor Porter who helped introduce me to the field of dendroclimatology. Thanks for the helpful conversations, always going the extra mile to make sure I understood concepts and for including me in so many of your projects. Again, the experience I gained was incredible and much appreciated.

Thanks to my colleagues at Parks Canada, especially Phil Wilson and John McKenzie who allowed me to gain great workplace experience while also working around my schedule.

And last, but certainly not least, I owe my deepest gratitude to my family and my fiancée Linsey Hern, for supporting me throughout all my studies. I wouldn't have been able to do it without your help and understanding.

Financial and logistical support provided by: the Cumulative Impacts Monitoring Program; Natural Sciences and Engineering Research Council of Canada; Northern Scientific Training Program; Environment and Natural Resources, Government of the Northwest Territories; Aurora Research Institute; Aboriginal Affairs and Northern Development Canada; and Carleton University.

TABLE OF CONTENTS

LIST OF TABLES

LIST OF FIGURES

LIST OF EQUATIONS

CHAPTER 1

1.1 Introduction

It has been well documented that anthropogenic activities have prompted a shift in climate conditions for a wide array of global environmental patterns (Hegerl et al., 2007). These effects are exaggerated in northern Canada (areas north of 60°N), where a loss of snow cover has resulted in a positive feedback system (Christensen et al., 2007). Between 1948 and 2005, mean annual air temperatures in northern Canada have increased approximately 2.0°C, while Canada, as a whole, has warmed by an average of 1.2°C (Prowse et al., 2009). Such findings highlight the sensitivity of northern environments, and the importance of reacting to an accelerated pace of change.

Lake area has dramatically increased in response to rising water levels in the Mackenzie Bison Sanctuary (MBS), north of Fort Providence, NT. Bomblies et al. (2001) observed that increases in lake level are driven by changes in the local climate. As a relatively flat region, small deviations in hydrology have the potential to cause a disproportionately large amount of change in the physical size of lakes. These changes have significant ecological impacts on the plants and animals found in this area, killing shoreline vegetation and grassland habitat which in turn influence the distribution of animals such as moose (*Alces alces*) and wood bison (*Bison bison athabascae*); (Environment and Natural Resources Government of the Northwest Territories [ENR GNWT], 2010). Bison are important for maintaining the structure, composition, and stability of plant and animal communities (Gates et al., 2010). The Mackenzie bison herd, originating from a population base of 18 individuals, has thrived in the MBS. Still,

there are significant challenges facing the survival of the Mackenzie herd, including anthrax breakouts, mass drownings as a result of falling through ice covered lakes, loss of habitat due to lake expansion, and the spread of tuberculosis and brucellosis. In order to provide effective herd management, decision makers must understand if lake expansion is part of a longer-term cycle or perhaps indicative of a new set of normal or baseline conditions.

The objectives of this thesis are twofold: (1) to examine long-term climate variability in the MBS to determine if shifting climatic conditions may be responsible for recent lake expansion, and (2) to examine the spatial extent of lake expansion in the MBS and determine if current lake surface area within the sanctuary is greater or less than previous decades. The objectives will be explored through the development of climatically sensitive tree ring chronologies from white spruce (*Picea glauca*) and jack pine (*Pinus banksiana*) sites near Fort Providence, NT, and the analysis of remotely sensed data. The dendrochronological analysis will be used to reconstruct past climate for the Fort Providence region, helping to better understand the long-term climate patterns for this region and allow recent trends to be examined over a much longer time period than afforded by the short instrumental data available. This research will provide important details about possible climatic drivers of recent lake level fluctuations in the region, information which is critical to understanding changes in lake level and their implications for bison habitat.

1.2 Thesis structure

This thesis will be organized as follows: Chapter 1 has provided a brief introduction to the research topic. Chapter 2 provides a literature review in relation to the Mackenzie bison population and applications of remote sensing and dendroclimatology in related studies. Chapter 3 offers an overview of the study area, as well as a description of the methods employed for this study. Chapter 4 presents the results of the analyses, while the discussion of results in regards to their respective foci are presented in Chapter 5. Chapter 6 summarizes the major conclusions of the study and suggests avenues for future research in this region.

CHAPTER 2
LITERATURE REVIEW

2.1 The Mackenzie Bison Herd

Wood bison, listed as a threatened species under the Species at Risk Act (SARA) and the Committee on the Status of Endangered Wildlife in Canada (COSEWIC), are an important natural resource. Thought to have originally existed in numbers as great as 150,000 in 1800, wood bison succumbed to the pressure of hunting, predation, and disease, dropping to an estimated 250 individuals by 1891 (ENR GNWT, 2010). Additional stressors, such as interbreeding between transported plains bison (*Bison bison bison*) and wood bison threatened to eliminate the wood bison species altogether (Parks Canada, 2012). However, in 1959 a herd of 18 isolated wood bison were found within a remote area of Wood Buffalo National Park (WBNP). These bison were subsequently transferred to the MBS where their numbers have grown (ENR GNWT, 2010). Until recently, the MBS herd was the largest free-ranging bison population in Canada that remained free of tuberculosis and bovine brucellosis. An early 2008 population survey estimated roughly 1600 individuals existed (ENR GNWT, 2010). Unfortunately, a particularly devastating anthrax outbreak occurred that summer, killing at least 440 bison over an 8-week period (Government of the Northwest Territories [GNWT], 2012). Recovery efforts for this threatened species have been restricted due to the proximity of diseased herds and the continued threat of interbreeding by plains bison, cattle, and domesticated bison (ENR GNWT, 2010). The following examines the ecological and economic significance of wood bison, specifically of those found in the MBS population.

2.1.1 Disease Control

Tuberculosis and brucellosis are cattle diseases that can infect mammals of all forms, including humans. A number of bison populations surrounding the MBS are infected with these diseases (Figure 2.1), the prevalence of which has not declined in the last 40 years (GNWT, 2012). Interaction between these herds could introduce widespread infection in the Mackenzie Bison herd, adding a further population stressor. Preventing the spread of these diseases is considered to be one of the highest priorities of the bison conservation effort (Strong and Gates, 2009). The infection threat not only restricts the MBS range, but also represents an avenue for widespread contamination within the MBS and beyond (Tessaro et al., 1992). These diseases lead to numerous health-related complications for bison, including death, but the most widespread effects "may be related to immune function, energy balance or reduced reproduction, which can lower bison population growth rates" (ENR GNWT, 2010, p. 7). Modelling suggests that a combination of brucellosis, tuberculosis, and predation are the likely drivers of population change in WBNP from 1970 to 1999, where populations have dwindled from over 10,000 individuals to 2,200 (Joly and Messier, 2004).

2.1.2 Economic Impacts

The risk of contact and spread of disease by displaced MBS herds also has the potential to cause economic losses through indirect means. For example, the Canadian beef industry, which exports an estimated 2.2 billion dollars of product annually (CBC News, 2006), could suffer massive financial losses with the introduction of tuberculosis or brucellosis from bison contact. If these diseases are detected in livestock, the

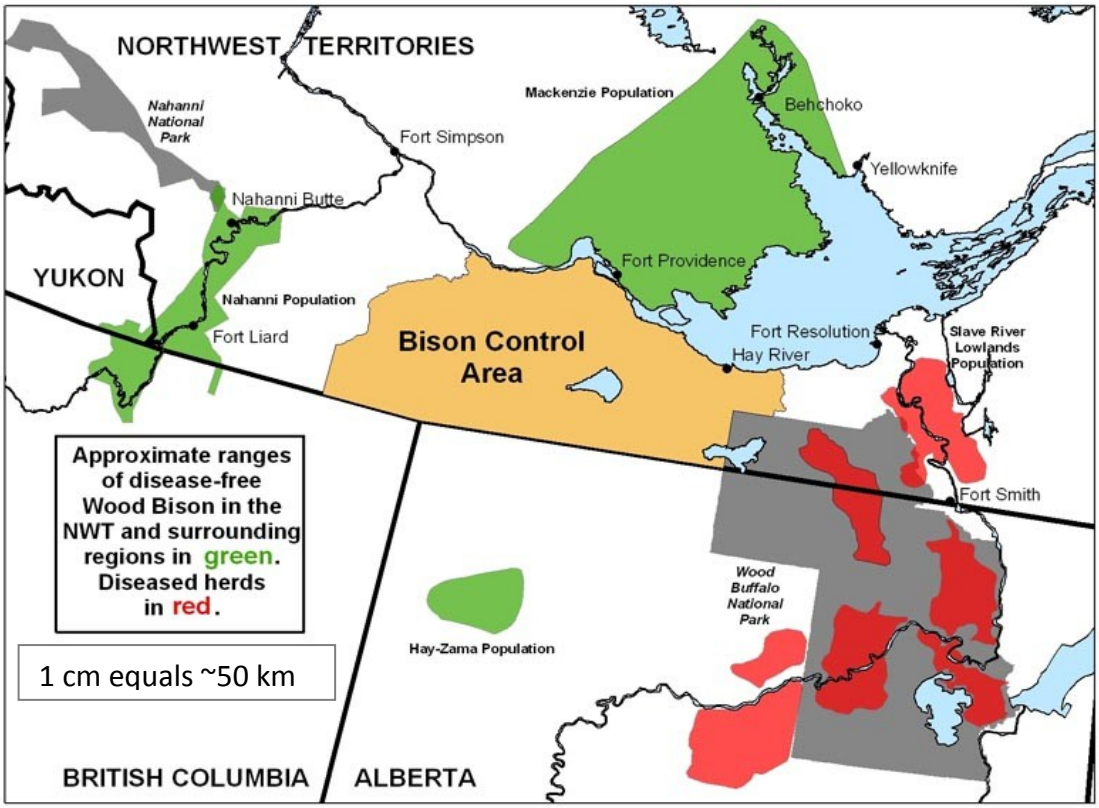

Figure 2.1. Location of the Mackenzie bison herd and nearby herds in the Northwest Territories, Yukon Territory, and Alberta. Herds depicted by green shading represent ranges of disease-free wood bison while those in red are wood bison herds with confirmed bovine brucellosis and tuberculosis. The yellow shaded region represents the Bison Control area where bison movement is not permitted so disease-free and diseased animals do not come in contact with one another. Map from ENR GNWT, 2011.

Canadian Food Inspection Agency must be notified immediately, and the infected cattle destroyed. News of infection in even a single cow in the Canadian cattle industry could result in the boycott of Canadian livestock and associated products, as was experienced in 2003 with the discovery of bovine spongiform encephalopathy (BSE, otherwise known as mad cow disease; ENR GNWT, 2010). Between 2003 and 2005, the government was forced to provide close to 2 billion dollars in relief funding for cattle farmers affected by BSE (CBC News, 2006).

Additionally, a strong bison population allows for potential economic benefits such as tourism and outfitting in local communities (ENR GNWT, 2010). Risk of bison infection and/or migration could reduce these economic opportunities.

2.1.3 Ecological Diversity

Subspecies diversity provides genetic, behavioural, and morphological variation, which in turn enhances biodiversity and evolutionary potential for bison as a whole (Gates et al., 2010). It is therefore important to manage bison herds in a way that minimizes contact between wood bison and other potential genetic threats, such as interbreeding with plains bison or cattle.

There are several distinguishing features between wood bison and plains bison. Although wood bison are typically larger, they do not appear as such due to a lack of chaps and a small neck mane (Figure 2.2). Furthermore, the highest point of the hump on a wood bison is well forward of the front legs, whereas the hump of a plains bison is directly over the front legs (Parks Canada, 2009).

Figure 2.2. A wood bison bull (top) and plains bison bull (bottom). Top image by P. deMontigny, bottom image from Gates et al. (2010).

2.2 Remotely sensed data

It is important to consider how the landscape has changed in order to understand potential pressures on the Mackenzie bison herd. The Mackenzie herd is relatively dense, at an overall density of 0.2 bison/km^2 compared to 0.05 bison/km^2 in WBNP (Gates and Larter, 1990). It has been observed that the primary motivation for MBS herd movement is in response to bison density increases, with a calculated critical value of 0.5-0.8 bison/km^2 (Gates and Larter, 1990). As more land is inundated by expanding lakes, the loss of habitat increases density and makes the Mackenzie herd a more likely candidate to travel to/through the Bison Control Area, a patrolled buffer zone separating the Mackenzie herd from diseased herds in WBNP. There is clear evidence of expanding lakes, such as a submerged boat launch road leading to Caen Lake (Figure 2.3), and, although remote sensing results exist for a limited number of individual lakes (van der Wielen, 2012) as well as all of Canada at coarse scale (250 m x 250 m pixels; Carroll et al., 2011), to what extent the phenomena occurs regionally, or even if these changes are statistically significant remains largely unknown. Remote sensing technology allows for measurement of historic lake levels, providing the opportunity to put recent landscape changes into context.

2.2.1 Imagery acquisition

The availability of remotely sensed data continues to grow as sensor design and rocket technology improves and affordability increases (Gao, 2009). There are multiple satellite platforms to choose from, each providing a combination of unique and

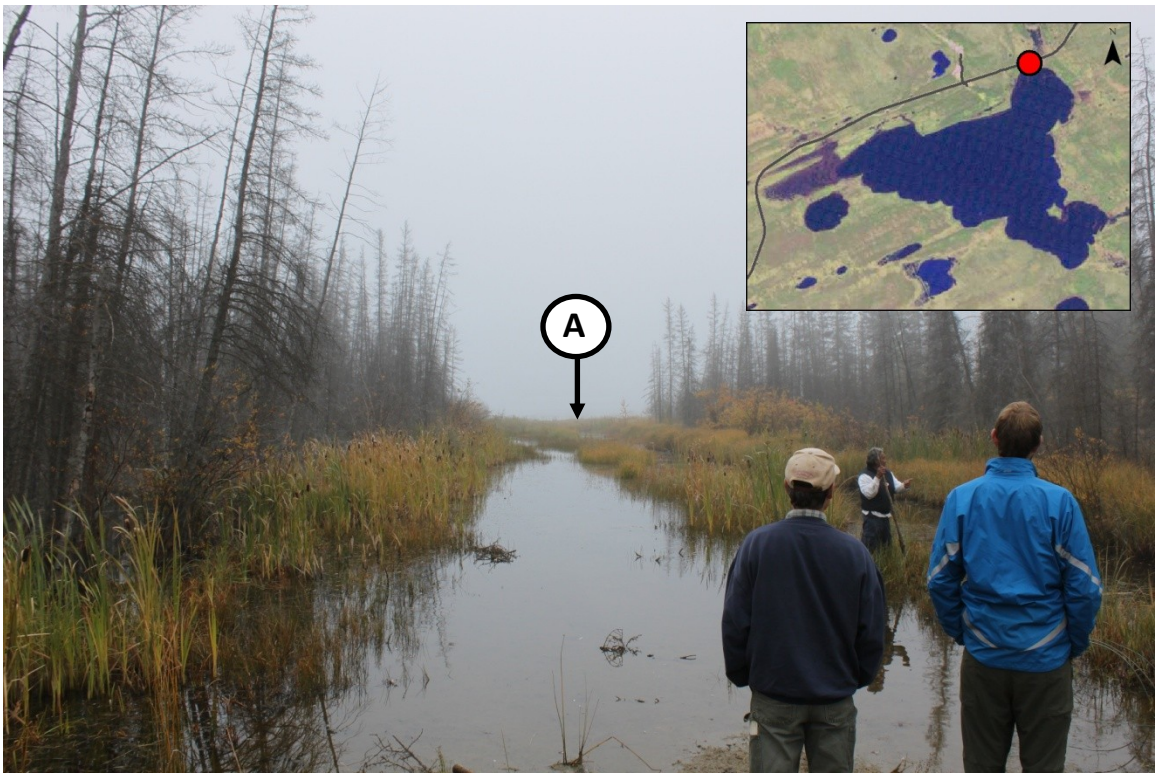

Figure 2.3. Submerged boat launch at Caen Lake (see Figure 3.6 for the location of Caen Lake). Evidence of the boat launch extends a few metres beyond the edge of the vegetation (Point A). Photo by P. deMontigny.

redundant features. The perceived advantages and disadvantages vary from one user to the next and are dependent on the project at hand. It is therefore important to first establish which attributes are essential to the project in considering which data to use (Gao, 2009). Spatial coverage and temporal resolution are common priority factors in the data selection process. Additionally, cost, data storage size, and processing times are also typically considered (Gao, 2009). LANDSAT 5 Thematic Mapper (TM) was chosen as the best option for this project, as it addressed the most essential factors. This imagery dates back to 1984, cycles on a 16-day period, and is free to access via the United States Geological Survey (USGS) Earth Explorer website (http://earthexplorer.usgs.gov/). Additionally, the 30m pixel size, although of coarse resolution, translates into a manageable database, both in terms of storage memory and processing efficiency.

In order to make accurate conclusions concerning multi-year environmental changes, it is important to eliminate seasonal variation (Anderson and Milton, 2006). A consistent and purposeful time period limits the impact of seasonal trends and allows for a measurement of true change. LANDSAT 5 TM is a passive sensor, measuring the natural radiation reflected by land surfaces. The presence of snow greatly impacts passive data collection, not only in high snow conditions where land features are shielded, but also in low snow conditions where the spectral signature of the image is affected (Jin et al., 2002). As such, images with snow are to be avoided. Furthermore, in northern Canada, evaporation has a strong effect on summer lake levels (Marsh and Bigras, 1988), and higher air temperatures are generally associated with an increase in

evaporation (Arnell et al., 2001). To avoid the greatest potential influence of summer temperatures, albeit using this over-simplified understanding of lake modelling, September, with an average maximum temperature of 13.2°C, was subjectively chosen to minimize influences of evaporation and snowfall.

2.2.2 Imagery correction

LANDSAT 5 TM data needs to be geometrically rectified to correct for distortions which are inherent to all satellite sensors. The rotation and curvature of the Earth results in a skewed image, as does off-nadir distortion, scanning mirror inconsistency, and shifted sensor position/orientation (Gao, 2009). Ground Control Points (GCPs) are used to match features on the imagery with the corresponding real world coordinates of those features. The USGS applies pre-processing to all downloaded imagery; files are corrected to Standard Terrain Correction Level 1T, using the Level 1 Product Generation System (LPGS). A range of 1,847 to 2,771 automated GCPs are integrated into the imagery for this project, with a root-mean-square error (RMSE) range of 0.103 to 0.199 pixels. RMSE is an accuracy indicator of the GCPs used, and while no true minimum threshold exists, a RMSE limit of one pixel is typically enforced (Gao, 2009). It was decided that image orthorectifcation was not needed due to the nature of the landscape (relatively flat) and the simplified land cover analysis (two classes: water and land). This is an acceptable standard for coarse or medium resolution satellite imagery analysis when a shift in topographic relief is considered minimal (Gao, 2009).

In addition to the positional corrections applied by the USGS, there is still a significant amount of correction that the user must undertake (Gupta, 2003). For

example, although LANDSAT 5 TM imagery is geometrically corrected using GCPs, an accuracy error of up to 250 metres (equivalent to the length of approximately 8 pixels) may exist for low-relief areas and must be dealt with accordingly (Gao, 2009). Additionally, LANDSAT 5 TM captures information simultaneously through the use of sixteen detectors, introducing the possibility that each detector may record slight differences in radiometric signal. This can lead to striping in the image, and is described by Chander et al. (2004, p. 2749) as the "most significant radiometric artifact observed in all of the LANDSAT imaging sensors".

Clouds and haze must also be accounted for, as the presence of these features can impact the accuracy of land cover classification dramatically (Kaufman, 1987). Furthermore, images must be radiometrically calibrated. LANDSAT 5 TM stores data as a digital number, a relative value based on the theoretical range of pixel values, ranging between 0 (no radiation) and 255 (maximum radiation). Digital numbers are converted to at-sensor radiance measurements by the user with the aid of gain and bias rescaling values supplied in lookup tables (such as is provided in Chander et al., 2009). This process accounts for calibration error, and, although LANDSAT 5 TM was equipped with an internal calibrator to correct for radiometric changes, it was later discovered that calibration values had errors of up to 15% (Chander et al., 2009). Gain and bias rescaling values greatly improve calibration results when used with the digital number to radiance equation. In addition to calibrating data, digital number values are also converted to physical absolute units of spectral radiance ($W \cdot m^{-2} \cdot sr^{-1} \cdot \mu m^{-1}$). The at-sensor radiance is then used to compute a top of atmosphere reflectance value, which helps calibrate for

differences in sun angle, ground surface irradiance, and Earth-Sun distance (Chander et al., 2009).

2.2.3 Land classification

While LANDSAT 5 TM provides the best opportunity to examine the study area over time, the 30m x 30m pixel resolution limits the classification accuracy of a traditional pixel based analysis. Traditional pixel classification schemes, such as Maximum Likelihood or Minimum Distance Classifiers, label pixels as a distinct class, allowing for only one classification type per pixel. These results, often referred to as crisp pixels, ignore the reality that real world land cover types are rarely pure. This is especially relevant at the 30m x 30m scale of LANDSAT 5 TM, where the assumption of pure pixels is likely inappropriate for most situations (Zhang and Foody, 1998). The implementation of more advanced remote sensing techniques is therefore required in order to reliably determine lake area change. Fuzzy classification is advantageous in this scenario as it provides "more information and potentially a more accurate result, especially for coarse spatial resolution." (Lu and Weng, 2007). Fuzzy logic was first introduced by Zadeh (1965) to deal with situations of partial truth. Fuzzy classification allows for a single pixel to be labelled to multiple classes, producing a separate membership grade for each class (for example, a pixel can have a membership of 0.2 for water, 0.4 for forest, and 0.4 for bedrock).

2.2.4 Accuracy assessment

No classification process derived from remote sensing imagery, including fuzzy classification, is error free, as there are a wide variety of potential error sources (Okeke and Karnieli, 2006). Therefore, it is important to report the level of accuracy for image classification results, quantifying the quality of the classification. It should be noted that accuracy refers to the agreement between reference data samples and classification results, and is not necessarily a measure of ground truth conditions (Foody, 2002). Although fuzzy logic is often applied to land classification studies, little attention has been given to accuracy assessment. This has led to a significant number of studies which have incorrectly applied traditional methods to report accuracy values (Gao, 2009). Traditional measures of accuracy are designed to be used specifically with crisp data and are not appropriate for mixed pixels (Zhang and Foody, 1998). Conversely, in order to apply fuzzy membership algorithms, reference data must also be fuzzy. Unfortunately, fuzzy reference data are not always feasible or possible, especially for studies examining historical imagery (Okeke and Karnieli, 2006). Foody (1999) and Okeke and Karnieli (2006) note that when fuzzy ground truth data are unavailable, it is appropriate to examine only those pixels which are pure (crisp) or have a strong association to one land cover type. These pixels are selected as potential evaluation pixels and are transformed to crisp values through defuzzification. The classification data, also transformed to crisp values in order to support interpretation and visualisation (Gao, 2009), allows for an error matrix to be compiled with traditional assumptions. Although there are

disadvantages associated with this method, particularly the availability of pure pixels, it ensures data conform to assumptions necessary for meaningful analysis.

There are four commonly reported components of accuracy assessment: producer's accuracy, user's accuracy, overall accuracy, and the Kappa statistic. Producer's accuracy (1 - error of omission) is the probability that a reference pixel has been correctly classified, whereas user's accuracy (1 - error of commission) is the probability that a classified pixel represents the correct class (Liu et al., 2007). Overall accuracy is computed by dividing the number of correct pixels by the total number of pixels. The Kappa value (K) is a measure of classification accuracy after removing chance agreement (Liu et al., 2007). Kappa values range from 1.0 (100% more effective than random assignment) to 0.0 (no improvement over random assignment).

The Mann-Kendall test statistic (Equation 2.1; Mann, 1945; Kendall, 1975) is often applied to environmental studies to assess trend (Zhang et al, 2011) and is recommended for general use by the World Meteorological Organization. Schlagel and Newton (1996) highlight two main advantages of the Mann-Kendall test; first, it is non-parametric, so data do not need to be normally distributed, and second, results are minimally impacted if gaps or outliers exist in the data series. Kendall's tau (τ) is a measure of correlation comparing the ranking of a data point and its relation to an increase in time (Hamed, 2008). A higher Kendall's tau value indicates a greater correlation between time and the response variable.

$$S = \Sigma_{i=1}^{n-1}\Sigma_{j=i+1}^{n}(x_i - x_j) \qquad \textit{(Eq. 2.1)}$$

where x_i and x_j are two subsets of data where i = 1, 2, …, n and j = i+1, i+2, …, n. Each data value is then compared with the remaining data values. If a data value from a later time period is higher (lower) than a data value from an earlier time period, *S* increases (decreases) by 1. The net result determines *S* (Karmeshu, 2012).

In cases where n ≥ 10, Mann-Kendall is assumed to be normally distributed, allowing variance to be calculated from measured values as opposed to theoretical distributions (Drapela and Drapelova, 2011). A z-score and p-value are then calculated. The Mann-Kendall test only indicates if a trend exists, not the magnitude of change. Unfortunately, while the Sen's slope statistic does provide a physical measure of change per unit time, data need to be equally spaced in time (Sen, 1968). As a result, only the relative trend will be examined for this study.

2.3 Records of climate variability

Although remote sensing analysis provides insight into the recent history of lake levels, the root causes for the observed changes are still difficult to ascertain from visual sources alone. Climate data are often used to determine the influential variables of environmental phenomena, while also providing a longer record of observation than afforded by remote sensing. A longer record is more likely to capture a greater range of variability of conditions, allowing for more informed conclusions to be made. Lake levels in North America typically correlate well with large atmospheric patterns such as the

Arctic Oscillation (AO), Pacific Decadal Oscillation (PDO), and the Pacific/North American (PNA) pattern (Gibson et al., 2006; Leira and Cantonati, 2008; Wiles et al., 2009).

The AO is a normalized index which measures atmospheric pressures associated with winds north of 20°N latitude. In positive phases of the AO, strong winds confine cold polar air to arctic regions (roughly 55°N), whereas negative phases allow cold air to flow south, resulting in large storms in mid-latitude regions (National Weather Service, 2005).

The PDO is an index which examines temperature and pressure anomalies of the North Pacific Ocean, similar to El Nino/Southern Oscillation (ENSO), but with two defining features: the PDO events can last 20-30 years (as opposed to 6-18 months for ENSO), and the PDO primarily affects North America, followed by secondary effects in the tropics (opposite of ENSO). Positive phases result in warmer and drier conditions in northwestern North America, while negative phases are linked to cooler and wetter conditions (Mantua and Hare, 2002).

PNA values, also reported as a normalized index, use 1981-2010 data as a baseline reference (National Weather Service, 2012). In positive phases of PNA, an atmospheric ridge develops across western North America, allowing warm, moist maritime air to move further north while deflecting “moisture-bearing cyclonic systems from the Pacific” (Trouet and Taylor, 2009). This results in above average temperatures and below average precipitation in northwest North America (Sheridan, 2003). At the same time, a trough develops in eastern North America, forcing polar air southward, creating wetter and cooler conditions. The opposite occurs in negative phases of PNA

(Climate Prediction Center Internet Team, 2012; Figure 2.4). These modes of atmospheric variability impact air mass movement, driving air temperature, storm patterns, precipitation, and evaporation regimes, all of which are important factors in the hemispheric climate and regulation of water bodies (Labrecque et al., 2009). Unfortunately, records of these large scale climate systems are temporally short, limiting analysis opportunities.

2.4 Dendroclimatology

In place of instrumental or remotely sensed records, proxy data sources can be used to reconstruct past climatic conditions. Dendrochronology is a scientific discipline which uses tree rings to obtain calendar dates of specific phenomenon through the cross-dating of common growth patterns in tree ring series, including the pattern of wide and narrow growth rings. A key sub-field of this discipline is dendroclimatology. Dendroclimatology examines the link between tree ring growth and the climate in a specific area.

Tree ring data, through the use of numerous samples collected from multiple sites, can be used to identify regional scale variability (Gunnarson, 2001). These proxy reconstructions can accurately represent hydrologic phenomena, allowing investigations of past environmental variables that are not generally available through historical climate data (Landwehr, 1986; Liu et al., 2010). Among the many factors that can influence the growth of trees, precipitation and temperature are two of the most important aspects. These factors can also have a great influence on the water table and

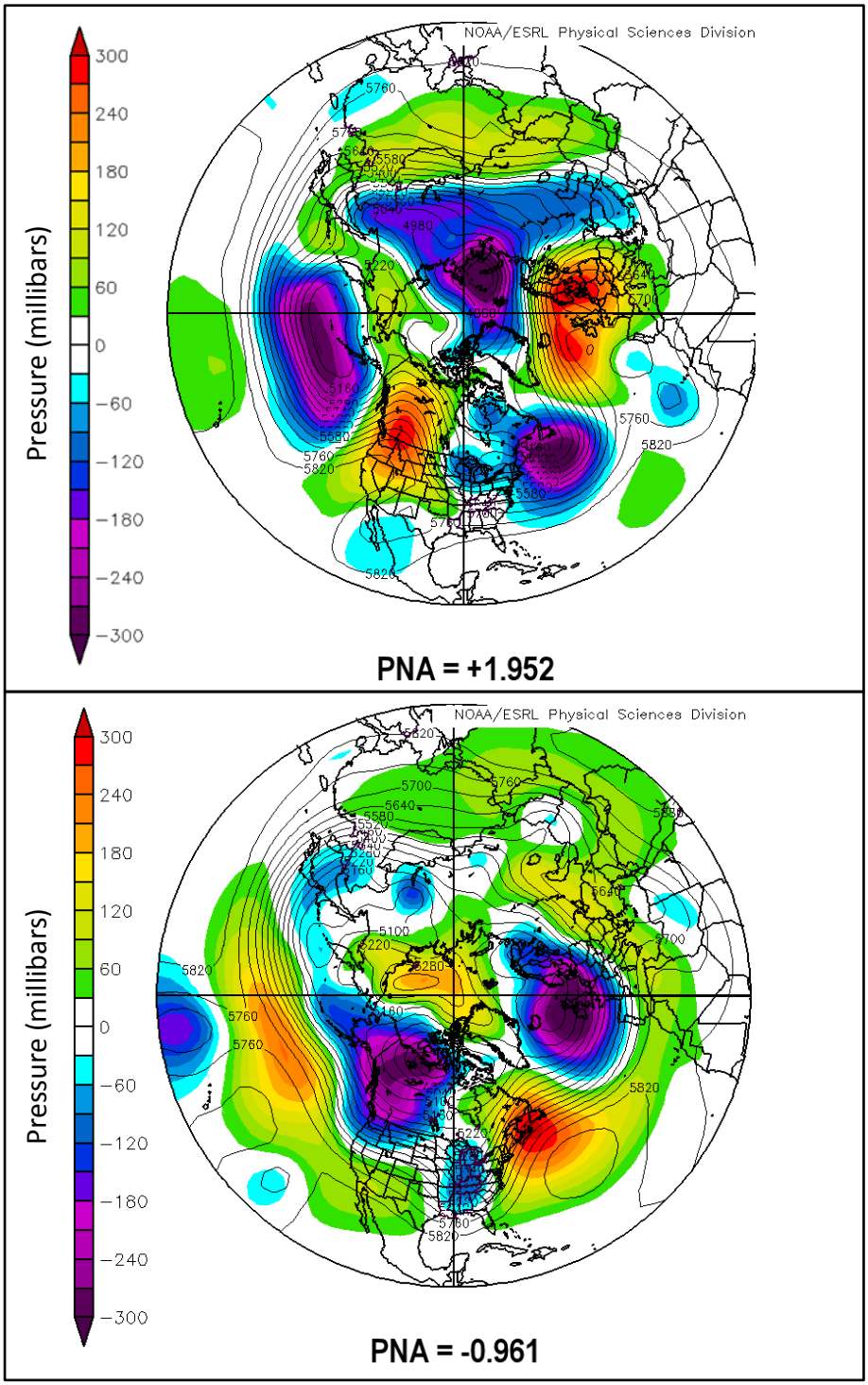

Figure 2.4. Postive (top) and negative (bottom) phases of the Pacific North American (PNA) pattern. Colours indicate pressure, with PNA index values specified at the bottom of each image. PNA index values are relative to 1981-2010 normals. Image from National Weather Service Forecast Office (2009).

other hydrologic properties which can impact lake levels. On the landscape, precipitation directly influences the water balance and provides runoff, while temperature indirectly alters hydrology by influencing runoff and evaporation properties (Quinn, 2006). As such, significant changes in precipitation and temperature regulate both tree growth and lake levels, providing an indirect record of past hydrological conditions through tree-ring analysis (Begin, 2001).

2.5 Principles of Dendroclimatology

In his seminal book "Tree Rings and Climate", Harold C. Fritts (1976) outlines several key principles utilized in dendroclimatological research. These principles are widely accepted and employed in the field of dendrochronology (Martinelli, 2004; Speer, 2010). The following describes the principles outlined by Fritts (1976), which are used as the theoretical framework for this project.

2.5.1 Uniformitarian Principle

The first of these principles is the Uniformitarian Principle. This principle indicates that the processes which influenced the past are the same processes which influence the present. As noted by Fritts (1976), this does not necessarily mean that past climates were the same as present day, but that the same type of relations are assumed to be constant (i.e., the types of weather patterns which exist today are assumed to have been in existence in the past).

2.5.2 Principle of Limiting Factors

The Principle of Limiting Factors is the foundation of dendrochronology; it is only possible to crossdate tree rings if a limiting environmental factor exists. The factor must be present for a long period of time and influence a large enough geographic area so as to influence multiple trees in a similar manner (Fritts, 1976). A biological process, such as the growth of tree-rings, cannot proceed faster than the constraints placed upon it by the most limiting factor (Fritts, 1976). A factor may at first be limiting, but become less important as conditions change. If conditions change significantly, and the limiting factor no longer becomes important, the biological process will increase until a new limiting factor is placed upon it. For example, Porter and Pisaric (2011) found that all sampled sites in Old Crow Flats, Yukon, exhibited a positive response to summer temperatures prior to 1950, but the climate-growth response at some sites changed to a negative relation between tree growth and summer temperature after 1950. It is assumed that the variation in the tree ring widths is caused by limiting factors which can be readily identified. However, one must be careful not to assume that growth factors are static for a single sample.

2.5.3 Ecological Amplitude

Ecological Amplitude is the third principle presented by Fritts (1976). The assumption is that the sensitivity of species will increase as one moves closer to the margin of a species' natural range, thus limiting factors will be more evident under such conditions. This principle is why many dendrochronological studies are conducted near the growth margins of a species (Begin, 2001; Büntgen et al., 2005) where the stress

imparted by limiting factors will be most significant, such as along the northern treeline in Canada.

2.5.4 Selective sampling and site selection

The final principle is that of selective sampling and site selection. A tree whose growth is limited by a particular growth factor is more prone to produce variable ring widths than trees with complacent ring widths. Variable ring widths provide more climate variability information. Proper site selection can help to maximize the signal contained in tree ring records by sampling sites where limiting factors are most important. For example, trees growing on steep slopes with thin soils are likely to be limited with respect to precipitation because the thin soils retain little moisture and the steep slopes encourage precipitation to move rapidly downslope. Conversely, on relatively flat sites, soils tend to be much deeper and moisture is more abundant. Thus, trees growing in such environments often have complacent growth with similarly sized tree rings from one year to the next (Figure 2.5). Fritts (1976) further explains that sampling should be constrained to a particular species in order to minimize genetic differences. This sampling strategy appears to be contrary to normal statistical assumptions, which typically require a completely random approach, however Lamarche et al. (1982) argue that it is important to choose the specific site and the trees within it, so that all sampled trees will have the same or similar climate signals. Furthermore, fieldwork and laboratory analysis are often expensive and time consuming, requiring that information be extracted as efficiently as possible.

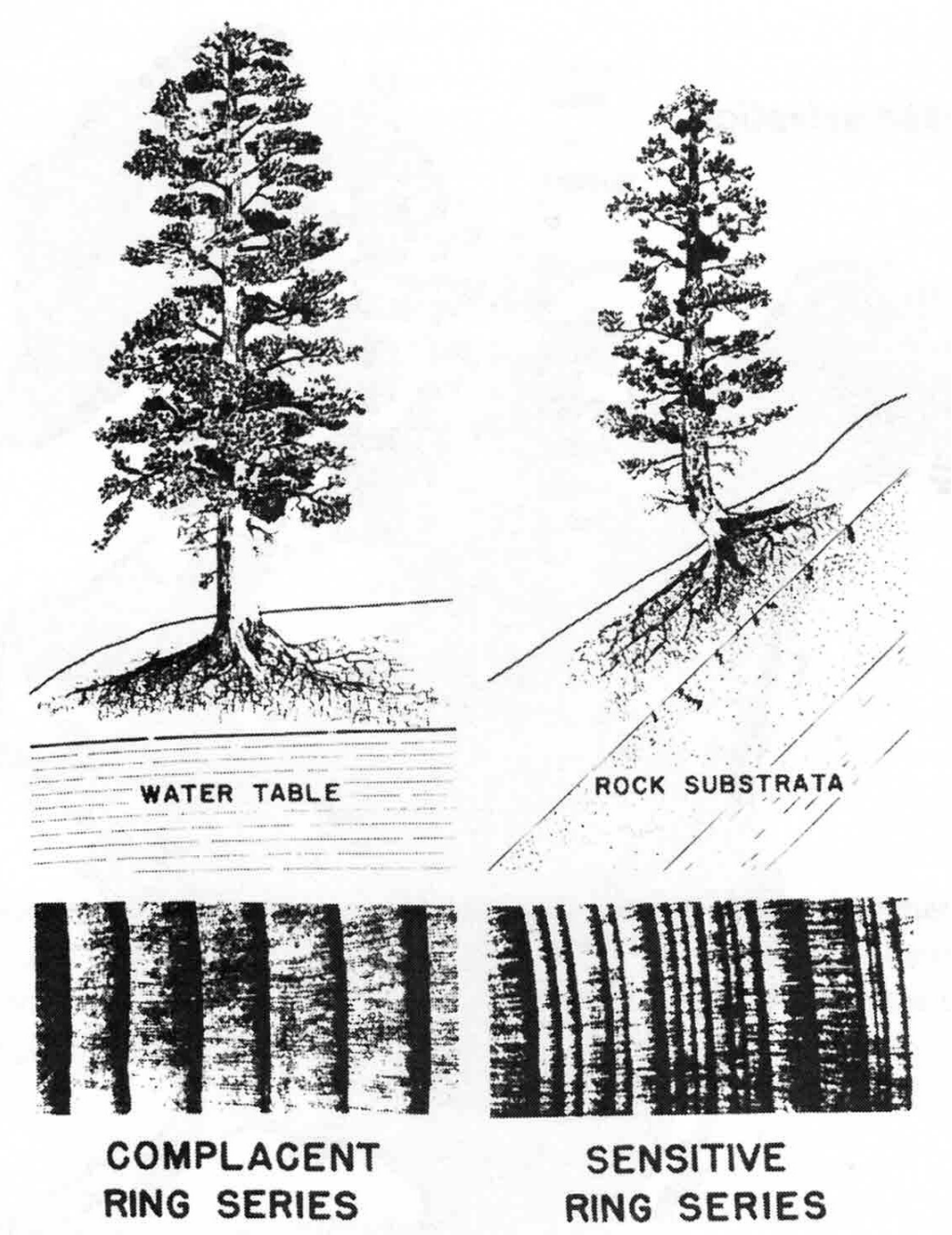

Figure 2.5. The tree on flat terrain (left) has reliable access to water and is therefore more likely to produce complacent ring widths. At right, the sloped landscape promotes runoff and restricts water availability to the tree, producing sensitive ring widths. Image from Speer (2010).

2.6 Dendrochronology

Fritts (1976) describes in detail appropriate sampling and analysis methods. Many of these methods are adapted from Stokes and Smiley (1968). Tree samples are typically collected with an increment corer (a hollow tube with a drill bit head) which extracts a small sample of wood roughly the diameter of a drinking straw (Figure 2.6). When sampling, there are external clues which may help to indicate the relative age of trees and the variability of ring widths by observing the structure and form of the tree. Fritts (1976) observed that older trees exhibited features which proved to be good indicators of age, such as a "gnarled snag top from which all small branches have disappeared". This is in agreement with the characteristics Schulman (1956) had previously described as being common to many different species of conifers. Fritts (1976) recommends two radii per tree be sampled from at least 20 trees in order to maximize the climate signal and reduce individual tree anomalies. There are often problematic samples however, such as cores with questionable dating, which may have to be excluded from the final analysis (Fritts, 1976). Having an excess of sample cores allows for problematic cores to be removed when needed. The collection of 30 trees per site is thought to ensure enough samples are available for the final model.

2.6.1 Standardization and the creation of tree ring indices

Trees display a natural decline of ring width over time, a pattern known as the biological growth trend. As trees age they add yearly growth around an ever increasing trunk size, leading to narrower rings that are simply the result of the biological growth trend and not due to climatic factors. This age related trend must be removed. This can

Figure 2.6. A tree sample, partially concealed by a drinking straw, beside a pre-grooved wood core mount. Photo by P. deMontigny.

be accomplished in a number of ways, but no matter the method, allows for younger, fast growing portions of a tree to be made comparable to older, slower growing portions of the tree (Fritts, 1976). Tree ring measurements are also transformed into dimensionless units during standardization, called tree ring indices, which allow for a better comparison across sample sites than raw measurements do.

Tree ring indices are then tested to determine if ring width patterns correlate with climate variables, and, if such a relation exists, the indices can then be used to develop a model based on this relation. With a model in place, recorded climate measurements are replaced by the predicted values, and a comparison done to assess the quality of the model. There are many statistical measures for calibrating and validating a tree ring climate reconstruction, including the correlation coefficient (r), coefficient of determination (r^2), and adjusted coefficient of determination (r^2_{adj}). These statistics, used extensively in sciences, compare the linear regressions of the reconstructed climate values and known instrumental records. In addition to reporting these common measures, statistics specific to dendroclimatological analysis will also be used in this study; the sign test (ST; Equation 2.2), the reduction of error (RE; Equation 2.3) and the coefficient of efficiency (CE; Equation 2.4) are three such measures.

$$\mathrm{ST} = \Delta x_i = x_i - x_{i-1} \qquad \textit{(Eq. 2.2)}$$

$$\mathrm{RE} = 1 - [\Sigma(y_i - \hat{y}_i)^2 / \Sigma(y_i - \bar{y}_c)^2] \qquad \textit{(Eq. 2.3)}$$

$$\mathrm{CE} = 1 - [\Sigma(y_i - \hat{y}_i)^2 / \Sigma(y_i - \bar{y}_v)^2] \qquad \textit{(Eq. 2.4)}$$

where x_i is the first-differences of each series, y_i is one of n measured values, $\hat{y}_i$is the estimated value, $\bar{y}_c$ is the mean of the measured values in the calibration period, and $\bar{y}_v$ is the mean of the measured values in the verification period.

2.6.2 Sign test

The ST is a non-parametric test which is also popular due to its simplicity. It indicates if the general trend between the reconstructed and the measured data is comparable. The ST only measures if values change in a similar manner from the mean, not the magnitude of change. For example, if both reconstructed and actual recorded temperature values indicate warming compared to the mean, then that year would be in agreement. Sign tests for each year are tallied, and if the number of agreements is greater than the number of disagreements (by more than would be expected by chance alone), then the reconstruction will be considered reliable to some degree.

2.6.3 Reduction of Error and Coefficient of Efficiency

A split period calibration-validation procedure is used to calculate RE and CE values. Here, the model is assessed by comparing the relation between modeled values and actual recorded instrumental values. A portion of instrumental data, usually half, is used to calibrate the reconstructed values. The calibration/validation periods are then reversed, and the process is repeated. Output values of RE and CE are measures of shared variance between the actual and modelled series, essentially a test to determine if the model has predictive skill (Meko, 2011). Predicted values (validation) are compared to the mean of the instrumental record (calibration), producing the RE value.

The equation is very similar to a coefficient of determination equation, but can range from $-\infty$ to +1 (as opposed to -1 to +1). Meko (2011) notes that the much larger range for RE suggests that a RE value close to the r^2 value is evidence of validation. Similarly, Cook et al. (1994) and Mann et al. (1998) propose that if the model provides a better prediction of climate compared to just applying an average, RE and CE will be positive, and a stronger climate reconstruction can be presented. Of the three measures, ST and CE are the most rigorous tests (Cook et al., 1994). While CE also compares predicted values to the mean of the instrumental record and ranges from $-\infty$ to +1, the "difference between the RE and CE lies in the denominator. Although this difference appears to be trivial, in fact large differences in the RE and CE can occur" (Cook et al. 1994, p. 402). The ST, RE, and CE are commonly reported in the dendroclimatological literature, and appear to be a useful measurement of calibration and validation.

2.7 Northern dendrohydrology and dendroclimatology

Dendroclimatology has been used in multiple regions and climatological applications (Case and MacDonald, 1995; Büntgen et al., 2005; Cook et al., 2007). In northern Canada, recent interest in the region has resulted in the development of multiple dendroclimatological reconstructions. For example, Pisaric et al. (2009) used twelve jack pine sites to develop a 325-year (1680-2005, statistically robust from 1819-2005) June precipitation record for the Yellowknife area, extending the previous precipitation record by ~260 years. Results correlated well with other North American dendroclimatological studies and large scale atmospheric patterns, showing the mid-20th century as the longest sustained period of dry conditions. Youngblut and Luckman

(2008) reconstructed maximum June-July temperatures from 1684–1995 for southwestern Yukon using seven white spruce chronologies, with the mid-1900's encompassing some of the warmest temperatures of the reconstruction. June-July temperatures were found to be 0.49°C warmer in the 20th century than the 1684-1899 average. Meko (2006) studied eight white spruce sites as well as 46 other tree ring chronologies obtained from the International Tree Ring Data Bank (ITRDB), to reconstruct water levels for Lake Athabasca. Lake levels were determined by comparing tree ring widths to known lake levels and running a principal component analysis. The statistically significant relation between white spruce growth and water levels in the Peace Athabasca Delta allowed for Lake Athabasca water levels to be extended back to 1801, revealing 1890 as the year of lowest reconstructed water levels. The success of these studies suggests that it is likely possible to reconstruct climate for the Fort Providence region and establish a relation to lake expansion.

2.8 Palmer Drought Severity Index

Previous work completed in the Fort Providence region (deMontigny and Pisaric, 2011) indicated a significant correlation existed between tree growth and the Palmer Drought Severity Index (PDSI; Palmer, 1965). PDSI is a climate index designed to measure the intensity, duration, and spatial extent of drought (Shabbar and Skinner, 2004). Computing PDSI is a multi-step process; the following explanation is derived from Wells et al. (2004). PDSI is calculated monthly, using evapotranspiration (*ET*), recharge (*R*), runoff (*RO*), loss (*L*), potential evapotranspiration (*PE*), potential recharge (*PR*), potential runoff (*PRO*), and potential loss (*PL*). The four potential values are weighted

using local climate data (Equation 2.5 – 2.8) to derive Climatically Appropriate for Existing Conditions (CAFEC) values for *PE* (α_i), *PR* (β_i), *PRO* (γ_i), and *PL* (δ_i)

$$\alpha_i = \frac{\overline{ET_i}}{PE_i} \quad \textit{(Eq. 2.5)}$$

$$\beta_i = \frac{\overline{R_i}}{PR_i} \quad \textit{(Eq. 2.6)}$$

$$\gamma_i = \frac{\overline{RO_i}}{PRO_i} \quad \textit{(Eq. 2.7)}$$

$$\delta_i = \frac{\overline{L_i}}{PL_i} \quad \text{(Eq. 2.8)}$$

where i is the month and the top bar indicates an average value. For example, the average evapotranspiration for January (Equation 2.9) would be calculated as

$$\bar{E}_1 = \frac{\sum E_1}{\text{number of years of data}} \quad \textit{(Eq. 2.9)}$$

The CAFEC values are then combined to determine CAFEC precipitation, $\dot{P}$ (Equation 2.10), which indicates the amount of precipitation needed to maintain a normal soil moisture level.

$$\dot{\text{P}} = a_i + \beta_i + \gamma_i - \delta_i \quad \textit{(Eq. 2.10)}$$

The difference between the CAFEC precipitation value and the actual amount of precipitation that fell in a given month (*P*) is calculated, providing a measure of moisture departure (*d*; Equation 2.11).

$$d = P - \dot{P} \qquad \textit{(Eq. 2.11)}$$

As *d* will be dependent on local conditions, comparisons across varying temporal and spatial scales become problematic. Palmer (1965) developed PDSI to examine drought conditions in Kansas and Iowa, regions in which soil properties differ significantly in certain aspects (i.e., potential run off; Palmer, 1965). As a result, measurements are normalized, allowing for comparison between locations. To normalize values, a climatic characteristic, *K* (refined from *Ḱ*), is used to weight *d* (Equations 2.12 and 2.13),

$$\acute{\mathrm{K}}_i = 1.5 \log_{10}\left(\frac{\frac{\overline{PE_i} + \overline{R_i} + \overline{RO_i}}{\overline{P_i} + \overline{L_i}} + 2.8}{\overline{D_i}}\right) + 0.5 \qquad \textit{(Eq. 2.12)}$$

$$K_i = \frac{17.67}{\sum_{j-1}^{12} \overline{D}_j \acute{\mathrm{K}}_j} \acute{\mathrm{K}}_i \qquad \textit{(Eq. 2.13)}$$

where $\overline{D_i}$ is the average moisture departure for the given month, and the value of 17.67 is a constant derived by Palmer (1965) from data of nine locations across seven states. The climatic characteristic (*K*) is then used to calculate a moisture anomaly index (*Z*; Equation 2.14), which makes it possible to compare PDSI both temporally and spatially.

$$Z = dK \qquad \textit{(Eq. 2.14)}$$

Finally, a monthly PDSI value can be calculated to indicate climatic conditions (Equation 2.15)

$$PDSI_t = 0.897 \cdot PDSI_{t-1} + (1/3)\, Z_t \qquad \textit{(Eq. 2.15)}$$

where $PDSI_t$ is the PDSI value for time period t, and Z_t is the moisture anomaly index for time period t, independent of past months data. Conditions must be evaluated over months/seasons to allow for proper assessment of abnormal dry or wet environments (Shabbar and Skinner, 2004).

PDSI values have been developed for much of North America by Cook et al. (2007) and the data are freely available through the North American drought atlas (http://iridl.ldeo.columbia.edu/SOURCES/.LDEO/.TRL/.NADA2004/.pdsi-atlas.html). Grid point 49 (62°.5' N, 117°.5 W) and grid point 50 (117°.5' W, 60°.0' N) were the two data points nearest to the study sites used in deMontigny and Pisaric (2011). Although correlations were highest between the tree ring chronologies and PDSI in the study by deMontigny and Pisaric (2011), the climate-growth relationship was convoluted in recent decades as the trees sampled in that study became submerged by rising water levels (Figure 2.7). As a result, sample sites situated in areas unaffected by rising lake levels were sought for this study, to ensure a more dependable climatic relationship.

2.9 Atmospheric circulation patterns

Sea surface temperatures, typically examined as a deviation from normal conditions (called sea surface temperature anomalies; SSTAs), have been used to

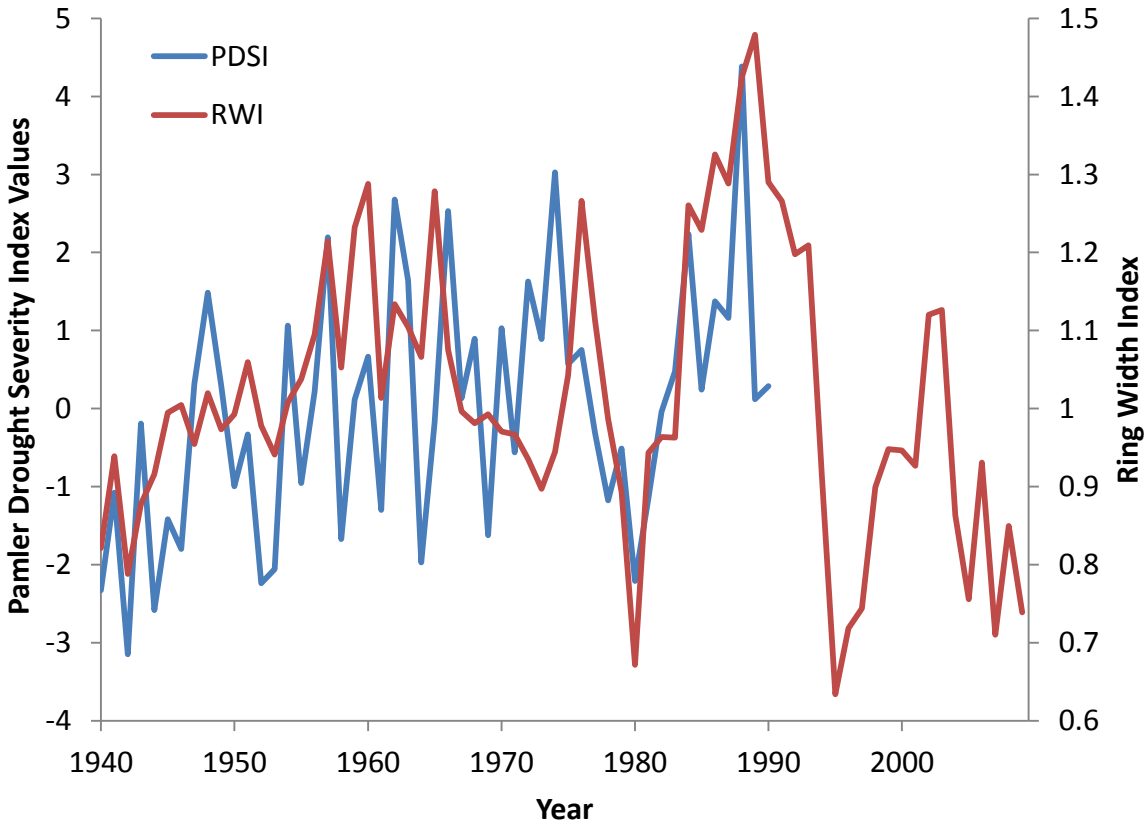

Figure 2.7. Results from deMontigny and Pisaric (2011). PDSI values (blue) compared to the black spruce regional chronology (red).

successfully predict regional precipitation and temperature (Colman and Davey, 2003).

The Hadley Centre Sea Surface Temperature version two dataset (HadSST2) provides monthly SSTA values extending from 1850-present within a 5° latitude x 5° longitude global grid. Anomalies are relative to the 1961-1990 climate normal. Unlike many SSTA datasets, HadSST2 data are not interpolated, but are checked for quality and bias (Rayner et al., 2006). SSTs also impact atmospheric patterns such as the previously mentioned AO, PDO, and the PNA pattern, all of which will be consequently examined for this project.

CHAPTER 3
STUDY AREA AND METHODS

3.1 Study area

The study region is located within the Great Slave Plain High Boreal and Great Slave Lowland Mid-Boreal Level IV Ecoregions (Ecosystem Classification Group [ECG], 2007). Situated in a discontinuous permafrost zone, the terrain is flat, with minimal topographic variability throughout the landscape. Elevation ranges between 125 and 300 m a.s.l. (ECG, 2007), with highest elevations occurring in the northern half of the study area. There are thousands of small and shallow lakes surrounded by black spruce (*Picea mariana*) forest. White spruce and jack pine stands are present on well-drained sites (ECG, 2007).

3.1.1 Geology

There are two main top layer subsurface geologic formations which encompass the majority of the MBS: the Hay River Formation and the Horn River Formation (Figure 3.1). Both are remnants from the Paleozoic Era, specifically the Devonian Period (~416-360 mya; Douglas, 1974; Douglas, Norris, and Norris, 1974; 1975). These sedimentary formations are characterized by black or grey shales containing 40% clay (Farrokhrouz and Asef, 2013) and fine-grained limestone, which “contributed significant silt and clay to the matrix of local glacial till” (EcoDynamics Consulting, 2008, p. 5).

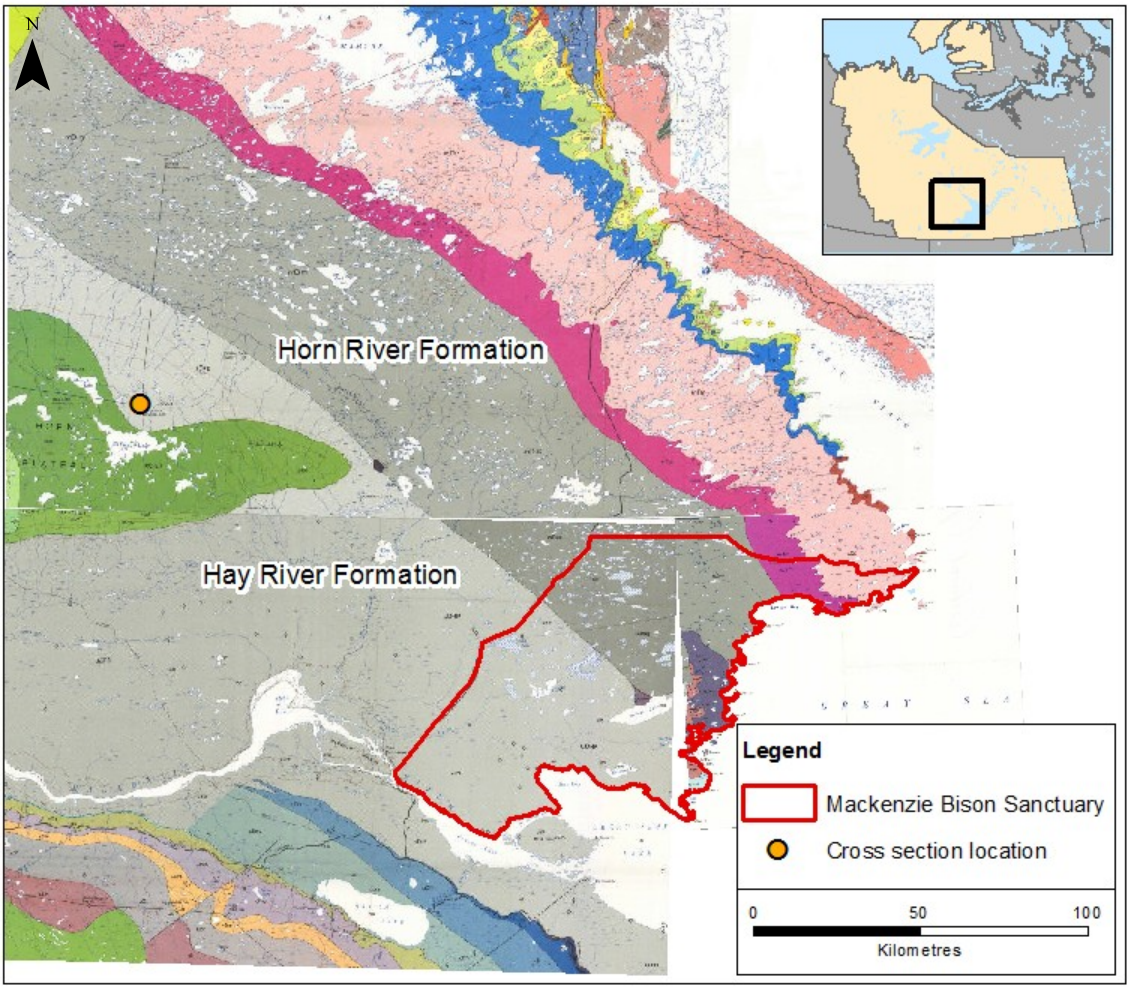

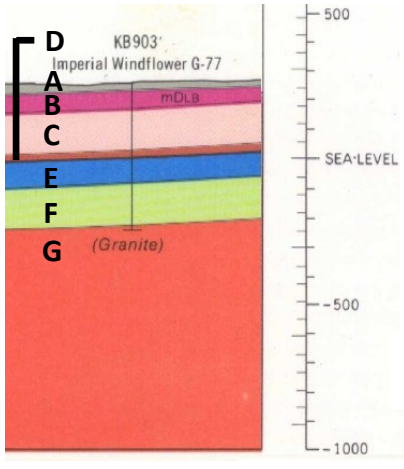

Geologic formation: material

A - Horn River: shale, limestone.
B - Lonely Bay: limestone.
C - Chinchaga: gypsum, limestone, dolomite.
D - Mirage Point: dolomite, shale, gypsum.
E - Chedabucto Lake: dolomite, shale.
F - La Martre Falls: shale, dolomite, salt crystal casts.
G - Granite

Figure 3.1. Subsurface geology for the study region and surrounding area. The Hay River and Horn River formations cover the majority of the MBS (top). A nearby cross-section of subsurface layers is also shown (left). Images derived from Douglas (1974), Douglas, Norris, and Norris (1974; 1975).

3.1.2 Glacial Lake McConnell

The Laurentide ice sheet, which covered the entire study area during the last glaciation, has also helped define the current landscape. As the ice sheet retreated, Glacial Lake McConnell formed, extending from Great Bear Lake to Lake Athabasca (Figure 3.2; Smith, 1994). In addition to the glacial till left by the melting ice sheet, glaciolacustrine beach deposits and fluvial-lacustrine deposits from Glacial Lake McConnell provided a massive source of silt, clay, sand and gravel (EcoDynamics Consulting, 2008). Drainage improves moving north within the MBS and beyond due to glacial till (ECG, 2007).

3.2 Climate

Winter seasons are long and cold, while summers are short and cool (ECG, 2007). The climate record for the immediate study area, Fort Providence, NT, is incomplete for long periods during the length of record from 1943 to present (Figure 3.3). In such cases, Fritts (1976) suggests that information can be gathered from neighbouring areas, assuming that the regions exhibit similar exposure and elevation. These areas should also be within a 160 kilometer distance of the site, using a minimum of two neighbouring weather stations. Hay River and Yellowknife represent the closest opportunities to study long term instrumental records for the general region. Although Fritts (1976) indicates that correlations may be substantially reduced if the weather station is more than 32 kilometers away, both Hay River and Yellowknife temperature records correlate well with the Fort Providence climate data that does exist ($r \geq 0.98$, p-

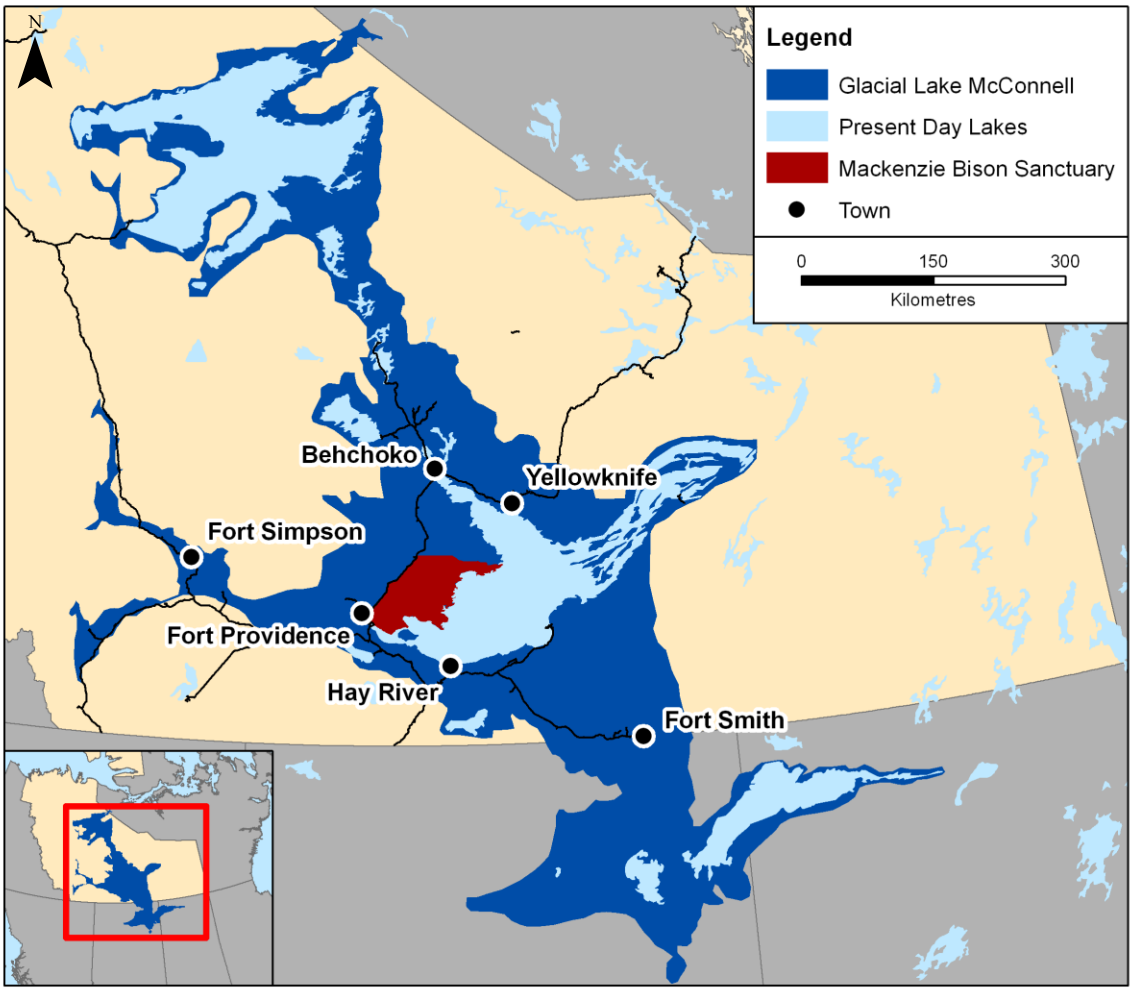

Figure 3.2. Maximum extent of Glacial Lake McConnell. Image derived from Smith (1994).

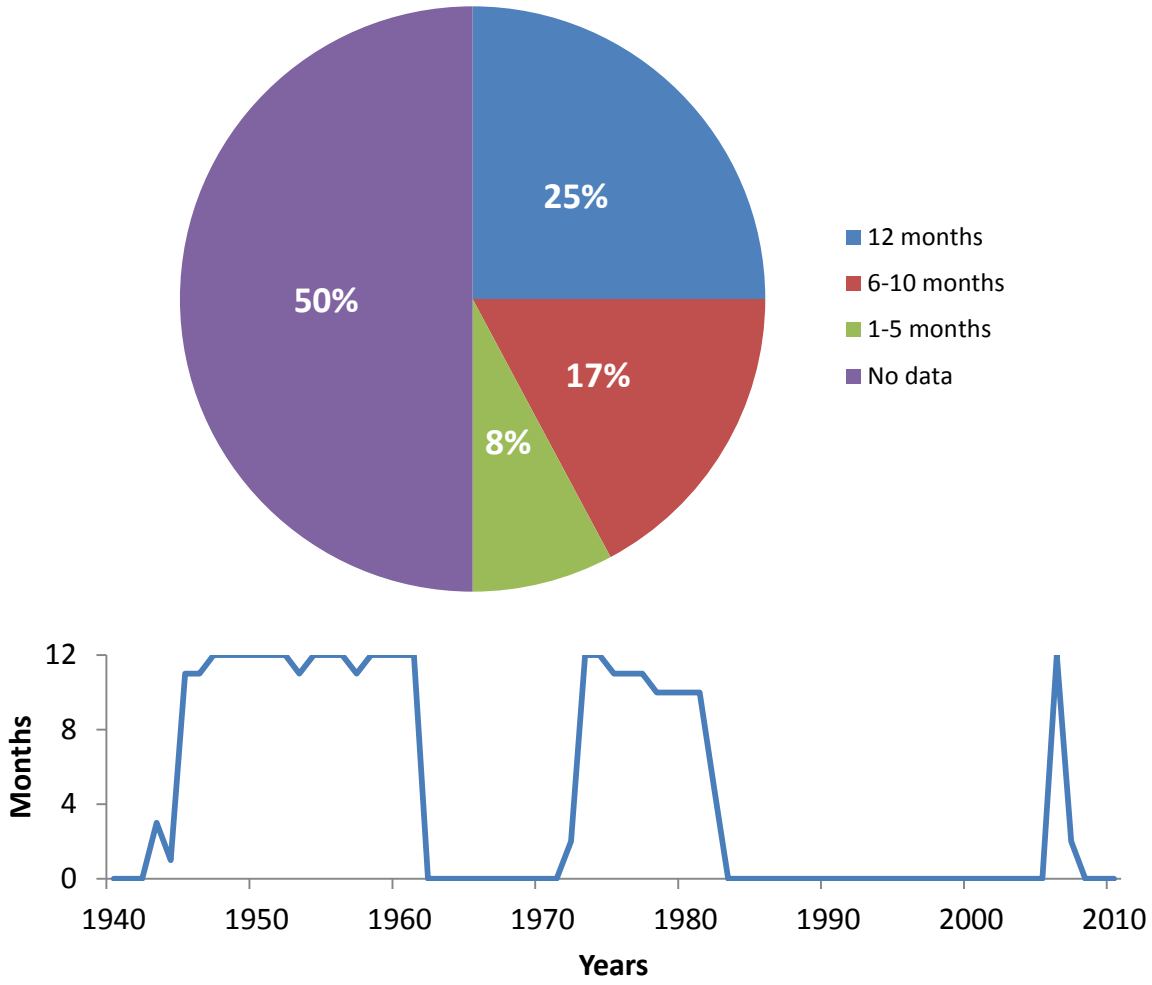

Figure 3.3. A summary of the existing climate data for Fort Providence, NT (1943-2007). The bottom graph shows the temporal distribution of climate data.

value ≤ 0.01), suggesting there is significant similarity between the records. Precipitation however, is only moderately correlated (r ≥ 0.51, p-value ≤ 0.01).

Using an averaged value for the three stations, a 30-year climate normal (1981-2010) was created. The thirty year daily average is to satisfy the minimum time period recommended by the World Meteorological Organization (WMO) to eliminate inter-annual variations (WMO, 1989). The mean annual temperature is -3.2°C. Annual precipitation is approximately 317mm, with the majority falling during summer months (ECG, 2007; Figure 3.4).

3.3 Remotely sensed data

3.3.1 Image Standardization

As discussed in Chapter 2, LANDSAT 5 TM data were selected as the most suitable source of remote sensing imagery. To limit the seasonal variability of imagery, a semi-objective date range was established. A reference point, based on ± 1 standard deviation of the September maximum temperature climate normal, resulted in a date range of August 12th to October 13th. This date frame is similar to the August to October time frame suggested by van der Wielen (2012) to study lake area change in the MBS.

Images with less than 10% cloud cover, and no-to-minimal clouds within the area of interest, were selected. Using this method, 13 images were obtained for the period 1986-2011 (Table 3.1). A combination of two LANDSAT 5 TM scene footprints were needed to capture a meaningful observation period. In order to provide a consistent area of analysis however, the spatial extent was limited to where the two footprints

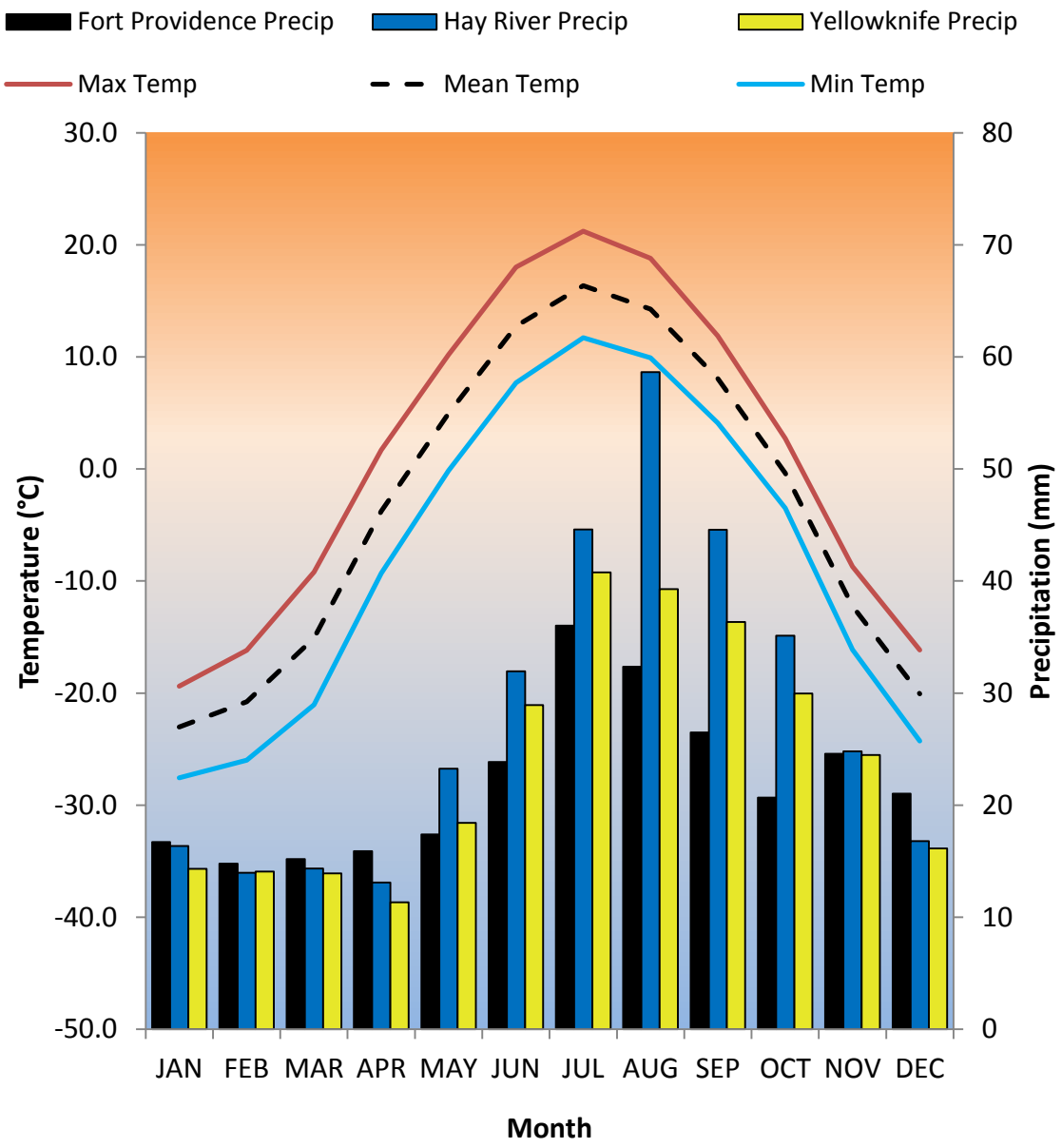

Figure 3.4. Fort Providence, Hay River, and Yellowknife climate normal (1981-2010). Maximum (red line), mean (dotted line), and minimum (blue line) temperature values were derived by averaging the three sites together; temperatures between sites are highly correlated ($r \geq 0.98$, p-value ≤ 0.01). Precipitation totals are shown for Fort Providence (black), Hay River (blue), and Yellowknife (yellow). Average Fort Providence precipitation data was derived from all available Fort Providence data (1943-2007).

Table 3.1. LANDSAT 5 TM images used in analysis. There are thirteen images between 1986-2011.

Year	Date	Scene ID
1986	Sept. 9	LT50480171986252PAC00
1989	Sept. 1	LT50480171989244PAC00
1992	Aug. 17	LT50470171992230PAC00
1993	Sept. 21	LT50470171993264PAC00
1994	Aug. 30	LT50480171994242PAC00
1997	Sept. 23	LT50480171997266PAC00
1999	Sept. 13	LT50480171999256PAC00
2001	Aug. 17	LT50480172001229LGS01
2003	Oct. 3	LT50470172003276PAC02
2004	Sept. 26	LT50480172004270PAC01
2005	Sept. 6	LT50470172005249PAC01
2007	Aug. 18	LT50480172007230PAC02
2011	Aug. 22	LT50470172011234PAC03

overlap. As a result, eastern portions of the MBS have been excluded from analysis (Figure 3.5). Although cloud-free images were sought in imagery acquisition, occasional clouds were still present in four of the images (1986, 1989, 1994, and 1997). These small areas were masked from analysis using the Haze Removal tool, part of the Atmospheric Correction (ATCOR) wizard in PCI Geomatica 2013.

Images were radiometrically calibrated with Equation 3.1. Top of atmosphere reflectance values were also calculated, using Equation 3.2 (Finn et al., 2012). Earth-Sun distance (D), ground surface irradiance (I), and sun angle (SA) were extracted using a combination of the metadata file (included in each LANDSAT 5 TM image) and lookup tables.

$$L_\lambda = G_{rescale} * DN_\lambda + B_{rescale} \qquad \textit{(Eq. 3.1)}$$

$$P_\lambda = \frac{(\pi * L_\lambda * D^2)}{(I * \sin(\pi * SA/180))} \qquad \textit{(Eq. 3.2)}$$

3.3.2 Image Classification

Following standardization, images were classified into two broad categories, water and land. Indices, such as the Normalized Difference Vegetation Index (NDVI; Rouse et al., 1973) and Normalized Difference Water Index (NDWI; Gao, 1996), combine spectral information from multiple bands, exaggerating differences between vegetated and non-vegetated surfaces. LANDSAT 5 TM records information in seven spectral bands, the combination of which can lead to increased accuracy in feature classification

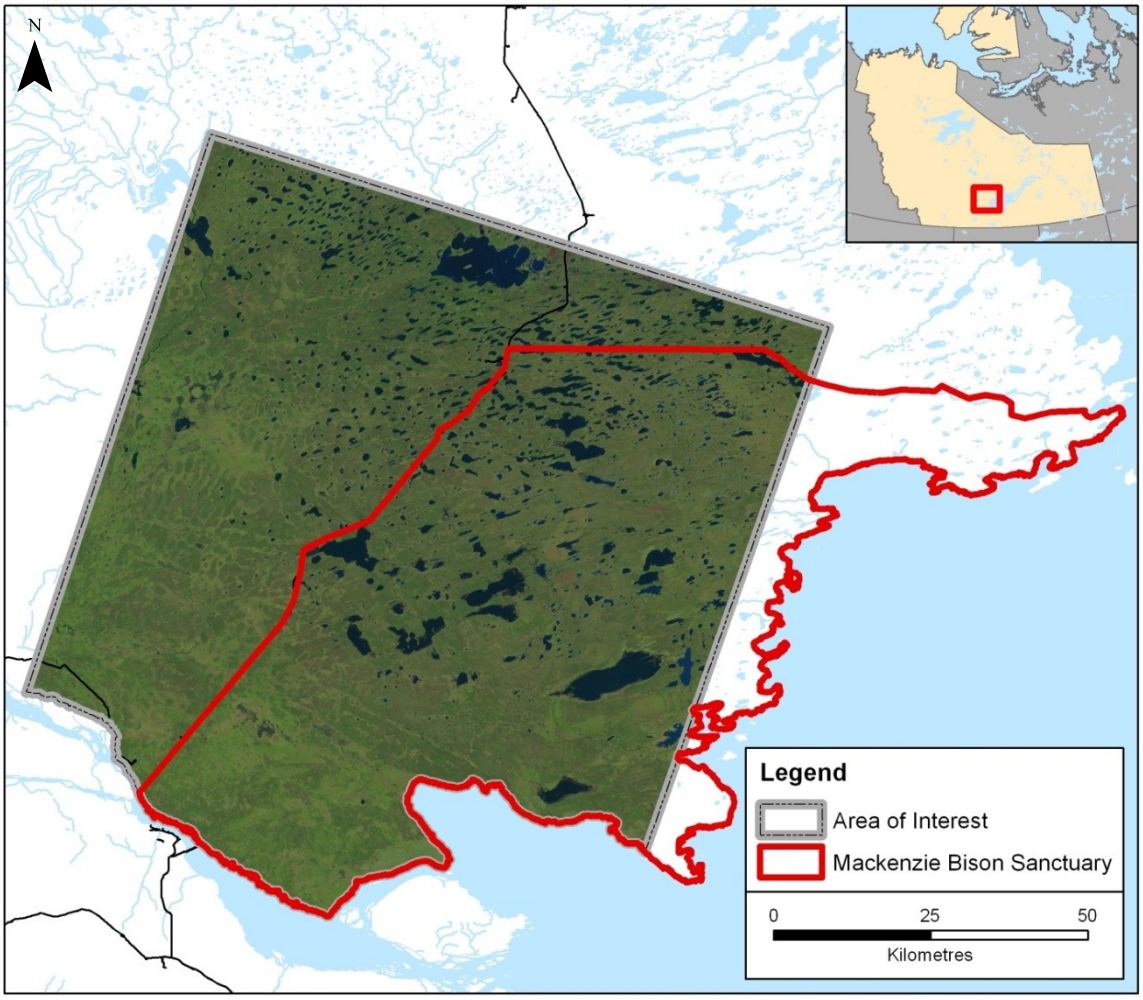

Figure 3.5. Map of the Mackenzie Bison Sanctuary (red) compared to the area of analysis (grey). Great Slave Lake and south of the Mackenzie River and Great Slave Lake have also been excluded from analysis.

(Gao, 1996). Unfortunately, flooded tree stands and floating vegetation appear to negatively impact index classification results, severely underestimating the size of lakes.As a result, only the near-infrared (NIR) band was used for analysis. The NIR band has been used successfully in other studies to delineate shoreline boundaries (Van and Binh, 2009). Additionally, the images for this study demonstrate a bi-modal distribution of data, providing a reliable distinction between water and land features.

Per-pixel, top of atmosphere reflectance values were transformed to fuzzy membership values using a sigmoid membership function (Equation 3.3), where $f1$ is the spread value and $f2$ is the midpoint value. The spread value, which ranges between 1 and 10, controls how rapidly the fuzzy membership curve decreases from 1 to 0. A lower spread value results in a less abrupt transition to a 0 membership value (ESRI, 2011). A spread value of 5 was applied to all images for this project using the Fuzzy Membership tool in ArcMap. A midpoint value of 0.5, the middle range of membership values of the input raster, was also implemented. To classify water, low reflectance values (water) were given a membership of 1.0, high reflectance values (land) received a membership of 0.0, with all other values ranging between 1.0 and 0.0 membership. The resulting raster was then hardened (converted to crisp values) based on the membership of interest (three thresholds were examined for this project: 1.0, ≥0.5, and ≥0.1), producing a raster with only two categories: water or land.

$$\mu(x) = \frac{1}{1+\left(\frac{x}{f2}\right)^{f1}} \qquad \textit{(Eq. 3.3)}$$

A minimum mapping unit (MMU) of 0.81 hectares (9 pixels) was implemented for this study, a standard cautionary measure for 30 m pixel sensors (Knight and Lunetta, 2003). Features of less than 0.81 ha contribute to a 'salt and pepper' image and are not considered replicable (Lunetta and Balogh, 1999). A 3 x 3 pixel mode filter was implemented to generalize the image. The majority filter examines the central pixel of a 3 x 3 window and assigns a category class based on the value of the majority of pixels in the window. While this method does limit the ability to detect small changes in lake size, the result is a more reliable classification. Clustered pixels were grouped together using the Region Group tool in ArcMap. Clusters of eight pixels or less were reclassed as no-data and subsequently excluded from further analysis. The classified raster images were then converted to non-simplified vector shapefiles to calculate lake area.

In addition to examining the study site as a whole, the area was sub-divided into smaller zones of analysis to explore lake growth within the region. Turner et al. (2010) examined lake water balances in Old Crow Flats, Yukon using isotopic tracers ($\delta^{18}O$ and $\delta^{2}H$). They found that some lakes exhibited a strong reliance on snowmelt, others on rainfall, and still others relied on groundwater. The associated dependence was related to landscape conditions of the immediate area surrounding the lake, and varied widely even within a single study site. It may be advantageous therefore, to examine lake growth at the site level as opposed to regionally, where the varying response signals may be lost. A grid size of 10 x 10 km, or 10,000 ha, was chosen to conform to regional scale investigation standards in land cover change detection (Abdullah and Nakagoshi, 2006). Boundary grid squares with cells covering less than 50% of the total land area

were omitted from analysis, leaving 101 grid cells. Due to the number of grid locations examined at the regional scale, a decision was made to focus on a single membership type. A fuzzy membership of ≥0.5 was chosen, as 1.0 membership does not make full use of the available data (Foody, 1999). Additionally, Larter and Gates (1991) examined wood bison diet and habitat in the MBS and found the bison preferred wet and mesic meadows. As a result, areas with some water present were not interpreted as at great of risk to bison displacement, and the ≥0.1 membership results were not studied further. Four major lakes (Birch Lake, Boulogne Lake, Caen Lake, and Dieppe Lake; Figure 3.6) were also selected to examine lake growth at an even finer scale. A 500 m buffer was applied to the maximum extent of each lake to define a consistent area of analysis while capturing potential spatial distribution inconsistencies.

3.3.3 Sampling strategy

To test for accuracy, pixels from the original, unclassed imagery which had an obvious spectral association to a specific land cover type were used as reference data. From the resulting group of reference data, assessment pixels were determined with a stratified random sampling approach using the Geospatial Modelling Environment tool (Beyer, 2012). This method guarantees a specified number of pixels are selected for each class, but random selection within those classes ensures sampling conforms to scientific principles (Gao, 2009). Lillesand et al. (2007) recommend a minimum of 50 sample pixels per class as a rule of thumb, but up to 100 sample pixels for large areas. One hundred sample points were selected per class for this study.

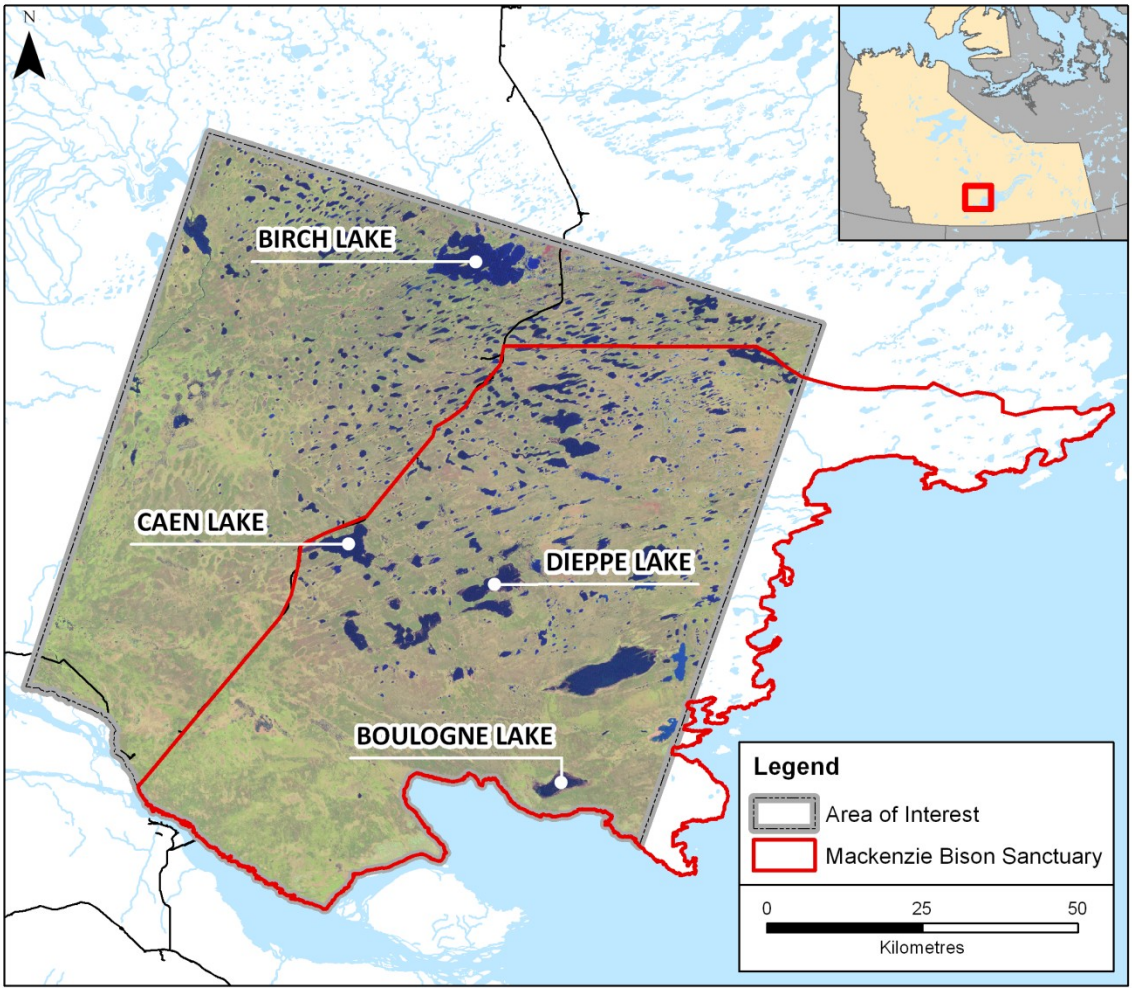

Figure 3.6. Locations of Birch Lake, Boulogne Lake, Caen Lake, and Dieppe Lake.

The associated land cover types of the reference and classified data within the assessment pixels were then compared (classified data being the imagery which had been classed according to fuzzy membership results). It should be noted that the majority of sampled pixels are likely within the interior area of a given class, which may inflate accuracy results.

3.3.4 Statistical Procedures

Lake level data analyzed for this study were found to be highly autocorrelated over the time series, a phenomenon inherent to the majority of environmental time series analyses (Buchberger, 1995). When a data series exhibits autocorrelation, sampling is no longer independent and the amount of meaningful information extracted is an overestimation of importance, as the influence of previous data points skews results. Mann-Kendall results are greatly impacted by autocorrelation, so data were corrected with an effective sample size approach described by Yue and Wang (2004). The original effective sample size approach compares the mean variance of an independent sample point with the variance of the remaining data (McGrath, 2009). The Yue and Wang (2004) method calculates the effective sample size based on the estimated detrended data, resulting in a better representation of significant change. A confidence level of 95% was applied.

3.4 Dendroclimatology

3.4.1 Sampling methods

Tree cores were collected from white spruce and jack pine (Table 3.2) and analysed separately to test for a common climate signal from multiple species chronologies. Site boundaries were neither uniform nor static, as site size is determined in the field by the ability to find an appropriate number of sensitive trees. For this study however, a radius of 500 m can be considered a conservative estimate of site size. Sites were selected at roughly 10 km intervals along Highway 3, which runs through the MBS from Fort Providence to Behchoko (Figure 3.7). A minimum (maximum) of 30 (39) trees were sampled per site. Samples were collected using Hagloff increment tree borers (with an internal diameter of ~4.3 mm)

3.4.2 Sample preparation and measurement

Cores were allowed to air dry and then mounted on pre-grooved wood core mounts, placed in a way that exposed the transverse (cross-sectional) surface (Fritts, 1976). The samples were then sanded with progressively finer sandpaper. A sandpaper grit sequence of 180, 320, 380, and 400 or 600 is recommended by Stokes and Smiley (1968) and was used as a guideline. Samples were dated (marked) under a microscope, highlighting each decade, half century, century, and problematic areas where absent or hard to see rings appear (Stokes and Smiley, 1968). A Velmex tree ring measuring system was used to provide precise ring width measurements (precise to 0.001 mm). Measurements were compared across multiple samples to ensure proper cross dating, using visual cues, the list method (Yamaguchi, 1991), and statistical cross dating with

Table 3.2. Summary of tree ring sample sites for the study area.

Site Code	Latitude	Longitude	Elevation (m)	Tree Species	Series Length (yrs)
FP01	61.55039	-117.15425	190	white spruce	1731-2010
FP02	61.69592	-116.91578	208	white spruce	1920-2010
FP03	61.43972	-117.37347	160	white spruce	1908-2010
FP05	61.85500	-116.62017	228	jack pine,	1930-2010
				white spruce	1927-2010
FP06	62.69056	-116.16417	227	jack pine	1861-2010
				white spruce	1718-2010
FP08	62.72614	-116.09828	248	jack pine	1852-2008
FP09	61.89714	-116.52744	240	white spruce	1796-2010
FP10	61.68000	-116.97806	254	white spruce	1885-2010
FP11	61.82097	-116.71217	227	jack pine,	1873-2010
				white spruce	1890-2010
FP12	61.73256	-116.87428	231	jack pine	1874-2010
FP13	62.14839	-116.26556	220	jack pine	1895-2010
FP14	62.03703	-116.31392	214	white spruce	1879-2010
FP15	61.63231	-117.12006	215	jack pine	1926-2010
FP16	61.53503	-117.21075	194	white spruce	1922-2010

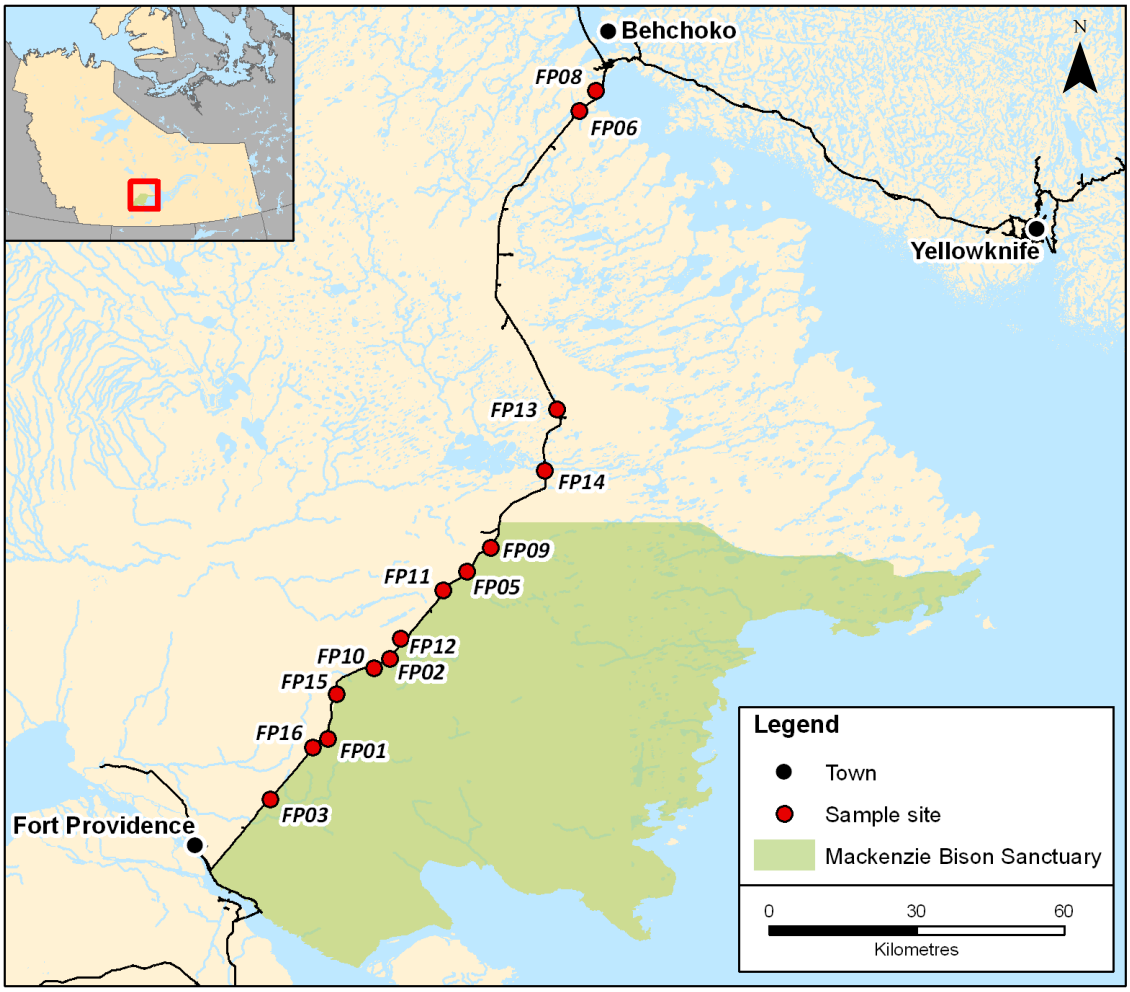

Figure 3.7. Map of tree ring sampling sites. There is a large gap between sites FP06 and FP13 due in part to recent fire activity in the area.

the computer program COFECHA (Holmes, 1983). The list method is a faster alternative to skeleton plotting, used in instances where there is a clear pattern of rings from living trees (Speer, 2010). Consistent marker rings are then used to cross date other cores.

3.4.3 Standardization

Two standardization methods were initially considered for this project: negative exponential curve (NEXP) and Signal-Free (SF). NEXP is employed extensively in the field of dendroclimatology (Speer, 2010), and SF, while still a relatively new concept, is quickly becoming a popular method. The NEXP method is a deterministic model, dividing the ring widths of each individual tree series by a known age-related curve (Gunnarson, 2001; Speer, 2010). For SF, a data-adaptive smoothed curve is used to develop a mean chronology. Raw ring width measurements are then compared to this mean chronology to remove the common climate signal, producing SF values (Porter, 2012). These values are an estimate of tree growth in an unchanging climate, with age related growth removed (Melvin and Briffa, 2008). The removal of the age related trend and development of NEXP ring width indices were completed using the ARSTAN software package (Cook and Holmes, 1986). A signal free enabled ARSTAN add-in (by Ed Cook, Lamont-Doherty Earth Observatory Tree-Ring Laboratory) was used to calculate SF values.

Standardization results varied widely between the two methods, especially in the early part of the series. It has been well documented that NEXP is likely to reduce at least some of the climate signal when removing the growth trend (Melvin and Briffa, 2008), however this technique is less prone to user error than empirical models such as

SF (Speer, 2010). Additionally, while SF provides a seemingly improved method for standardization, research in regards to this method has been limited (Briffa and Melvin, 2011; Anchukaitis et al., 2013). Further investigation is needed before SF can be applied with confidence. As such, SF results were not studied further.

3.4.4 Regional chronology

Assuming a consistent species sample and standardization technique, individual site chronologies have the potential to be combined into a single regional chronology. In dendroclimatology, this allows for a better understanding of the spatial distribution of climate (Speer, 2010). To determine if site chronologies were affected by similar influences and therefore appropriate for grouping, Principal Component Analysis (PCA) was used. PCA is used to understand multi-dimensional phenomena, reducing the number of influencing factors to a few key variables (Demsar et al., 2013). Data are mapped in a multi-dimensional matrix, with the factor explaining the greatest amount of variance labelled as Principal Component 1 (PC1) followed by PC2, PC3, and so on, ordered according to their eigenvalues (Desmar et al., 2013). If site chronologies are similar in influence then a regional chronology can be created.

3.4.5 Climate-growth relation

Although there are many methods for determining which climatic factors are most likely influencing tree growth, correlation coefficients were used for this study. Correlation coefficients can "provide information similar to analysis of variance and because correlation is a simpler concept and easy to compute, it is sometimes favored

over analysis of variance" (Fritts, 1976). A statistical equation using linear regression was subsequently developed to model climate based on tree ring width. This is a standard statistical technique for dendroclimatology (Speer, 2010).

The model derived for this study has been tested against the measures of statistical significance discussed in Chapter 2, providing confidence in reconstructed climate values, and will be presented in Chapter 4.

CHAPTER 4
RESULTS

4.1 Remotely sensed data

4.1.1 Landscape level changes

A range of lake surface area results for the entire study region, grouped by fuzzy membership threshold values and year, indicate an overall increasing trend (Figure 4.1). Mann-Kendall results indicate a statistically significant (p-value ≤ 0.05) positive trend for all three membership thresholds. With a Kendall's Tau value ranging between 0.615 and 0.692, there is a moderate correlation between lake area and time.

Examining the ≥0.5 membership results (Table 4.1), lake area ranges from 56,124 ha (or 5.7% of the total study area) in 1986 to a maximum of 106,711 ha (10.8% of the total study area) in 2007. Regional scale analysis shows that lake areal change is not uniform throughout the study area (Figure 4.2). This discrepancy is likely due to the greater number of lakes present in the northern and central regions of the study area (rows A-F in Figure 4.2), which averages 2,690 more lakes than the south (Table 4.1). Based on the Mann-Kendall test, thirty three of the 101 grid cells exhibit statistically significant change, all of which are associated with an increase in lake area. From 1986 to 2011, lake area within the statistically significant grid cells increased 8% to 1620% (p-value ≤ 0.05; minimum of 9 ha, maximum of 5,174 ha), with an average growth of 210% (1,122 ha). Kendall's Tau values ranged between 0.538 and 0.795.

Remotely sensed lake area results were compared to climate variables. Global summer (June-August) SSTAs correlate moderately well (0.582, p ≤ 0.05) with lake

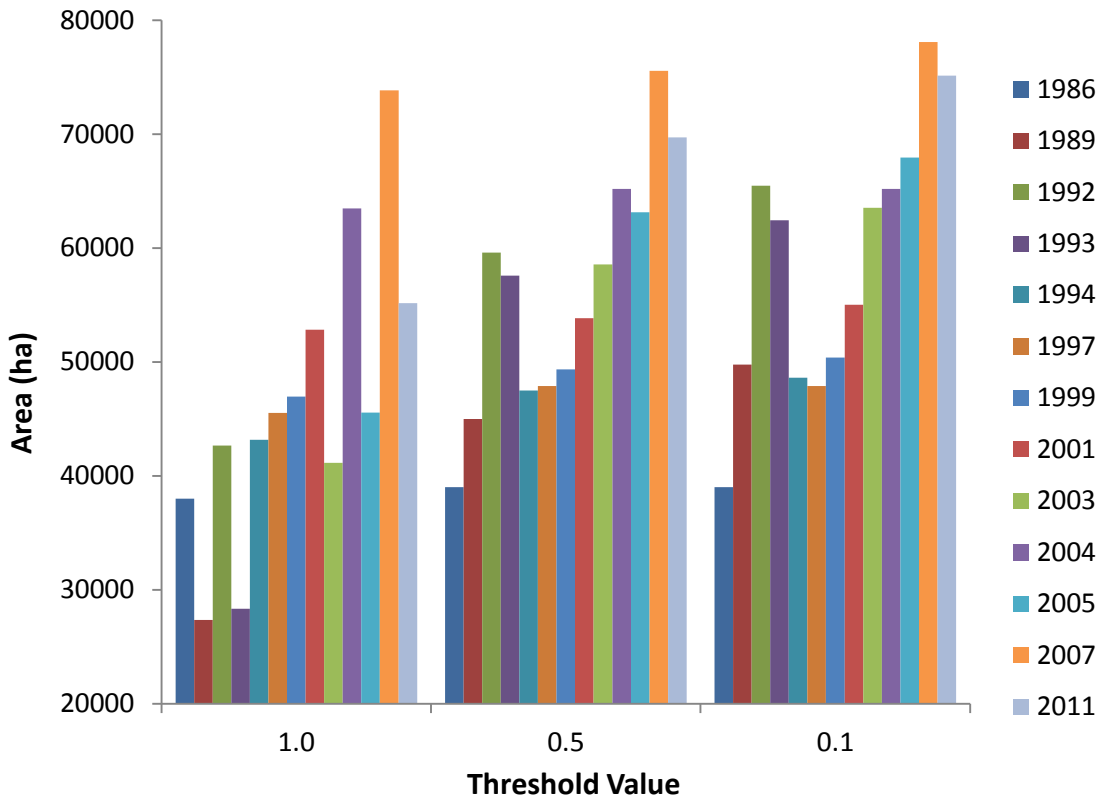

Figure 4.1. Total lake area (in hectares) within the study region. Results are grouped according to fuzzy membership threshold value.

Table 4.1. Summary of remote sensing analysis by region for ≥0.5 membership results.

	Overall Study Area			North/Central (rows A-F)			South (rows G-K)		
Year	# of Lake Objects	Area (ha)	% of Area	# of Lake Objects	Area (ha)	% of Area	# of Lake Objects	Area (ha)	% of Area
1986	3,577	56,124	5.7	3,151	50,197	8.4	426	5,927	1.5
1989	2,671	59,895	6.1	2,336	51,199	8.5	335	8,695	2.2
1992	3,200	77,564	7.9	2,810	66,952	11.2	390	10,612	2.7
1993	3,026	74,330	7.5	2,641	64,717	10.8	385	9,612	2.5
1994	1,815	59,573	6.0	1,611	51,811	8.6	204	7,761	2.0
1997	8,449	78,609	8.0	6,404	69,003	11.5	2,045	9,606	2.5
1999	3,211	65,974	6.7	2,841	59,125	9.9	370	6,849	1.8
2001	4,282	74,575	7.6	3,571	66,595	11.1	711	7,980	2.1
2003	3,017	76,078	7.7	2,657	66,531	11.1	360	9,548	2.5
2004	5,310	88,882	9.0	4,242	76,438	12.7	1,068	12,444	3.2
2005	3,472	81,401	8.2	2,988	70,409	11.7	484	10,993	2.8
2007	7,212	106,711	10.8	5,675	89,669	14.9	1,537	17,042	4.4
2011	3,135	87,804	8.9	2,748	73,111	12.2	387	14,692	3.8

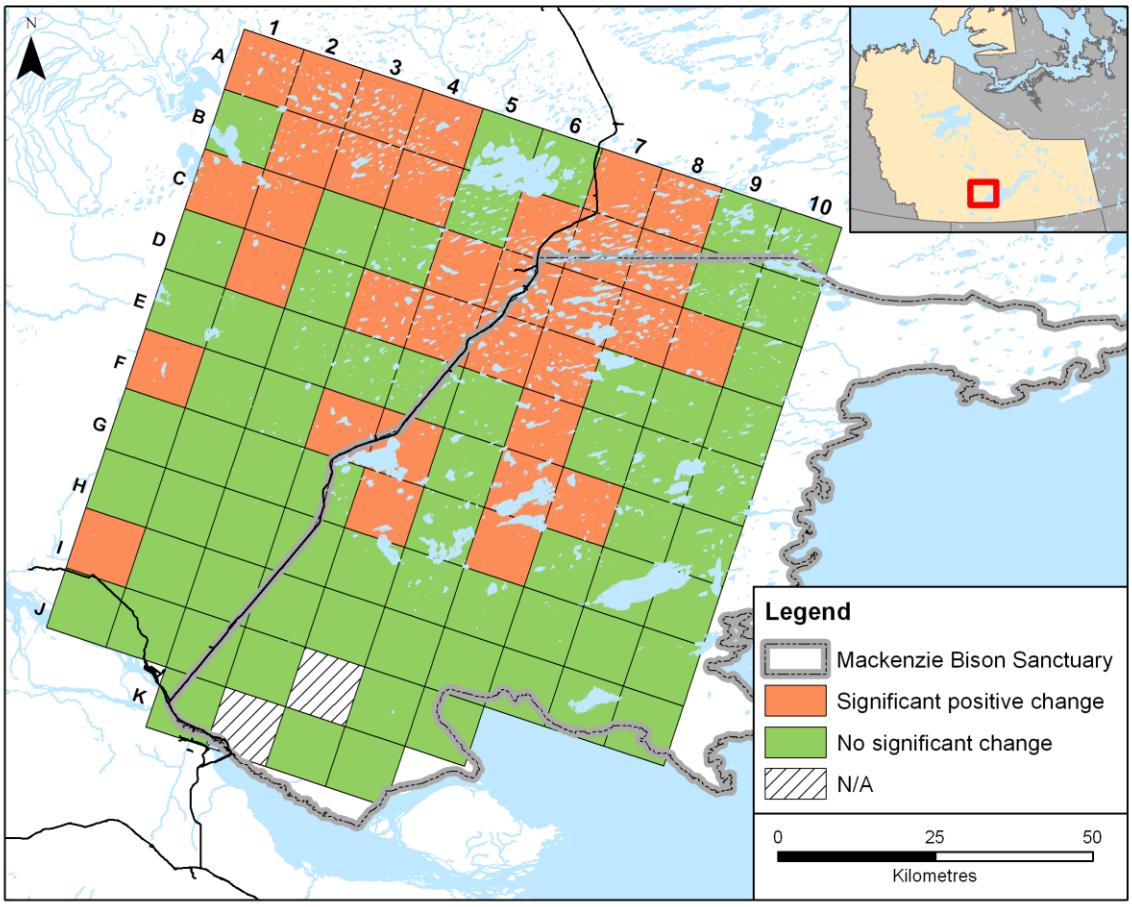

Figure 4.2. Grid map of the study area, highlighting areas of significant positive change (red) and non-significant change (green) in lake area. Significance was determined using the Mann-Kendall test statistic (p-value <0.05). N/A = Not Applicable, meaning no lakes are present within these grid cells.

growth in the study area, but July to October PNA values correlate best ($r = 0.649$, p-value ≤ 0.05; Figure 4.3).

Accuracy results for the classified data using the ≥0.5 fuzzy membership are high, with overall accuracy ranging between 80% and 99%. According to the user's accuracy results, the classification of water was more accurate than that of land. Consequently, in a two class map such as this, the producer's accuracy is inversely related (land is more accurately classified). The majority of erroneous pixels were located near the lake edge. Table 4.2 displays the overall accuracy and Kappa statistic (K) results.

4.1.2 Individual Lakes

To examine trends at a finer scale, remote sensing results related to Birch Lake, Boulogne Lake, Caen Lake, and Dieppe Lake were extracted and interpolated (Figures 4.4-4.7). Expansion rates for these lakes were estimated to be 4.25 ha/yr (0.2%/yr), 69 ha/yr (58%/yr), 63 ha/yr (3%/yr), and 83 ha/yr (12%/yr), respectively. It is important to note that Figures 4.4-4.7 are of varying scale, particularly Birch Lake and Boulogne Lake. Mann-Kendall results indicate that Caen Lake is the only study lake where the null hypothesis (that there is no statistically significant trend) can be rejected (p-value ≤ 0.05).

Birch Lake has an outlet to the south west, which may have contributed to its relatively stable water levels during the period of analysis. The three remaining lakes have experienced visually apparent lake growth, however even in low water level years, the extent of present lake levels are discernible via discolouration of the ground. This suggests that historical lake levels had previously reached current levels. Caen Lake and

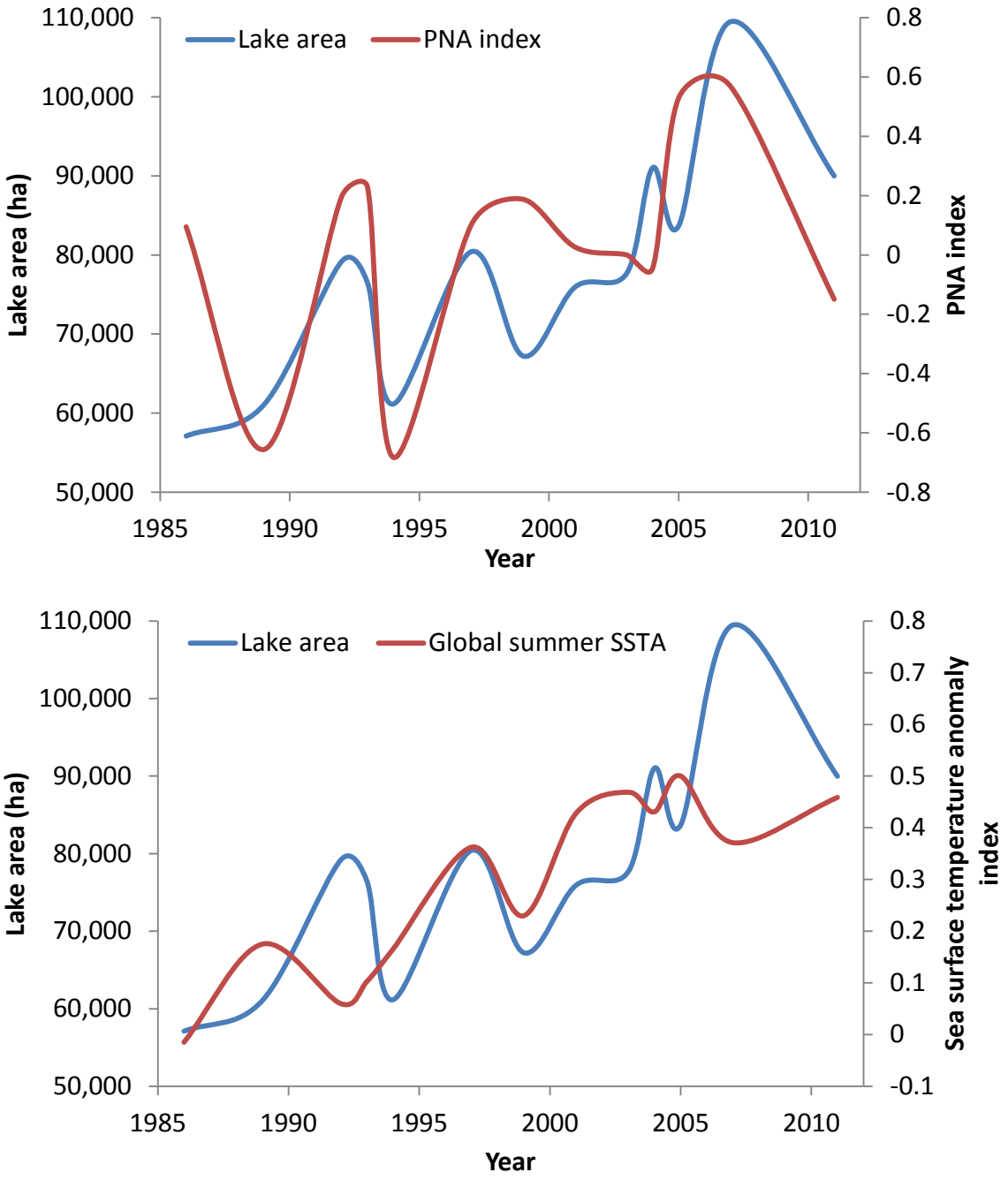

Figure 4.3. Lake area (blue) is correlated with (a) July to October Pacific North American pattern values (r = 0.649, p-value ≤ 0.05) and (b) global summer sea surface temperature anomalies (0.582, p ≤ 0.05).

Table 4.2. Summary of accuracy results by year (1986-2011). The table continues on the following two pages. K = Kappa statistic.

1986	Reference Total			
Remote Sensing Classification	Class	Water	Land	User's Accuracy
	Water	72	0	100
	Land	28	100	78
	Producer's accuracy	72	100	200

Overall accuracy = 86%, K = 0.72

1989	Reference Total			
Remote Sensing Classification	Class	Water	Land	User's Accuracy
	Water	91	0	100
	Land	9	100	92
	Producer's accuracy	91	100	200

Overall accuracy = 96%, K = 0.91

1992	Reference Total			
Remote Sensing Classification	Class	Water	Land	User's Accuracy
	Water	96	0	100
	Land	4	100	96
	Producer's accuracy	96	100	200

Overall accuracy = 98%, K = 0.96

1993	Reference Total			
Remote Sensing Classification	Class	Water	Land	User's Accuracy
	Water	98	0	100
	Land	2	100	98
	Producer's accuracy	98	100	200

Overall accuracy = 99%, K = 0.98

1994	Reference Total			
Remote Sensing Classification	Class	Water	Land	User's Accuracy
	Water	82	0	100
	Land	18	100	85
	Producer's accuracy	82	100	200

Overall accuracy = 91%, K = 0.82

Table 4.2 (Cont'd). Summary of accuracy results by year (1986-2011). The table continues on the following page. K = Kappa statistic.

1997	Reference Total			
Remote Sensing Classification	Class	Water	Land	User's Accuracy
	Water	60	0	100
	Land	40	100	71
	Producer's accuracy	60	100	200

Overall accuracy = 80%, K = 0.60

1999	Reference Total			
Remote Sensing Classification	Class	Water	Land	User's Accuracy
	Water	76	0	100
	Land	24	100	81
	Producer's accuracy	76	100	200

Overall accuracy = 88%, K = 0.76

2001	Reference Total			
Remote Sensing Classification	Class	Water	Land	User's Accuracy
	Water	74	0	100
	Land	26	100	79
	Producer's accuracy	74	100	200

Overall accuracy = 87%, K = 0.74

2003	Reference Total			
Remote Sensing Classification	Class	Water	Land	User's Accuracy
	Water	93	0	100
	Land	7	100	93
	Producer's accuracy	93	100	200

Overall accuracy = 97%, K = 0.93

2004	Reference Total			
Remote Sensing Classification	Class	Water	Land	User's Accuracy
	Water	82	0	100
	Land	18	100	85
	Producer's accuracy	82	100	200

Overall accuracy = 91%, K = 0.82

Table 4.2 (Cont'd). Summary of accuracy results by year (1986-2011). K = Kappa statistic.

2005	Reference Total			
Remote Sensing Classification	Class	Water	Land	User's Accuracy
	Water	93	0	100
	Land	7	100	93
	Producer's accuracy	93	100	200

Overall accuracy = 97%, K = 0.93

2007	Reference Total			
Remote Sensing Classification	Class	Water	Land	User's Accuracy
	Water	70	0	100
	Land	30	100	77
	Producer's accuracy	70	100	200

Overall accuracy = 85%, K = 0.70

2011	Reference Total			
Remote Sensing Classification	Class	Water	Land	User's Accuracy
	Water	91	0	100
	Land	9	100	92
	Producer's accuracy	91	100	200

Overall accuracy = 96%, K = 0.91

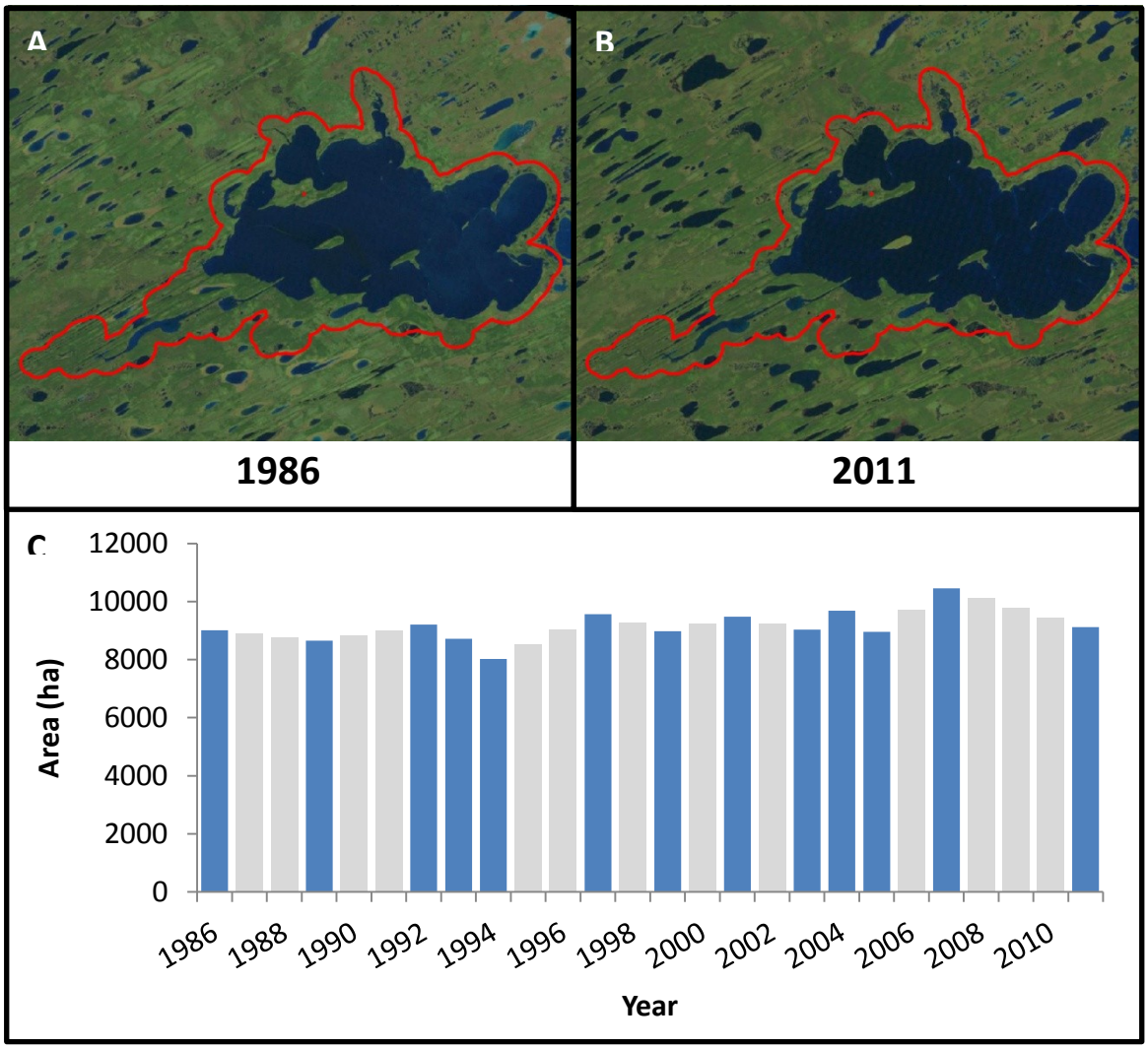

Figure 4.4. Birch Lake in (A) 1986 and (B) 2011. (C) Lake surface area results, in hectares, for the area of interest (red) are presented (bottom). Remote sensing results (blue) and interpolated values (grey) are shown. Map scale 1:140,000.

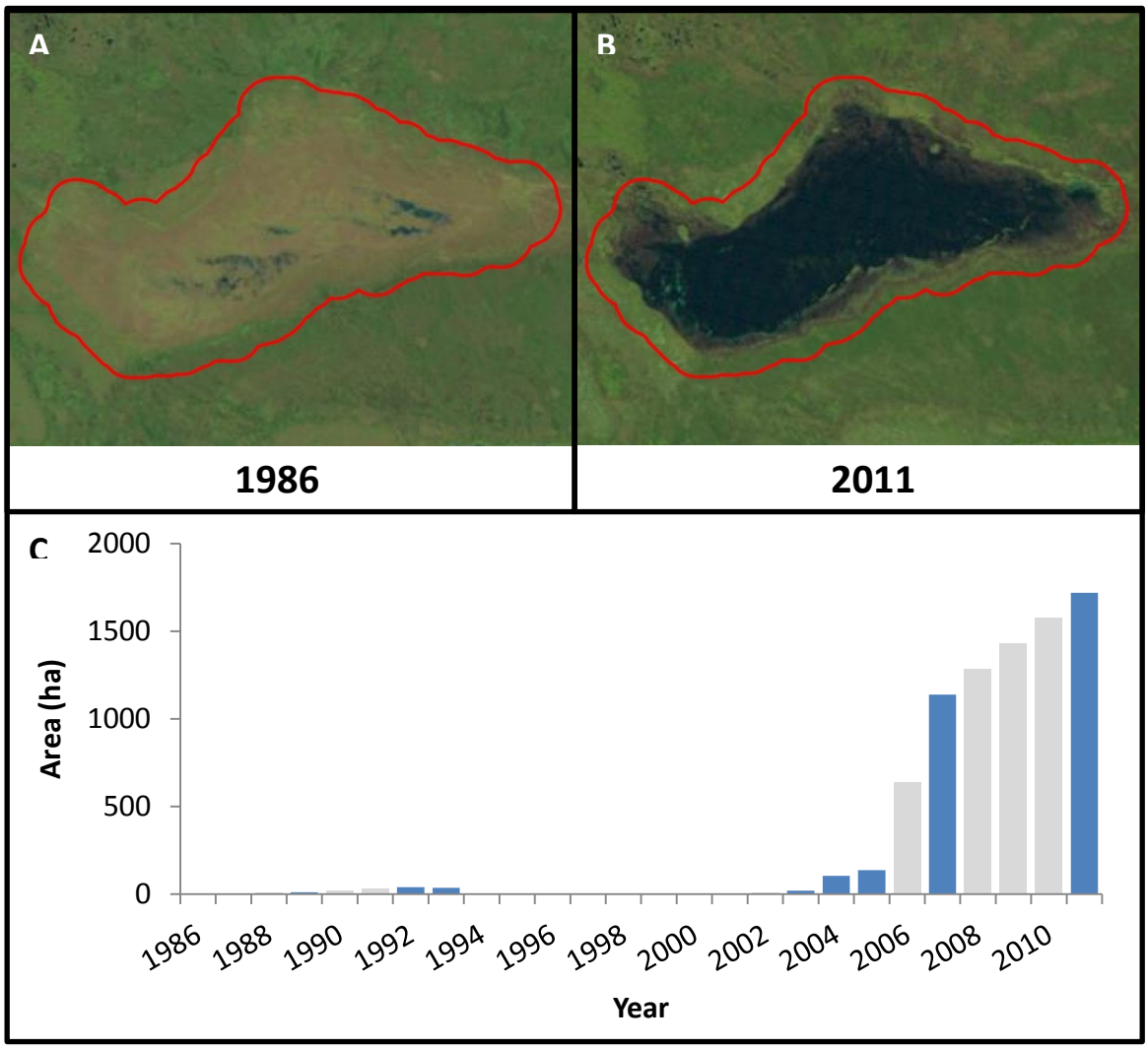

Figure 4.5. Boulogne Lake in (A) 1986 and (B) 2011. (C) Lake surface area results, in hectares, for the area of interest (red) are presented (bottom). Remote sensing results (blue) and interpolated values (grey) are shown. Map scale 1:56,000.

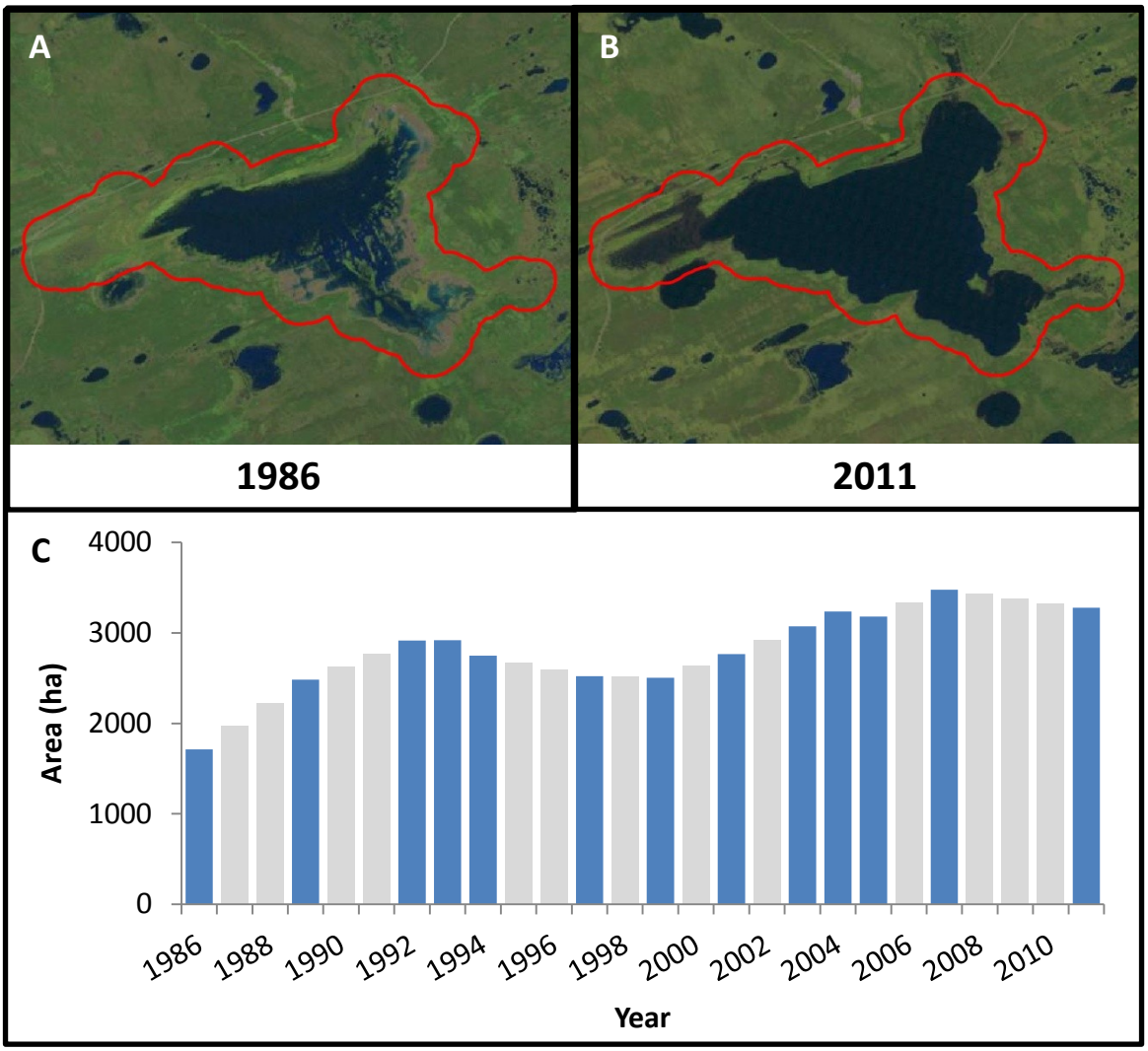

Figure 4.6. Caen Lake in (A) 1986 and (B) 2011. (C) Lake surface area results, in hectares, for the area of interest (red) are presented (bottom). Remote sensing results (blue) and interpolated values (grey) are shown. Map scale 1:85,000.

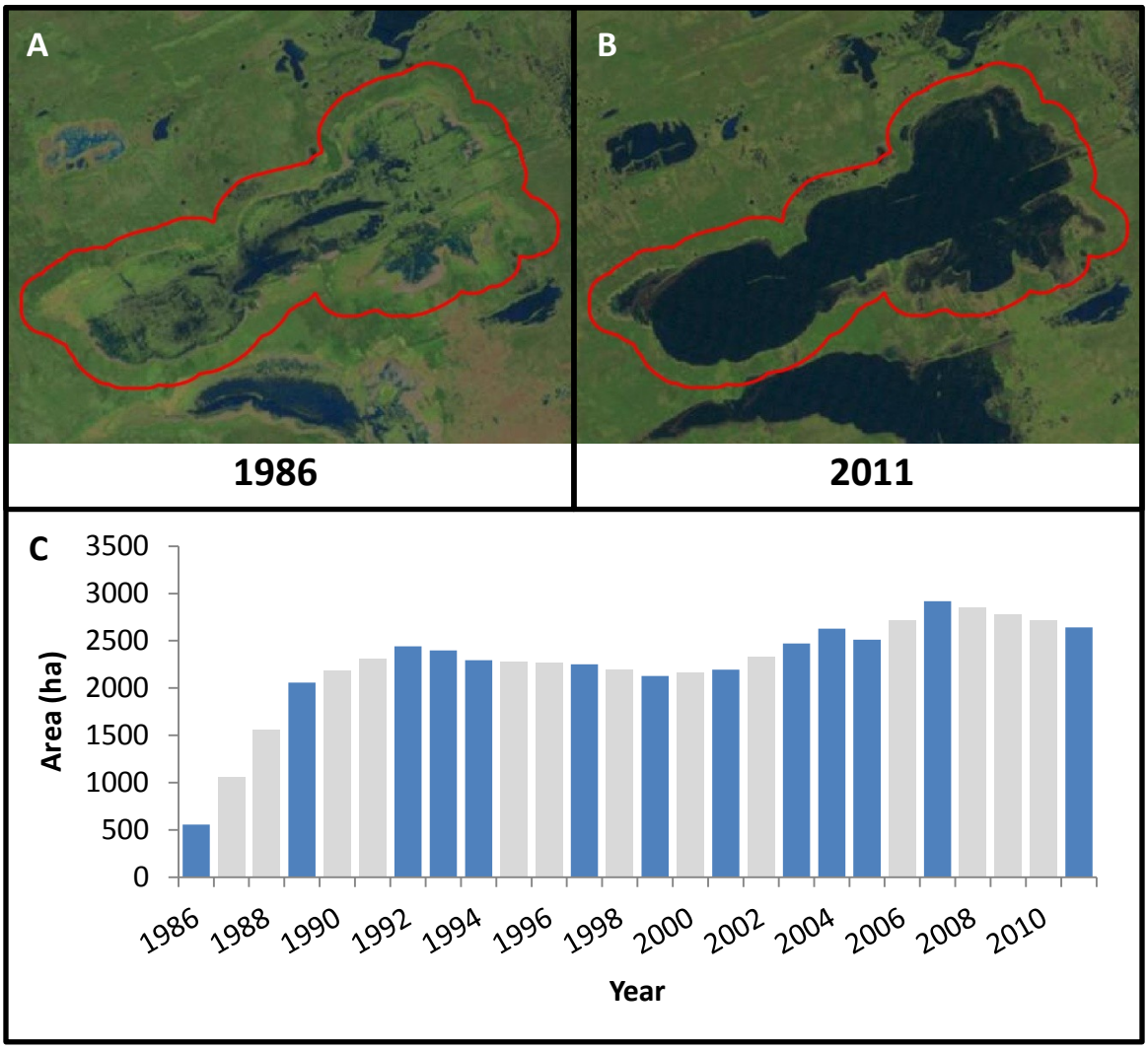

Figure 4.7. Dieppe Lake in (A) 1986 and (B) 2011. (C) Lake surface area results, in hectares, for the area of interest (red) are presented (bottom). Remote sensing results (blue) and interpolated values (grey) are shown. Map scale 1:69,000.

Dieppe Lake have followed an almost identical growth pattern. These lakes are geographically close to one another, suggesting growth may be controlled by the immediate environment.

4.2 Dendroclimatology

4.2.1 Site chronologies

The longest usable site chronologies for white spruce from this study date back to 1880 (sites FP06 and FP09) and 1864 for jack pine (sites FP06 and FP08). A chronology is only considered usable if the Expressed Population Signal (EPS) value is above 0.85 (Briffa and Jones, 1990) and more than one site chronology spans the given time period. EPS is one of the resulting statistical outputs of ARSTAN and provides a quality measure of the chronologies. FP01 was excluded from further analysis due to low EPS values (1820-1920 EPS < 0.85, with a minimum of 0.5), while the periods of analysis for the remaining sites were shortened to varying degrees (Table 4.3).

4.2.2 Assessing similarities of growth trends between site chronologies

In combination with site correlations (Table 4.4), a Principal Component Analysis (PCA) was conducted to determine which sites to include in the regional chronology. Site correlations varied widely and PCA plotting clustered in multiple groups (Figure 4.8). White spruce sites FP03, FP10, FP11, FP14, and FP16 encompass the largest group, with sites FP02/FP05 and FP06/FP09 the least similar. PC1 explains 52% of the variance for white spruce sites, and was compared to climate variables (Table 4.5). PC1 correlates

Table 4.3. Summary of data used to develop site chronologies. Usable series is determined by EPS being greater than 0.85.

Site Code	# of Series	# of trees	Series Inter-correlation	Mean Measurement (mm)	Mean Sensitivity	Series Length	Usable Series	# of Usable Years	Autocorrelation
WHITE SPRUCE									
FP01	34	18	.453	.27	.205	1731-2010	Not usable	-	.869
FP02	60	30	.660	.96	.175	1920-2010	1930-2010	81	.778
FP03	60	31	.683	.95	.229	1908-2010	1923-2010	88	.775
FP05	51	26	.602	1.00	.164	1927-2010	1932-2010	79	.810
FP06	44	25	.497	.38	.189	1718-2010	1880-2010	131	.863
FP09	62	34	.656	.71	.201	1796-2010	1880-2010	131	.826
FP10	60	31	.729	.92	.236	1885-2010	1917-2010	94	.841
FP11	40	20	.701	1.03	.236	1890-2010	1915-2010	96	.720
FP14	58	29	.619	.74	.200	1879-2010	1897-2010	114	.818
FP16	44	22	.702	1.25	.219	1922-2010	1930-2010	81	.789
JACK PINE									
FP05	78	39	.595	.67	.213	1930-2010	1938-2010	73	.935
FP06	20	10	.647	.43	.236	1861-2010	1864-2010	147	.867
FP08	57	30	.679	.39	.347	1852-2008	1864-2008	145	.750
FP11	56	28	.695	.54	.282	1873-2010	1877-2010	134	.806
FP12	43	22	.619	.57	.229	1874-2010	1876-2010	135	.895
FP13	54	30	.605	.91	.210	1895-2010	1898-2010	113	.867
FP15	56	29	.629	.93	.211	1926-2010	1928-2010	83	.932

Table 4.4. Correlation matrix between site chronologies of white spruce (top) and jack pine (bottom).

WHITE SPRUCE									
	FP02	FP03	FP05	FP06	FP09	FP10	FP11	FP14	FP16
FP02	1	.419**	.807**	-.006	.013	.567**	.466**	.436**	.329**
FP03	.419**	1	.367**	.256*	.494**	.669**	.304**	.585**	.717**
FP05	.807**	.367**	1	-.200	-.170	.415**	.296**	.435**	.070
FP06	-.006	.256*	-.200	1	.705**	.268**	.276**	.441**	.318**
FP09	.013	.494**	-.170	.705**	1	.534**	.198	.664**	.482**
FP10	.567**	.669**	.415**	.268**	.534**	1	.443**	.691**	.573**
FP11	.466**	.304**	.296**	.276**	.198	.443**	1	.335**	.588**
FP14	.436**	.585**	.435**	.441**	.664**	.691**	.335**	1	.348**
FP16	.329**	.717**	.070	.318**	.482**	.573**	.588**	.348**	1

JACK PINE							
	FP05	FP06	FP08	FP11	FP12	FP13	FP15
FP05	1	.232*	.207	.627**	.542**	.517**	.571**
FP06	.232*	1	.629**	.185*	.170*	.078	.089
FP08	.207	.629**	1	.164	.092	.220*	.101
FP11	.627**	.185*	.164	1	.690**	.587**	.323**
FP12	.542**	.170*	.092	.690**	1	.683**	.389**
FP13	.517**	.078	.220*	.587**	.683**	1	.438**
FP15	.571**	.089	.101	.323**	.389**	.438**	1

* = Correlation is significant at the 0.05 level (2-tailed).

** = Correlation is significant at the 0.01 level (2-tailed).

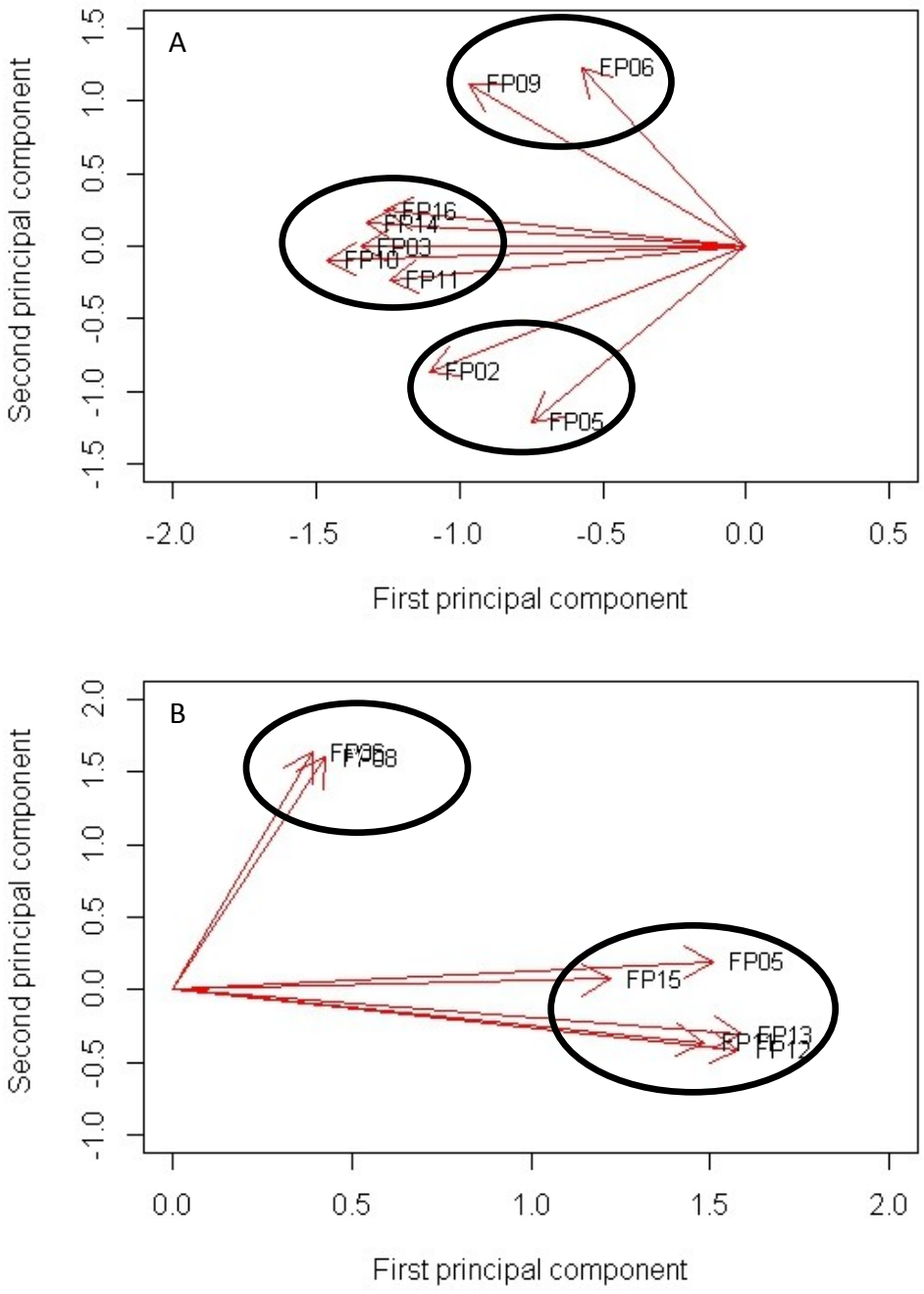

Figure 4.8. Principal Component Analysis results for (A) white spruce and (B) jack pine. Black circles indicate sample site groupings used for individual regional chronologies.

Table 4.5. Correlation between the first and second white spruce and jack pine Principal Components and selected climate variables. Only significant relations are shown.

	WS-PC1	WS-PC2	JP-PC1	JP-PC2
Maximum Temperature				
January				.237*
June	.369**			
November	.299*			
December		-.384**		.227*
Mean Temperature				
January				.219*
June	.298*			
November	.314*			
December		-.399**		.225*
Minimum Temperature				
November	.320*			
December		-.409**		
Precipitation				
February				-.233*
May				.259*
June	-.302*			.240*
October	-.326*			
December	-.334*		.243*	

* = Correlation is significant at the 0.05 level (2-tailed).

** = Correlation is significant at the 0.01 level (2-tailed).

weakly (r = 0.369, p-value ≤ 0.01) with maximum June temperatures (Figure 4.9). Jack pine sites FP06 and FP08 are least similar to the remaining jack pine sites (FP05, FP11, FP12, FP13, and FP15). PC1 explains 50% of the variance in jack pine sites, but correlations with climate variables were weak and were not interpreted further.

4.2.3 Tree ring chronologies

Due to low inter-site correlation, three White Spruce Average Chronologies (WSAC; Figure 4.10) and two Jack Pine Average Chronologies (JPAC; Figure 4.11) were initially created. These average chronologies were then compared against one another to develop a regional chronology. WSAC 1 did not correlate well with WSAC 2 or WSAC 3 (r = -0.11 and 0.36 respectively) and was not studied further, however WSAC 2 and WSAC 3 were highly correlated with one another (r = 0.75, p-value ≤0.01). Additionally, two existing tree ring datasets by Schweingruber (Bras d'Or Lake (SBL; n.d.[a]) and Fort Providence (SFP; n.d.[b])) were downloaded from the ITRDB. SFP and SBL are white spruce series, covering a time period of 1829-1988 and 1795-1988. SFP and SBL correlated moderately well with WSAC 2 and WSAC 3 (r = 0.61 and 0.62, and 0.59 and 0.62 respectively, p-value ≤ 0.01). As a result, a decision was made to combine these four chronologies (WSAC 2, WSAC 3, SFP, and SBL) into a single White Spruce Regional Chronology (WSRC; Figure 4.12) by averaging all chronologies equally. Correlations between JPAC 1 and JPAC 2 were low (r = 0.17); only JPAC 2 was used to create the Jack Pine Regional Chronology (JPRC; Figure 4.12).

Regional chronologies were tested against climatic variables (including at lagged time intervals). Correlations are generally weak, but diverse, suggesting that tree growth

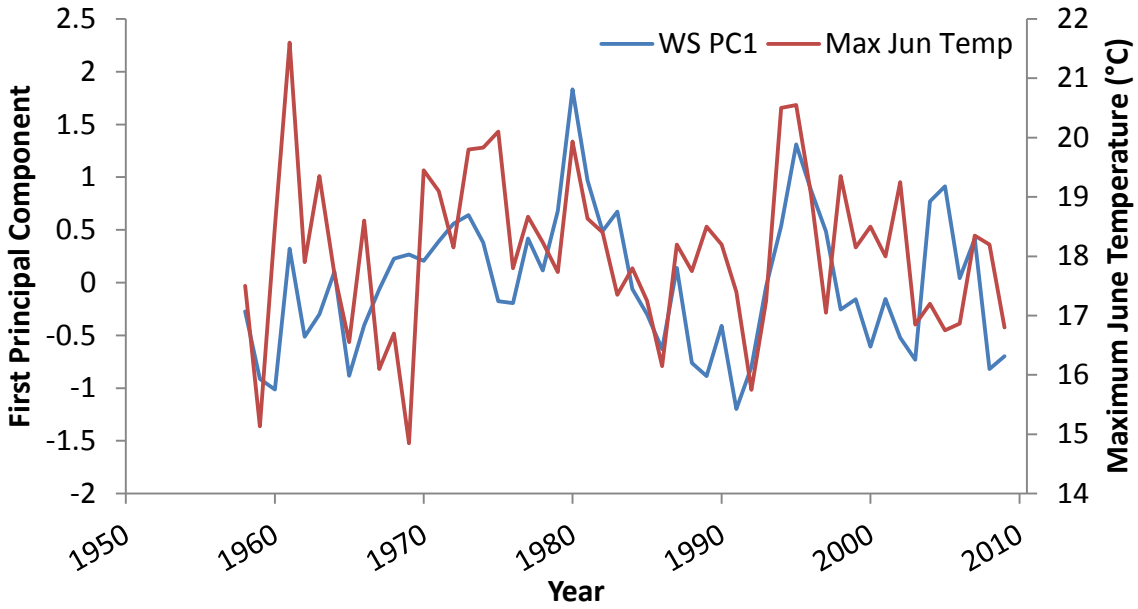

Figure 4.9. Comparison of Principal Component 1 of white spruce sites to maximum June temperatures.

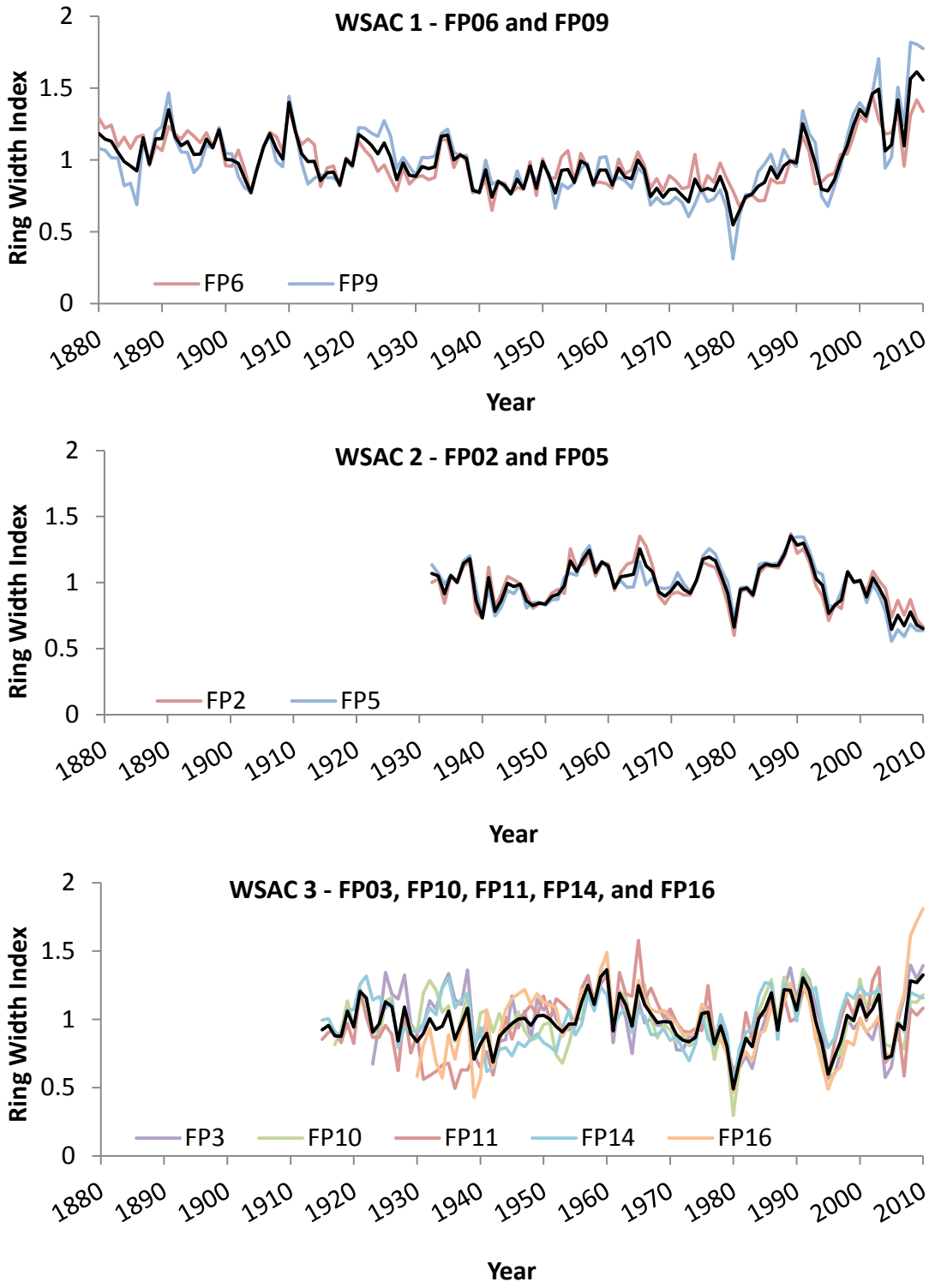

Figure 4.10. White spruce site chronologies (coloured lines) used to create the White Spruce Average Chronologies (WSAC; black line).

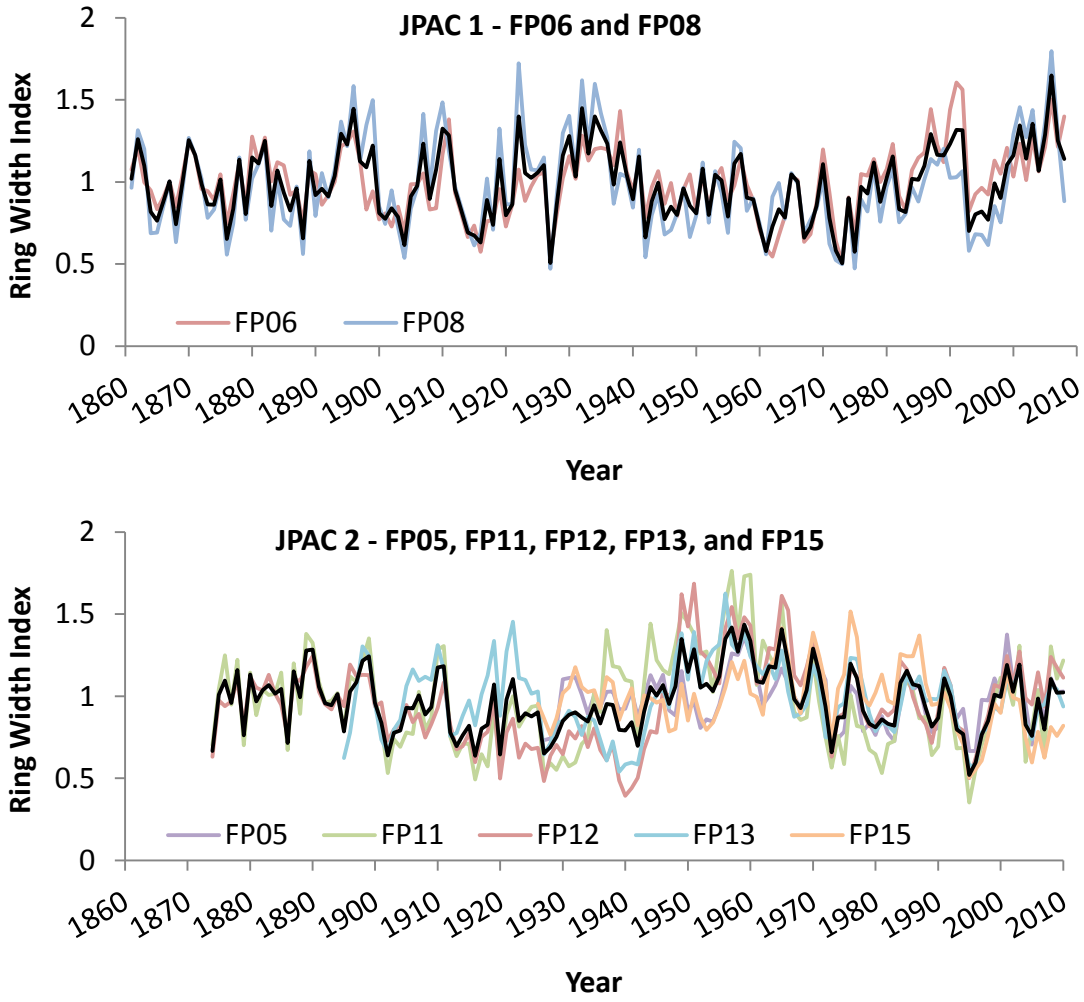

Figure 4.11. Jack pine site chronologies (coloured lines) used to create the Jack Pine Average Chronologies (JPAC; black line).

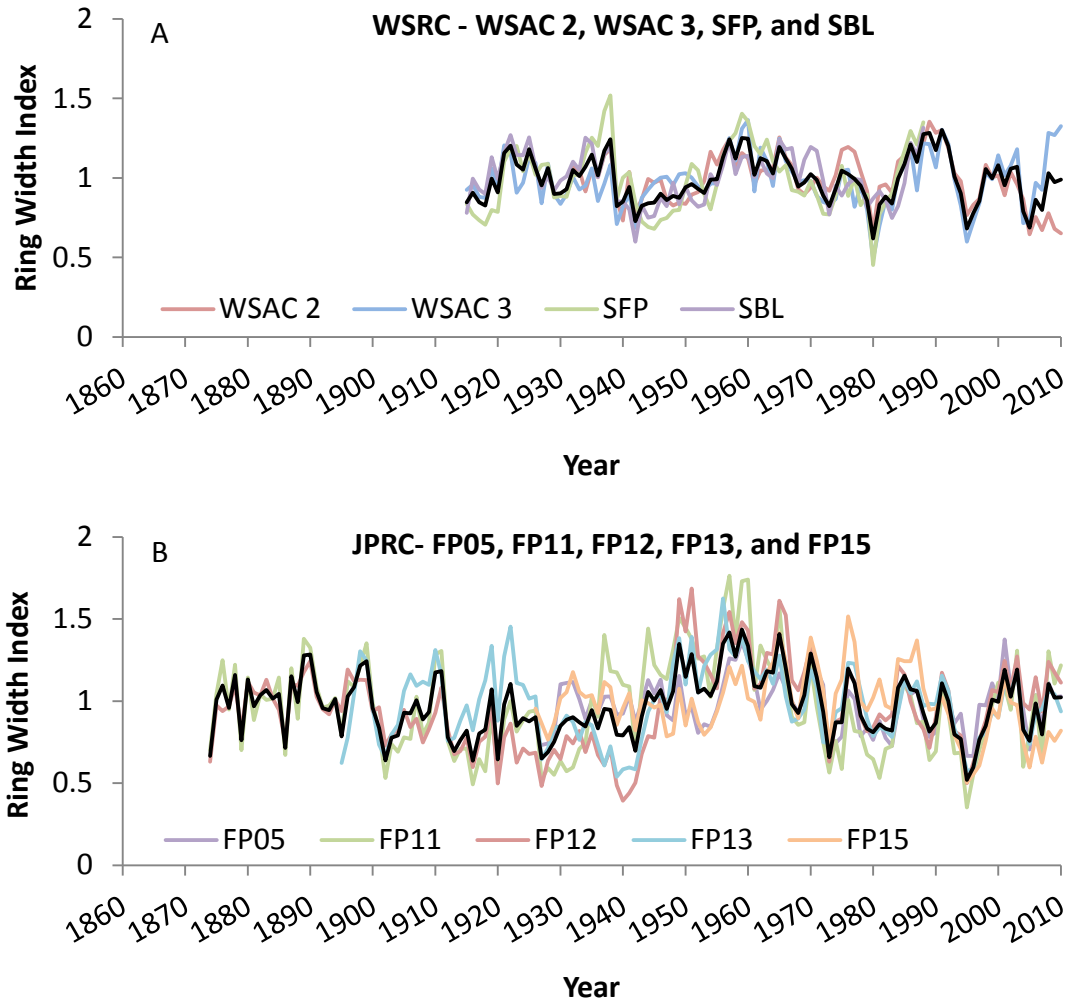

Figure 4.12. Regional chronologies (black line) for (A) white spruce and (B) jack pine.

was influenced by more than one limiting growth factor. WSRC negatively correlated with November maximum temperatures (r = -0.22, p-value ≤ 0.05), November minimum temperatures (r = -0.27, p-value ≤ 0.01), and October mean temperatures (r = -0.24, p-value ≤ 0.05), but is positively correlated with June (r = 0.28, p-value ≤ 0.01), July (r = 0.21, p-value ≤ 0.05), and December (r = 0.27, p-value ≤ 0.01) precipitation. JPRC correlates negatively but weakly with February maximum and mean temperatures (r = -0.23 and -0.19 respectively, p-value ≤ 0.05), but positively with June minimum temperatures (r = 0.21, p-value ≤ 0.05). JPRC also correlates weakly with large scale systems such as Arctic Oscillation and Pacific Decadal Oscillation (r = -0.30 and -0.31 respectively, p-value ≤ 0.05) as well as Pacific sea surface temperature anomalies (r = 0.26, p-value ≤ 0.05). All statistically significant correlations are presented in Table 4.6. As a general guide, Dancey and Reidy (2004) suggest that correlations of 0.4 to 0.6 should be considered as moderately associated. Anything less than 0.4 is considered a weak correlation and may have limited utility (Dancey and Reidy, 2004). As a result, only the WSRC/PDSI relation was examined further. WSRC correlates moderately well with PDSI (r = 0.49, p-value ≤ 0.01), following the low frequency trend of the data, while also capturing important high frequency events (such as a major dry year in 1980).

Based on the WSRC/PDSI relation, a model (Equation 4.1) was developed using linear regression in order to reconstruct PDSI:

$$y = 4.8375(x) - 4.8112 \qquad \textit{(Eq. 4.1)}$$

where y is the PDSI value for year t and x is the ring width of the regional chronology in year t.

Table 4.6. Correlation between the white spruce and jack pine regional chronologies and selected climate variables. Only significant relations are shown.

	WSRC	JPRC
Maximum Temperature		
February		-.233*
November	-.218*	
Mean Temperature		
February		-.191*
October	-.241*	
Minimum Temperature		
June		.213*
November	-.268**	
Precipitation		
June	.282**	
July	.213*	
December	.271**	
Palmer Drought Severity Index		
Grid Point 49	.490**	
Grid Point 50	.332**	
Teleconnection Patterns		
AO		-.304*
PDO		-.305*
Pacific SSTAs		
Year		.259*
Winter (DJF)		.238*
Spring (MAM)		.236*

* = Correlation is significant at the 0.05 level (2-tailed).

** = Correlation is significant at the 0.01 level (2-tailed).

Model testing suggests that the equation used produces a skilled model (p-value ≤0.05, RE >0.1, and CE >0.1; Figure 4.13). Reconstructed results correlate moderately with actual PDSI values for the full calibration period (r = 0.49, p-value ≤ 0.01) and sign test results (51 agreements, 25 disagreements) were also significant (p-value ≤ 0.05), indicating the agreement between variables is not a result of chance. Correlation, RE, and CE values for the early verification period (1915-1952) and late verification period (1953-1990) also strengthen confidence in the model (r = 0.53 and 0.44, RE = 0.33 and 0.23, CE = 0.28 and 0.19, respectively). As mentioned previously, positive RE and CE values indicate a skilled model.

Important aspects of the low frequency trend are retained in the reconstruction (Figure 4.13): a shift from positive to negative PDSI values in the late 1930s, high values in 1938 and 1988, and low values in 1942 and 1980. The PDSI reconstruction indicates that, on average, climate conditions in the MBS have remained stable between 1915 and 2011. Although there appears to be an almost cyclical pattern from 1940-1980, the reconstruction does not extend far enough back in time to make a definite conclusion regarding such claims. What is of great interest is the increase in variability in both the reconstructed and actual data (Figure 4.14). This indicates that dry years are becoming increasingly drier, while wet years are becoming gradually more wet.

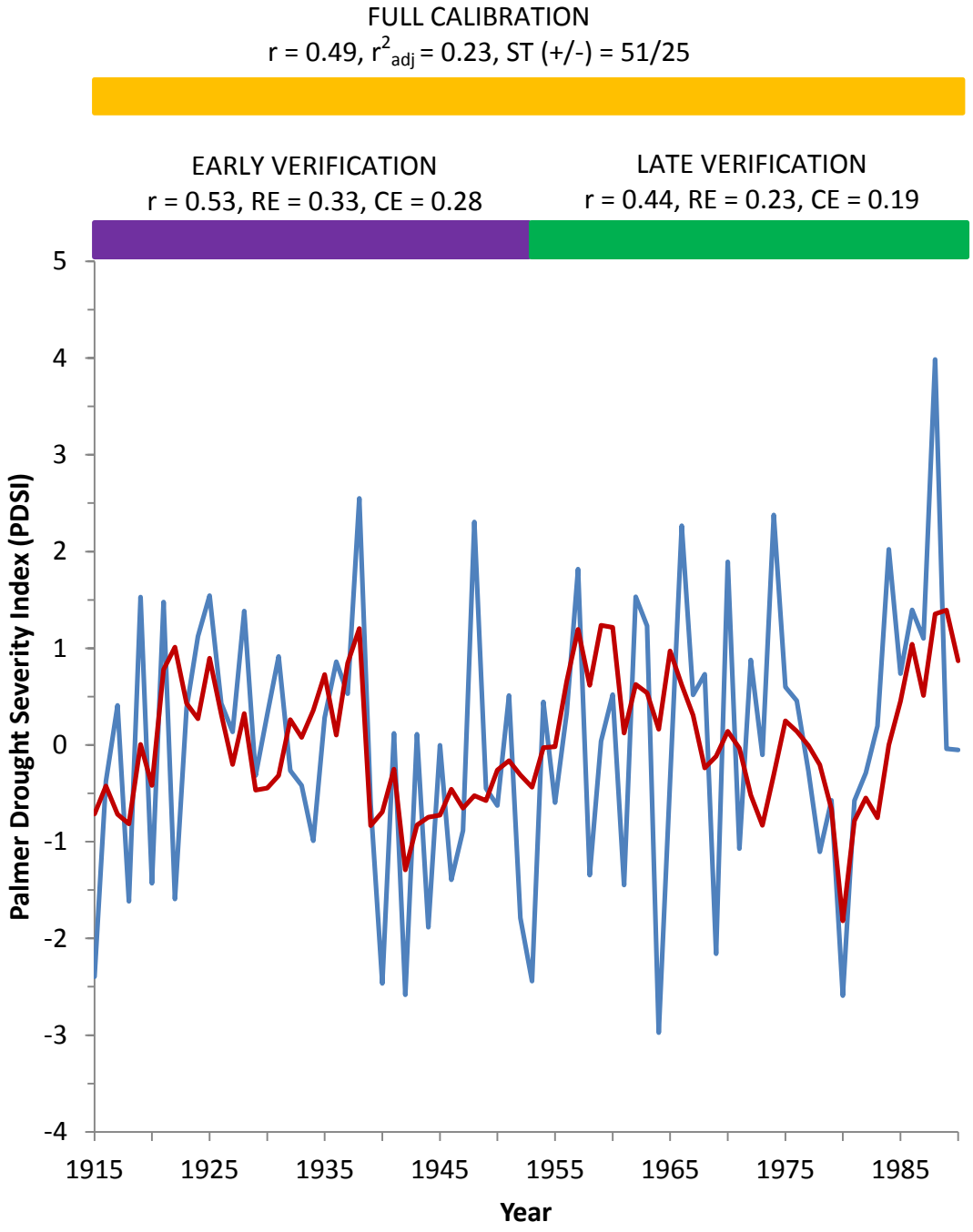

Figure 4.13. Reconstructed Palmer Drought Severity Index (PDSI) values (red) compared to calculated PDSI values (blue). The Sign Test results are statistically significant (p-value ≤ 0.05).

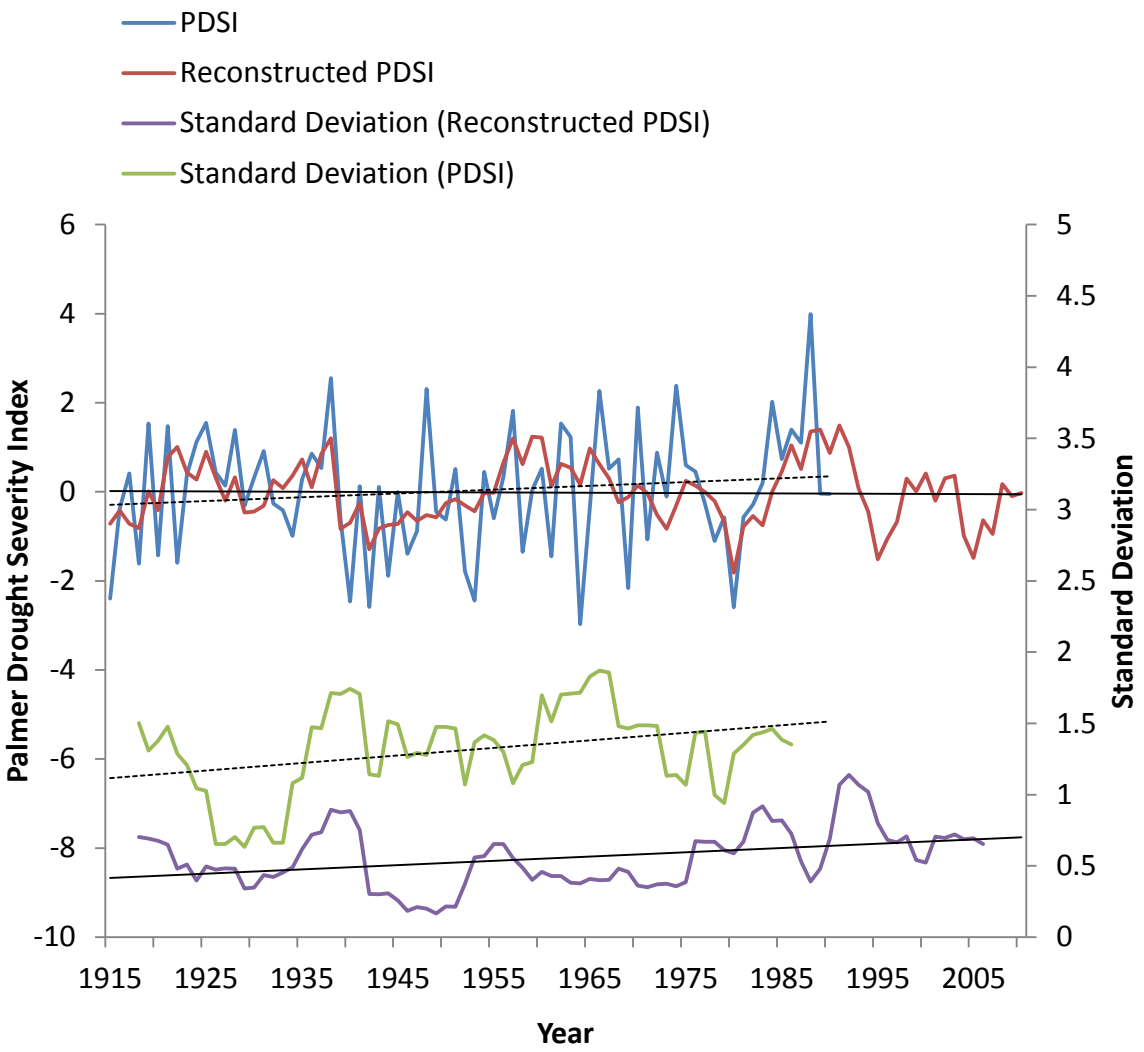

Figure 4.14. Reconstructed PDSI values (blue) show the overall climate average has been constant between 1915 and 2010. Variability (red) has increased.

CHAPTER 5
DISCUSSION

5.1 Remotely sensed data

5.1.1 Lake area

Recent studies examining lake area change in high latitude, discontinuous permafrost regions have regularly observed overall declining surface area (Labrecque et al., 2009; Roach et al. 2013). This does not appear to hold true in the MBS and surrounding area, where total lake area has either increased at a statistically significant pace, or has experienced no significant change; a result consistent with coarse scale analysis by Carroll et al. (2011). The majority of significant lake area change has occurred in the northern and central areas of the study region, both inside and outside of the MBS. While lake expansion may actually increase the surface area of wet meadows (the preferred habitat of wood bison; Larter and Gates, 1990), evidence indicates that wood bison are migrating due in part to the flooding (ENR GNWT, 2010). If lake expansion is contributing to bison movement, this is potentially a major problem, as remote sensing results suggest that lakes are expanding in a way that would direct bison south towards the Bison Control Area. The limited number of lakes in the southern MBS may result in an insufficient supply of wet and mesic meadows (preferred habitat locations for wood bison), further exasperating the problem as wood bison continue to seek out more suitable habitat. Therefore, it is important to address the results presented above, understanding what the implications of the findings are and how they relate to management of the Mackenzie herd.

The distribution of statistically significant growth, or lack thereof, in the southern MBS may appear surprising, as there is at least one clear example of drastic change (Boulogne Lake). While it has been suggested that Mann-Kendall results are susceptible to underestimating significance in small spatial scale conditions (Good and Lowe, 2006), the omission of these areas, at least in the case of Boulogne Lake, is likely related to the rapid and very recent acceleration of lake growth. In this case, of the 13 years of observation, only two, 2007 and 2011, exhibit large surface area differences; the majority of observations indicate very small surface area changes (Figure 4.4). As discussed, the Mann-Kendall statistic is not only used to test for differences, but how differences occur over time. Additionally, one of the primary benefits of the Mann-Kendall test is that calculations are minimally impacted by outliers. It appears that the 2007 and 2011 measurements of Boulogne Lake are treated as an anomaly, not representative of a change in conditions. As a result, lake expansion is likely more prevalent than indicated by the results of this study.

5.1.2 Atmospheric patterns

Years of larger lake area correspond to years dominated by positive July to October PNA values (and, to a lesser degree, warmer global summer SSTAs; Figure 4.3). This suggests that lake level variability is associated, at least to some degree, to the changing weather patterns delivered by the PNA. PNA has experienced an overall trend towards more

positive conditions since 1950 (Figure 5.1). Similarily, the Intergovernmental Panel for Climate Change (IPCC) reports that global SSTs have also increased in recent decades (Figure 5.2), a trend which is "virtually certain to rise significantly" in the future (Nicholls et al., 2007, p. 323). These estimates indicate a trend of warmer temperatures and less precipitation in the study area. This makes understanding lake growth less clear, suggesting two possibilities (1) lake growth is not a direct result of an increase in precipitation, or (2) large scale systems such as PNA and SSTAs are not appropriate for capturing regional climatic variability.

Spence and Rausch (2005) studied atmospheric patterns at a more regional scale and found that large scale systems in themselves may not be a reliable indicator of weather conditions. Using daily surface weather maps, they identified seven synoptic patterns for the Yellowknife region (Figure 5.3) and discovered that the low pressure cyclones, dependant on the Aleutian low, accounted for the majority of rainfall. The Aleutian low is a semi-permanent atmospheric pressure system in the North Pacific, which varies in intensity and, although typically centers near the Aleutian Islands, can vary in location (Rodionov et al., 2007). The Aleutian low influences the interaction between northern and tropical air masses in the Pacific; during strong Aleutian lows, warm, moist air from the tropics is pulled northward to polar regions (Zhu et al., 2007). Spence and Rausch (2005) discovered that low pressure cyclones often developed 2-4 days after an intense Aleutian low. Although the intensity and duration of the Aleutian low remained comparable between years of study, the frequency of low pressure cyclones was reduced by 50%, impacting precipitation levels (from 68.3mm in 1998 to

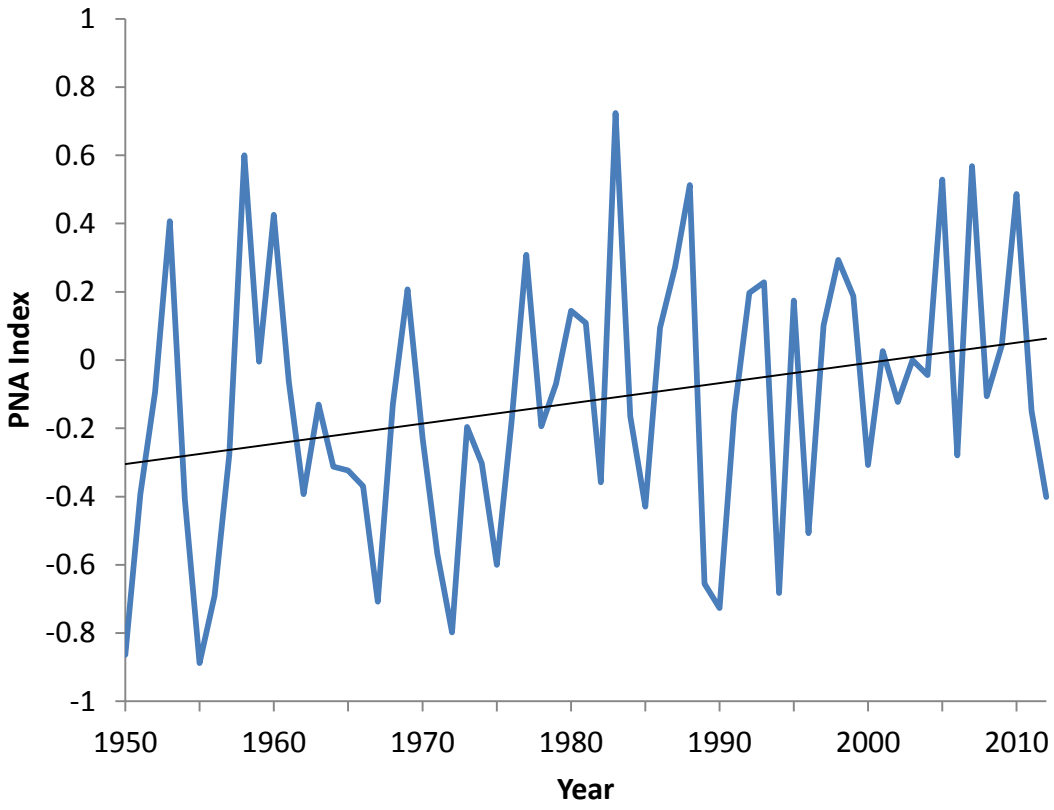

Figure 5.1. Historical PNA index values (1950-2012). Indices are relative to the 1981-2010 normal. Data from http://www.cpc.ncep.noaa.gov/data/teledoc/pna.shtml.

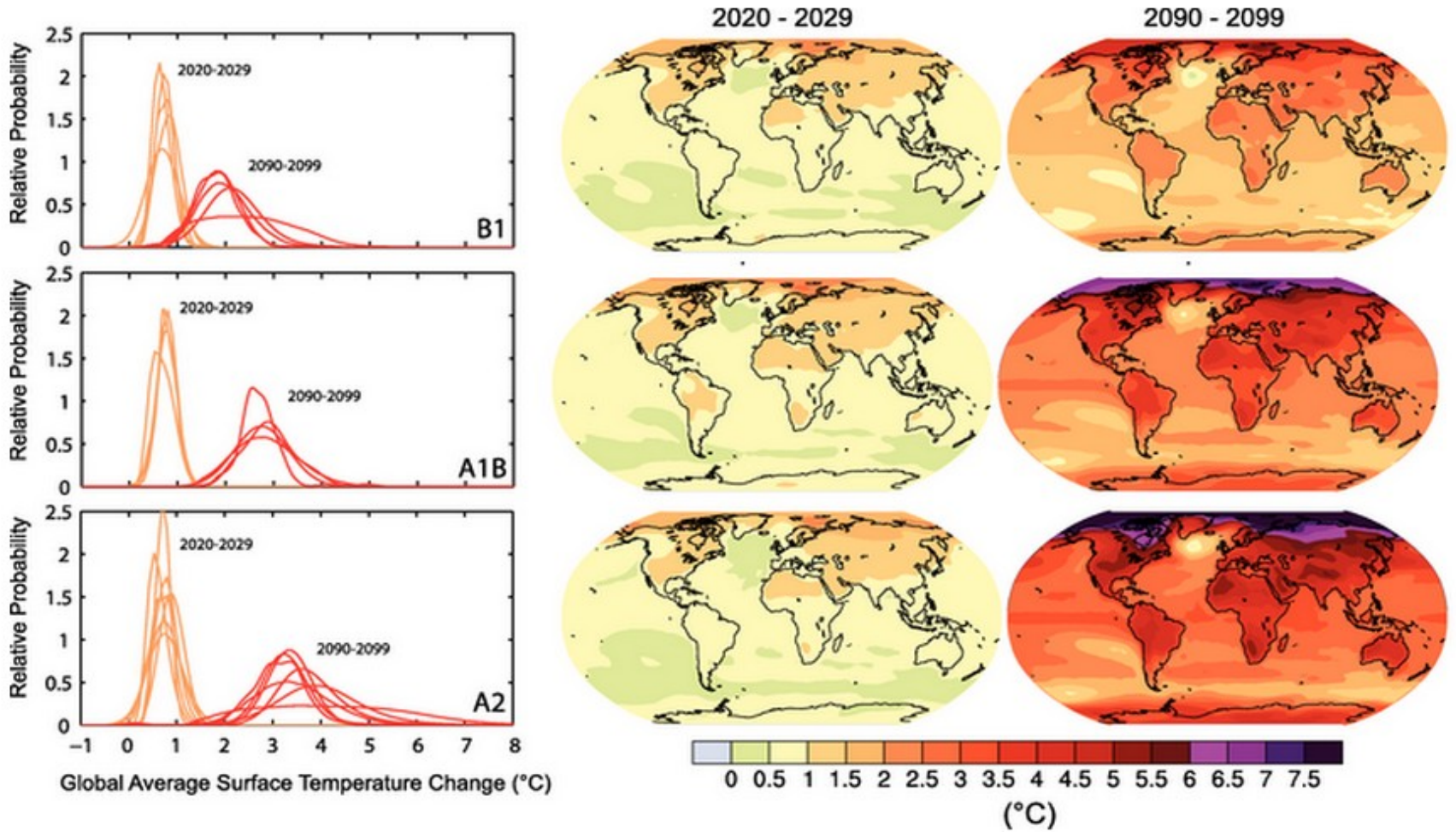

Figure 5.2. Predicted global surface temperature changes (both sea surface and land). Image from the Intergovernmental Panel on Climate Change [IPCC], (Nicholls et al., 2007).

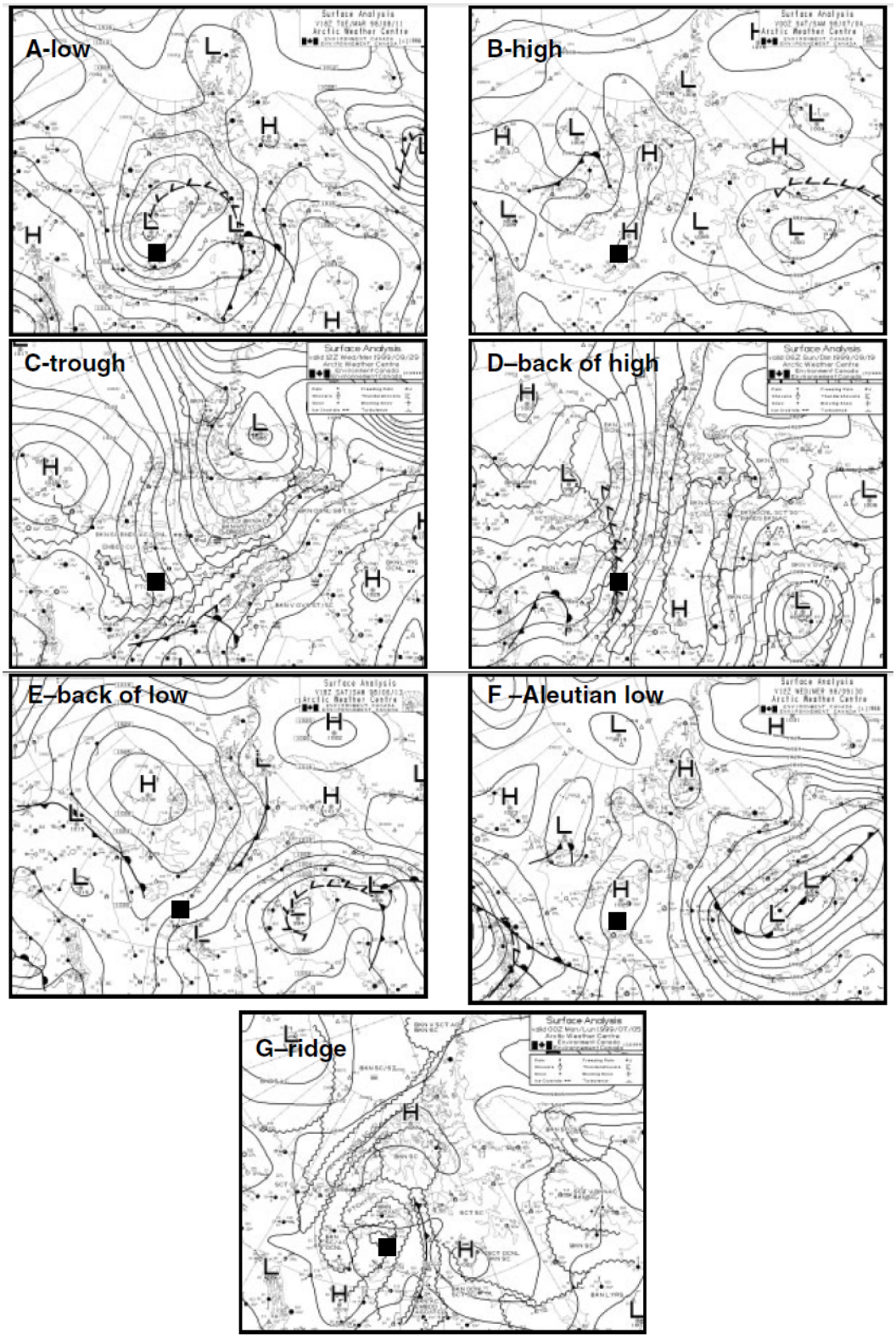

Figure 5.3. Seven synoptic patterns identified by Spence and Rausch (2005). Image from Spence and Rausch (2005).

46.7mm in 1999). The reduction in cyclone development was thought to be caused by a southern shift in the Aleutian low, where moist air, striking mountain ranges in coastal British Columbia, dissipated before having a chance to move north. As a result, Spence and Rausch (2005) concluded that while large scale systems such as the Aleutian low are important for cyclogenesis, regional mechanisms which modify cyclone development are equally important.

While it is clear that large scale atmospheric patterns can provide insight into climatic parameters which affect lake level fluctuations, the regional climatic conditions associated with a particular atmospheric pattern can be highly variable. Therefore, it is important to examine specific environmental variables directly (such as temperature and precipitation) in order to develop a true understanding of the long-term climate variability in a particular study area. Furthermore, as mentioned previously, lake area variability in the study region is not typical of results commonly reported in the literature. As a result, a large scale system such as the PNA may not provide sufficient insight as to what is affecting lake growth in and around the MBS.

5.2 Dendroclimatology

Typically, tree ring chronologies are associated with a particular climate variable such as temperature or precipitation (D'Arrigo et al., 2009; Pisaric et al., 2009; Luckman and Wilson, 2005; Case and MacDonald, 1995). In the MBS however, neither temperature nor precipitation records are individually highly correlated with any of the tree ring chronologies. This suggests that tree growth is affected by other critical limiting factor(s) and, as such, the identification of a single causal factor related to lake

expansion is probably not possible. Still, PDSI, which combines aspects of both temperature and precipitation, allows for the observation of general trends. PDSI results suggest that climate conditions have become more variable in recent years. If this trend continues, it poses a potential problem for managing the MBS herd, as climatic conditions become not only more extreme, but more extreme in both conditions. Other studies have observed or predicted an increase in intensity of the water cycle (Huntington, 2006); as temperatures continue to rise in northern Canada, water vapour is expected to increase. As a result, a greater amount of moisture will be present in the atmosphere, and therefore more precipitation could potentially fall during a given precipitation event (Meehl et al., 2005). However understanding extreme dry conditions is less obvious. Yoshikawa and Hinzman (2003), studying thermokarst ponds in Alaska, discovered that previous winter temperatures and snow depth were an important factor in controlling the freezing period of the active layer. In discontinuous permafrost zones, soils can drain quickly in non-frozen conditions, however once the active layer freezes, moisture is largely restricted to the surface, allowing for a greater amount of runoff and evaporation (Yoshikawa and Hinzman, 2003). For example, Yoshikawa and Hinzman (2003) note that the winter of 2000 was a heavy snowfall year so the active layer did not freeze until March 21, 2001. Conversely, there was little snow in the winter of 2001, and the active layer froze by late October. As a result, the water table was 25 cm below the ground surface in June of 2002, a trend which would completely drain the pond in roughly 1.5 years. Future monitoring of active layer freezing dates may provide insight

into the amount of influence the freeze date has on lake level variability in the MBS, especially when combined with climate conditions captured by calculated PDSI values.

It should be noted that although PDSI is used extensively by a variety of consumers, it is not without flaws. For example, Guttman et al. (1992) have questioned the applicability of PDSI outside of the central United States, as PDSI coefficients were developed through climate records from Iowa and Kansas. Furthermore, Alley (1984) criticizes PDSI for its weighting function (describing it as "weakly justified on physical or statistical grounds"), its high sensitivity to small precipitation changes in certain circumstances, and the subjective definition of wet or dry conditions (±0.5). Heddinghaus and Sabol (1991) respond to critiques of PDSI by claiming that, based on survey results, PDSI is typically only used to understand general patterns and that therefore exact conditions are irrelevant. Another potential concern is the northern PDSI data from Cook et al. (2007) used for this study, as values are derived from a limited number of data sources. PDSI was originally designed for the continental United States, where climate information is temporally and spatially superior to that of northern Canada. This method was then applied to the majority of North America by Cook et al. (2007). To address gaps in data, Cook et al. (2007) estimated PDSI for the 1900-1990 period of common overlap using interpolation, but acknowledge that Canadian data are "clearly under-represented". As a result, findings should be interpreted with caution, with attention focused on the general trend of data. While interpolated PDSI values offer a possibility of exploring past climate trends, there are certainly some glaring potential issues with interpreting this data without context.

Unfortunately, this is the best correlated metric and no other drought index has been as successful as PDSI. Until one is developed, the use of PDSI is widely accepted (Heddinghaus and Sobel, 1991). The following examines non-climatological influences which may be impacting the landscape at a more regional scale.

5.3 Non-climatological factors

5.3.1 Surficial deposits

Day (1968) discovered that the permeability of lacustrine deposits should be considered an important factor in determining water retention capability due to weak soil development in the region (a result of age and climate conditions). Still, it has been found that the soils in this region are generally well drained, and in fact the Twin Falls Series is considered unsuitable for agriculture because of its low water holding capacity (Day, 1968; EcoDynamics Consulting, 2008; see Table 5.1 and Figure 5.4 for a description and the spatial distribution of major soil types found in the region). Additionally, the drainage/permeability of soil and lacustrine deposits increases as one moves further north, where the majority of lake expansion occurs; the opposite effect one would expect. As such, it appears that the surficial materials are not a major factor in the observed lake expansion, although a more in-depth study of soil field capacity limits would be needed to confirm this conclusion.

5.3.2 Beaver Activity

Beavers (*Castor*) are often considered a keystone species due to their direct and far reaching impacts on the landscape (Gurnell, 1998). Dams, canals, and ponds built by beavers

Table 5.1. Description of major soil types found in the study area. Information is summarized from Day (1968).

SOIL	DESCRIPTION
Dieppe Series	Developed on moderately coarse textured beach deposits underlain by lacustrine deposits. The soils are slightly or moderately stony and consist of a thin organic layer, followed by gravelly loamy sand and gravelly sandy loam layers. Soils are well drained and permeable, however the underlying lacustrine silty clay is only moderately permeable.
Providence Series	Developed on moderately fine and fine textured lacustrine deposits. The soils are non to slightly stony and consist of a thin organic layer, followed by a silty clay loam layer. Soils are well drained and moderately permeable, however the underlying lacustrine deposit is only slowly permeable.
Sarristo Series	Developed on medium and moderately fine textured beach deposits underlain by silty clay loam lacustrine deposits. The soils are slightly to exceedingly stony and consist of a thin organic layer, followed by gravelly loam and gravelly sandy clay loam layers. Soils are imperfectly to moderately well drained and moderately permeable, however the underlying lacustrine deposits are only slowly permeable.
Twin Falls Series	Developed on coarse textured beach deposits that consist mainly of sand and gravel. The soils consist of sand, loamy sand, and sandy loam. Soils are rapidly drained and very rapidly permeable.

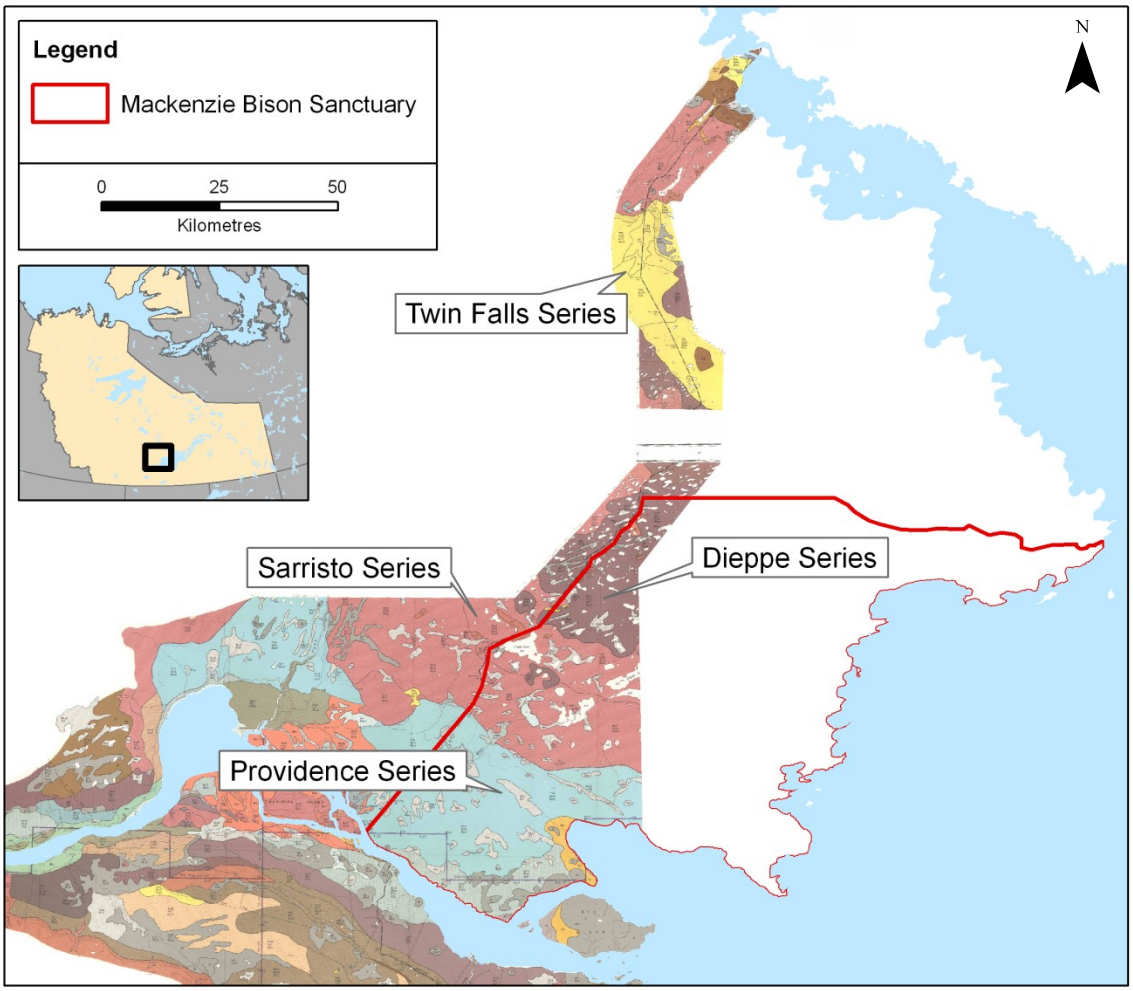

Figure 5.4. Soil map of the Fort Providence region. Image adapted from Day (1968).

influence hydrological variables in a variety of ways. Dams can block streamflow, causing the upstream water table to rise and expand. Even a low dam can flood a relatively large surface area, especially in flat topographic regions where the effects of beaver activity are typically magnified (Johnston and Naiman, 1987; Woo and Waddington, 1990). Furthermore, canals or diversion channels are used as travel and transport routes. These features have been documented at lengths greater than 100m and up to 1m in depth (Gurnell, 1998). If active for an extended period of time, channels may become downcut and serve as a permanent stream. This typically acts as a short diversion from normal streamflow, rejoining the channel shortly downstream, but may result in a drastic change in channel composition in some cases (Woo and Waddington, 1990). A species reintroduction project in Tierra del Fuego, highlights the potential large scale impacts of beaver activity and is described below.

In 1946, 25 pairs of North American beavers (*Castor canadensis*) from Canada were introduced to the Argentinian side of Tierra del Fuego (Jaksic et al., 2002). The population expanded relatively quickly and nearly 91% of streams in Tierra del Fuego were colonized by 1993 (Jaksic et al., 2002). Beavers eventually crossed waterways thought to be impassable, spreading beyond Tierra del Fuego to other islands and into mainland Argentina and Chile. Lizarralde (1993) estimated the beaver population range to be approximately 7,000,000 ha, with densities of up to 8.5 beavers/km^2 (Parkes et al., 2008). In Chile, beavers, officially labelled as pests since 1992, are blamed for killing riparian forests and causing millions of dollars of damage to infrastructure (i.e. triggering road washouts by using culverts as natural dams; Parkes et al., 2008). There have been

numerous attempts by the Chilean government to manage the beaver population, including a feasibility assessment for complete eradication (Parkes et al., 2008).

Unlike Tierra del Fuego however, the existence of natural predators in northern Canada limit beaver population growth. Still, beavers have the potential to spread rapidly in Canada. Colony sizes have a mean of roughly 5 individuals (± 1 SD; Rosell and Parker, 1995), with dispersal distances of less than ~15km (Leege, 1968), and sites are typically occupied for less than 6 years (Fryxell, 2001). Johnston and Naiman (1990) estimated that it would be possible for beavers to colonize roughly as far as 750 km over a 50 year period.

Beaver populations, which were severely depleted in the 16th to 19th centuries due to overtrapping, have partially recovered. Almost the entire pre-European contact range has been reoccupied in North America, but at densities of only one-tenth the numbers (Butler and Malanson, 2002). Effects are expected to escalate as beaver populations continue to recover (Butler and Malanson, 2002). Additionally, beavers prefer fine alluvial materials on low gradient streams for habitat (Gurnell, 1998). This suggests that the Fort Providence region represents a preferred habitat for beavers, the result of deposits left by Glacial Lake McConnell. Local residents who travel the land frequently, worked in association with children from the Fort Providence school system to identify areas of known beaver activity and their contribution to lake expansion in the MBS (Pisaric, personal communication; Figure 5.5). In the spring of 2013, data on the location of beaver activity was collected by the local hunters and trappers and the school children using handheld GPS units. A small number of lakes from the southern

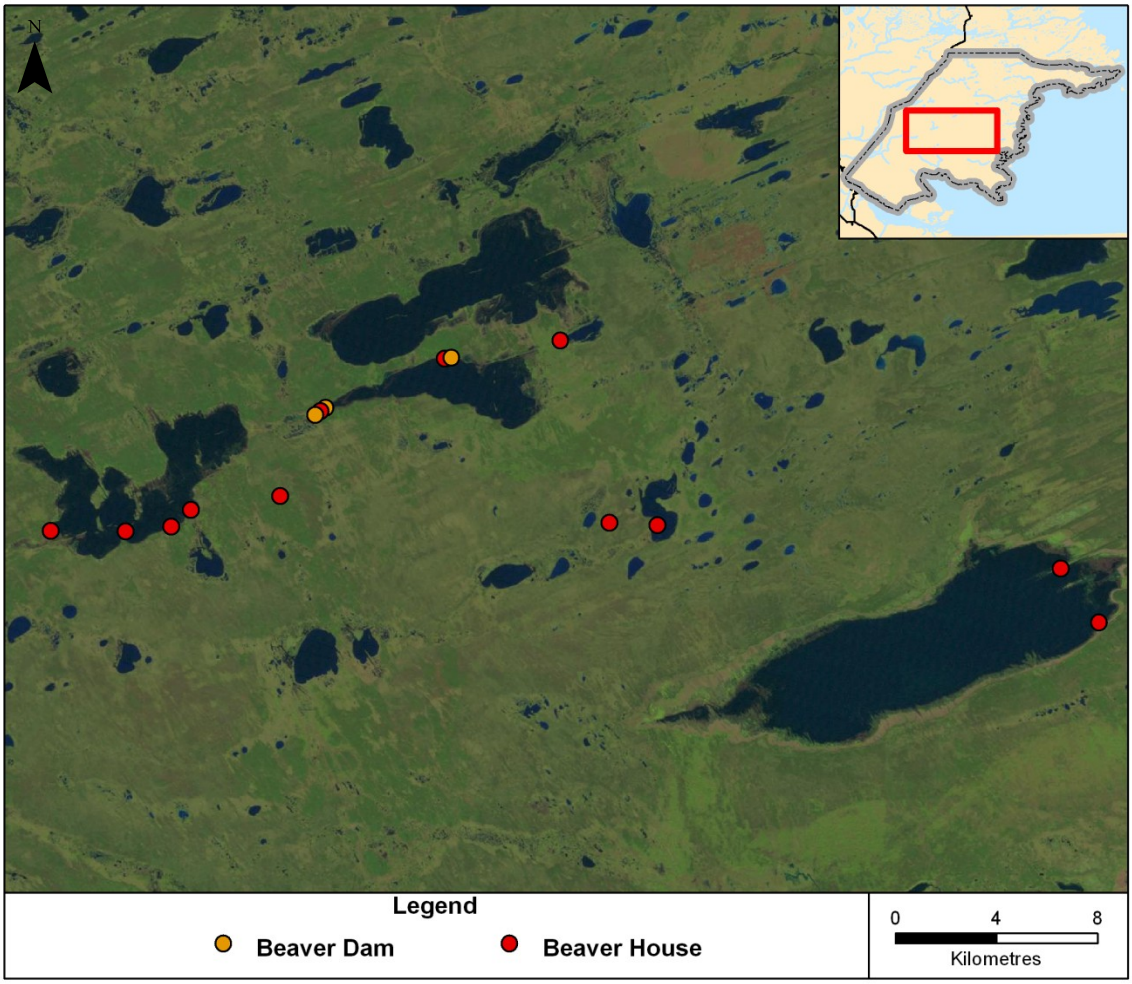

Figure 5.5. Beaver activity in the Fort Providence region, as mapped by local residents. Data from Pisaric (personal communication).

portion of the MBS were visited during this initial investigation. Unfortunately, at this point in time, there is not enough data to make reliable conclusions concerning the extent of beaver activity. As history has shown however, this variable should be considered seriously as it is a very real and potentially devastating source of landscape modification.

5.4 Limitations

Data availability and data collection were the largest limitations of this study. For example, in addition to the limited climate records, data regarding the underlying discontinuous permafrost (which may be significantly impacted by temperature changes) and beaver activity provided an inadequate amount of information to support any conclusions concerning these variables. Additionally, the collection of tree cores was restricted largely by budget constraints, as it was not possible to access remote locations for sampling; all sites were located along the highway. This, in combination with both past and recent fire activity, drastically reduced the number of suitable sample sites for dendroclimatological analysis.

Decisions regarding the acquisition and processing of imagery restricted the applications of the data. Although LANDSAT 5 TM imagery best met the requirements designated for this project, the pixel resolution limited classification accuracy. Imagery selection was limited due to subjective standards, such as the date range and cloud cover, which resulted in inconsistent time periods between observations. As a result, trend magnitude analysis could not be completed. It was also thought that increasing confidence in the classification of remote sensing imagery was an important factor in

assessing land cover change, so noise was removed from imagery. This reduced the ability to detect small changes however.

Finally, as a multidisciplinary study, it was not possible to examine all aspects of the project in great detail. For example, the accuracy and reliability of remote sensing results would have been greatly improved with the identification of a true fuzzy membership threshold value (i.e., the value at which water impacts wood bison movement). This would have likely required a detailed study of bison tracking and behaviour in the MBS in combination with measuring real world ground conditions, both of which were well beyond the scope of this project.

CHAPTER 6
CONCLUSION

6.1 General conclusions

Results confirm that lake area has steadily increased in the study region at a statistically significant rate. Remote sensing results also suggest that the observed changes are not uniform and that the majority of statistically significant change has occurred in the northern and central regions of the study area, where the majority of lakes are present. This is potentially a major problem for bison herd management, as bison are possibly being directed towards the bison management zone to the south of the MBS. Once in the bison management zone, bison can be shot by hunters or possibly come in contact with bison from areas to the south that may be infected with tuberculosis and bovine brucellosis.

Although lake area correlates moderately well with global summer SSTAs as well as the continental scale PNA pattern, lake variability is in contrast to what has typically been observed in the literature for high latitude, discontinuous permafrost regions. As such, it is unlikely that the results from this analysis can be extrapolated beyond the study area.

Lake expansion is likely the result of a multitude of variables. Non-climatological influences, particularly an increase in beaver activity, could also be contributors to this phenomenon. Unfortunately, data regarding these variables are limited for the region and must be studied in greater detail in order to make informed conclusions.

PDSI reconstructions indicate that climate has increased in variability between 1915 and 2010, resulting in more extreme wet and dry years. Management strategies

for the MBS should consider that lake area will likely continue expand in the future as climate variability is expected to increase.

6.2 Future research

The collection of active layer freezing dates may help to better understand year-to-year lake level variability. Long term analysis may provide insight lake growth when combined with climate data.

While it is believed the ≥0.5 membership results are the best representation of true conditions, this cannot be confirmed until better quality data is collected. The methodology used for this study is applicable to a broad range of analyses, however future work should focus on obtaining true lake area measurements in the field in order to reliably assess the accuracy of remote sensing results. The identification of historical water marks (discoloured ground) may also provide insight into the future spatial distribution of lakes. Additionally, it would be advantageous to extend the temporal record of imagery. Although there is limited availability, air photos do exist for the study area.

REFERENCES

Abdullah, S.A. and Nakagoshi, N. (2006). Changes in landscape spatial pattern in the highly developing state of Selangor, peninsular Malaysia. *Landscape and Urban Planning, 77*, 263-275.

Alley, W.M. (1984). The Palmer Drought Severity Index: limitations and assumptions. *Journal of Climate and Applied Meteorology*, 23, 1100-1009.

Anchukaitis, K.J., D'Arrigo, R.D., Andreu-Hayles, L., Frank, D., and Verstege, A. (2013). Tree-Ring-Reconstructed Summer Temperatures from Northwestern North America during the Last Nine Centuries. *Journal of Climate, 26* (10), 3001–3012.

Anderson, K. and Milton, E.J. (2006). On the temporal stability of ground calibration targets: Implications for the reproducibility of remote sensing methodologies. *International Journal of Remote Sensing, 27* (16), 3365-3374.

Arnell, N., Liu, C., Compagnucci, R., da Cunha, K., Hanaki, K., Howe, C., Mailu, G., Shiklomanov, I., and Stakhiv, E. (2001). Hydrology and water resources. Chapter 4 in *Climate Change 2001: Impacts, Adaptation and Vulnerability. Contribution of Working Group II to the Third Assessment Report of the IPCC.* Cambridge Press.

Begin, Y. (2001). Tree-ring dating of extreme lake levels at the subarctic–boreal interface. *Quaternary Research*, 55, 133–139.

Beyer, H.L. (2012). Geospatial Modelling Environment (version 0.7.2) [Software]. Available from http://www.spatialecology.com/gme/

Bomblies, A., McKnight, D.M., and Andrews, E.D. (2001). Retrospective simulation of lake-level rise in Lake Bonney based on recent 21-yr record: indication of recent climate change in the McMurdo Dry Valleys, Antarctica. *Journal of Paleolimnology*, 25, 477–492.

Briffa, K.R., and Jones, P.D. (1990). Basic chronology statistics and assessment. In: *Methods of Dendrochronology* [Cook, E.R., and Kairiukstis, L.A. (eds.)], Kluwer Academic, Dordrecht.

Briffa, K.R., and Melvin, T.M. (2011). A Closer Look at Regional Curve Standardization of Tree-Ring Records: Justification of the Need, a Warning of Some Pitfalls, and Suggested Improvements in Its Application. In: *Dendroclimatology: Progress and*

Prospects, Volume 11 [Hughes, M.K., Swetnam, T.W., and Diaz, H.F. (eds.)], Springer, Dordrecht.

Buchberger, S. (1995). Conditional Frequency Analysis of Autocorrelated Lake Levels. *Journal of Water Resources Planning and Management, 121* (2), 158–170.

Büntgen, U., Esper, J., Frank, D.C., Nicolussi, K., and Schmidhalter, M. (2005). A 1052-year tree-ring proxy for Alpine summer temperatures. *Climate Dynamics, 25*, 141-153.

Butler, D.R., and Malanson, G.P. (2002). The geomorphic influences of beaver dams and failures of beaver dams. *Geomorphology*, 71 (1), 48–60.

Carroll, M.L., Townshend, J.R.G., DiMiceli, C.M., Loboda, T., and Sohlberg, R.A. (2011). Shrinking lakes of the Arctic: Spatial relationships and trajectory of change. *Geophysical Research Letters, 38*, L20406.

Case, R.A., and MacDonald, G.M. (1995). A dendroclimatic reconstruction of annual precipitation on the western Canadian prairies since A.D. 1505 from Pinus flexilus James. *Quaternary Research*, 44, 267-275.

CBC (Canadian Broadcasting Corporation) News (2006). Mad Cow in Canada: The science and the story. Retrieved from: http://www.cbc.ca/news/background/madcow/

Chander, G., Helder, D.L., Markham, B.L., Dewald, J.D., Kaita, E., Thome, K.J., Micijevic, E., and Ruggles, T.A. (2004). Landsat-5 TM Reflective-Band Absolute Radiometric Calibration. *IEEE Transactions on Geoscience and Remote Sensing, 42* (12), 2747-2759.

Chander, G., Markham, B.L., and Helder, D.L. (2009). Summary of current radiometric calibration coefficients for Landsat MSS, TM, ETM+, and EO-1 ALI sensors. *Remote Sensing of Environment, 113*, 893-903.

Christensen, J.H., Hewitson, B., Busuioc, A., Chen, A., Gao, X., Held, I., Jones, R., Kolli, R.K., Kwon, W.T., Laprise, R., Magana Rueda, V., Mearns, L., Menéndez, C.G., Räisänen, J., Rinke, A., Sarr, A., and Whetton, P. (2007). Regional Climate Projections. In: *Climate Change 2007: The Physical Science Basis. Contribution of Working Group I to the Fourth Assessment Report of the Intergovernmental Panel on Climate Change.* [Solomon, S., Qin, D., Manning, M., Chen, Z., Marquis, M., Averyt, K.B., Tignor, M., and Miller, H.L. (eds)], New York, NY, USA, Cambridge University Press.

Climate Prediction Center Internet Team (2012). Pacific/North American (PNA). Retrieved from http://www.cpc.ncep.noaa.gov/data/teledoc/pna.shtml

Colman, A.W., and Davey, M.K. (2003). Statistical Prediction of Global Sea-Surface Temperature Anomalies. *International Journal of Climatology*, *23*, 1677-1697.

Cook, E.R., and Holmes, R.L. (1986). Guide for Computer Program ARSTAN. Tucson, Arizona: Laboratory of Tree-ring Research, University of Arizona.

Cook, E.R., Briffa, K.R., and Jones, P.D. (1994). Spatial regression methods in dendroclimatology: a review and comparison of two techniques. *International Journal of Climatology, 14*, 379-402.

Cook, E. R., Seager, R., Cane, M. A., and Stahle, D. W. (2007). North American drought: reconstructions, causes, and consequences. *Earth-Science Reviews*, 81, 93-134.

D'Arrigo, R., Jacoby, G., Buckley, B., Sakulich, J., Frank, D., Wilson, R., Curtis, A., and Anchukaitis, K. (2009). Tree growth and inferred temperature variability at the North American Arctic treeline. *Global and Planetary Change*, *65* (1), 71-82.

Dancey, C.P., and Reidy, J. (2004). Statistics without maths using SPSS for windows in Psychology. Harlow, England: Pearson Education.

Day, J.H. (1968). *Soils of the upper Mackenzie River Area, Northwest Territories*. Research Branch, Canada Department of Agriculture.

deMontigny, P., and Pisaric. M.F.J. (2011). *Lake level fluctuations and its impact on bison habitat: a climate reconstruction of the Fort Providence region, NWT*. Report submitted to Environment and Natural Resources, Government of the Northwest Territories. Ottawa, ON.

Demsar, U., Harris, P., Brunsdon, C., Stewart Fotheringham, A., and McLoone, S. (2013). Principal Component Analysis on Spatial Data: An Overview. *Annals of the Association of American Geographers, 103* (1), 106-128.

Douglas, R.J.W. (1975). *Geology, Trout River, District of Mackenzie* [map]. 1: 500,000. "A" Series Map 1371A. Ottawa, ON: Geological Survey of Canada.

Douglas, R.J.W., Norris, A.W., and Norris, D.K. (1974). *Geology, Great Slave, District of Mackenzie* [map]. 1: 500,000. "A" Series Map 1370A. Ottawa, ON: Geological Survey of Canada.

Douglas, R.J.W., Norris, A.W., and Norris, D.K. (1975). *Geology, Horn River, District of Mackenzie* [map]. 1: 500,000. "A" Series Map 1372A. Ottawa, ON: Geological Survey of Canada.

Drapela, K. and Drapelova, I. (2011). Application of Mann-Kendall test and the Sen's slope estimates for trend detection in deposition data from Beskydy Mts., the Czech Republic, 1997-2010. *Beskydy*, *4* (2), 133-146.

EcoDynamics Consulting (2008). *Northwest Territories Soil Survey Enhancement Project*. Report submitted to the Department of Industry, Tourism, and Investment, Government of Northwest Territories. Prince Albert, SK.

Ecosystem Classification Group (ECG) (2007). *Ecological Regions of the Northwest Territories – Taiga Plains*. Department of Environment and Natural Resources, Government of the Northwest Territories. Yellowknife, NT.

Environment and Natural Resources, Government of the Northwest Territories (2010). Wood Bison Management Strategy for the Northwest Territories. http://www.enr.gov.nt.ca/_live/documents/content/wood_bison_management_strategy.pdf

Environment and Natural Resources, Government of the Northwest Territories (2011). Mackenzie Bison Population. http://www.enr.gov.nt.ca/_live/pages/wpPages/Mackenzie_Bison.aspx.

ESRI (2011). ArcGIS Desktop Help 10.0 – Fuzzy Membership. http://help.arcgis.com/en/arcgisdesktop/10.0/help/index.html#//009z000000rn000000.htm

Farrokhrouz, M., and Asef, M.R. (2013). *Shale Engineering: Mechanics and Mechanisms*. Florida: CRC Press.

Finn, M.P., Reed, M.D. and Yamamoto, K.H. (2012). *A Straight Forward Guide for Processing Radiance and Reflectance for EO-1 ALI, Landsat 5 TM, Landsat 7 ETM+, and ASTER*. Retrieved from http://cegis.usgs.gov/soil_moisture/pdf/A%20Straight%20Forward%20guide%20for%20Processing%20Radiance%20and%20Reflectance_V_24Jul12.pdf

Foody, G.M. (1999). The Continuum of Classification Fuzziness in Thematic Mapping. *Photogrammetric Engineering and Remote Sensing, 65* (4), 443-451.

Foody, G.M. (2002). Status of land cover classification accuracy assessment. *Remote Sensing of Environment, 80*, 185-201.

Fritts, H.C. (1976). *Tree-rings and Climate*. New York: Academic Press.

Fryxell, J.M. (2001). Habitat suitability and source- sink dynamics of beavers. *Journal of Animal Ecology, 70*, 310-316.

Gao, B.C. (1996). NDWI - a normalized difference water index for remote sensing of vegetation liquid water from space. *Remote Sensing of Environment*, *58,* 257-266.

Gao, J. (2009). *Remotely Sensed Imagery*. Toronto, ON: McGraw-Hill.

Gates, C.C., Freese, C.H., Gogan, P.J.P., and Kotzman, M. (eds. and comps.) (2010). *American Bison: Status Survey and Conservation Guidelines 2010*. Gland, Switzerland: IUCN.

Gates, C.C., and Larter, N.C. (1990). Growth and dispersal of an erupting large herbivore population in northern Canada: The Mackenzie wood bison (Bison bison athabascae). *Arctic, 43*, 231-238.

Gibson, J.J., Prowse, T.D., and Peters, D.L. (2006). Hydroclimatic controls on water balance and water variability in Great Slave Lake. Hydrological Processes, 20, 4155-4172.

Good, P., and Lowe, J. (2006). Emergent Behavior and Uncertainty in Multimodel Climate Projections of Precipitation Trends at Small Spatial Scales. *Journal of Climate, 19* (21), 5554-5569.

Government of the Northwest Territories (2012). NWT wood bison (Bison bison athabascae). http://nwtspeciesatrisk.ca/tiki/tiki-index.php?page=WoodBison

Grissino-Mayer, H.D., Sheppard, P.R., Cleaveland, M.K., Cherubini, P., Ratcliff, P., and Topham, J. (2010). Adverse implications of misdating in dendrochronology: Addressing the re-dating of the “Messiah” violin. *Dendrochronologia*, 28, 149-159.

Gunnarson, B.E. (2001). Lake level changes indicated by dendrochronology on subfossil pine, Jämtland, Central Scandinavian Mountains, Sweden. *Arctic, Antarctic, and Alpine Research*, *33* (3), 274-281.

Gupta, R.P. (2003). Remote Sensing Geology (2nd ed.). New York, NY: Springer-Verlag.

Gurnell, A.M. (1998). The hydrogeomorphological effects of beaver dam-building activity. *Progress in Physical Geography, 22* (2), 167-189.

Guttman, N.B., Wallis, J.R., and Hosking, J.R.M. (1992). Spatial comparability of the Palmer Drought Severity Index. *Water Resources Bulletin, 28*, 1111-1119.

Hamed, K.H. (2008). Trend detection in hydrologic data: The Mann-Kendall trend test under the scaling hypothesis. *Journal of Hydrology, 349*, 350-363.

Heddinghaus, T.R., and Sobel, P. (1991). A review of the Palmer Drought Severity Index and where do we go from here? Preprints, Seventh Conference on Applied Climatology, Dallas, TX. American Meteorological Society, 242-246.

Hegerl, G.C., Zwiers, F.W., Braconnot, P., Gillett, N.P., Luo, Y., Marengo Orsini, J.A., Nicholls, N., Penner, J.E., and Stott, P.A. (2007). Understanding and Attributing Climate Change. In: *Climate Change 2007: The Physical Science Basis. Contribution of Working Group I to the Fourth Assessment Report of the Intergovernmental Panel on Climate Change* [Solomon, S., D. Qin, M. Manning, Z. Chen, M. Marquis, K.B. Averyt, M. Tignor and H.L. Miller (eds.)]. Cambridge University Press, Cambridge, United Kingdom and New York, NY, USA.

Holmes, R. L. (1983). Computer-assisted quality control in tree-ring dating and measurement. *Tree-Ring Bulletin*, *43*, 69-78.

Huntington, T.G. (2006). Evidence for intensification of the global water cycle: review and synthesis. *Journal of Hydrology*, *319*, 83-95.

Jaksic, F.M., Iriarte, J.A., Jimenez, J.E., and Martinez, D.R. (2002). Invaders without frontiers: cross-border invasions of exotic mammals. *Biological Invasions*, *4*, 157-173.

Jin, Y., Schaaf, C.B., Gao, F., Li, X., and Strahler, A.H. (2002) How does snow impact albedo of vegetated land surfaces as analyzed with MODIS data? *Geophysical Research Letters*, *29* (10), 121-124.

Johnston, C.A., and Naiman R.J. (1990). Aquatic patch creation in relation to beaver population trends. *Ecology*, *71*, 1617-1621.

Joly, D.O., and Messier, F. (2004). Testing hypotheses of bison population decline (1970–1999) in Wood Buffalo National Park: synergism between exotic disease and predation. *Canadian Journal of Zoology, 84*, 1165-1176.

Karmeshu, N. (2012). *Trend Detection in Annual Temperature & Precipitation Using the Mann Kendall Test: A Case Study to Assess Climate Change on Select States in the Northeastern United States*. Unpublished master's thesis, University of Pennsylvania, Philadelphia, Pennsylvania.

Kaufman, Y.J. (1987). The effect of subpixel clouds on remote sensing. *International Journal of Remote Sensing, 8* (6), 839-857.

Kendall, M.G. (1975). *Rank correlation methods*. London, UK: Griffin.

Knight, J.F., and Lunetta, R.S. (2003). An Experimental Assessment of Minimum Mapping Unit Size. *IEEE Transactions on Geoscience and Remote Sensing, 41* (9), 2132-2134.

Labrecque, S., Lacelle, D., Duguay, C.R., Lauriol, B., and Hawkings, J. (2009). Contemporary (1951-2001) Evolution of Lakes in the Old Crow Basin, Northern Yukon, Canada: Remote Sensing, Numerical Modeling, and Stable Isotope Analysis. *Arctic, 62* (2), 225-238.

LaMarche, V. C., Cook E. R., and Baillie, M. G. L. (1982). Sampling strategies. In *Climate from Tree-Rings*. Eds. M.K. Hugues et al. Cambridge University Press, Cambridge, UK.

Landwehr, J.M., and Matalas, N.C. (1986). On the nature of persistence in dendrochronologic records with implications for hydrology. *Journal of Hydrology*, 86, 239-277.

Larter, N.C., and Gates, C.C. (1991). Diet and habitat selection of wood bison in relation to seasonal changes in forage quantity and quality. *Canadian Journal of Zoology, 69* (10), 2677-2685.

Leege, T.A. (1968). Natural movements of beavers in south-eastern Idaho. *Journal of Wildlife Management*, *32*, 973-976.

Leira, M., and Cantonati, M. (2008). Effects of water-level fluctuations on lakes: an annotated bibliography. *Hydrobiologia, 613*, 171-184.

Lillesand, T., Keifer, R.W., and Chipman, J. (2007) Remote Sensing and Image Interpretation, 6th ed. Hoboken, NJ: John Wiley & Sons.

Liu, C., Frazier, P., and Kumar, L. (2007). Comparative assessment of the measures of thematic classification accuracy. *Remote Sensing of Environment, 107*, 606-616.

Liu, Y., Sun, J., Song, H., Cai, Q., Bao, G., and Li, X. (2010). Tree-ring hydrologic reconstructions for the Heihe River watershed, western China since AD 1430. *Water Research*, *44*, 2781-2792.

Lizarralde, M.S. (1993). Current status of the introduced beaver (Castor Canadensis) population in Tierra del Fuego, Argentina. *Ambio*, *22*, 351-358.

Lu, D. and Weng, Q. (2007) A survey of image classification methods and techniques for improving classification performance. *International Journal of Remote Sensing*, *28* (5), 823-870.

Luckman, R.A. and Wilson, G.M. (2005). Summer temperatures in the Canadian Rockies during the last millennium: a revised record. Climate Dynamics, 2*4*, 131-144.

Lunetta, R.S., and Balogh, M.E. (1999). Application of Multi-Temporal Landsat 5 TM Imagery for Wetland Identification, *Photogrammetric Engineering and Remote Sensing, 65* (11), 1303-1310.

Mann, H.B. (1945). Nonparametric tests against trend. *Econometrica, 13,* 245-259.

Mann, M.E., Bradley, R.S., and Hughes, M.K. (1998). Global-scale temperature patterns and climate forcing over the past six centuries. *Nature*, *392*, 779-787.

Mantua, N.J. and Hare, S.R. (2002). The Pacific Decadal Oscillation. *Journal of Oceanography*, *58*, 35-44.

Marsh, P. and Bigras, S.C. (1988). Evaporation from Mackenzie Delta Lakes, N.W.T., Canada. *Arctic and Alpine Research*, *20* (2), 220-229.

Martinelli, N. (2004). Climate from dendrochronology: latest developments and results. *Global and Planetary Change*, *40*, 129–139.

McGrath, N. (2009). *Effective Sample Size in Order Statistics of Correlated Data* (Master's thesis). Boise State University Theses and Dissertations. Retrieved from http://scholarworks.boisestate.edu/td/32

Meehl, G.A., Arblaster, J.M., and Tebaldi, C. (2005). Understanding future patterns of increased precipitation intensity in climate model simulations. *Geophysical Research Letters*, *32*, L18719.

Melvin, T.M., and Briffa, K.R. (2008). A “signal-free” approach to dendroclimatic standardisation. *Dendrochronologia, 26*, 71-86.

Meko, D. M. (2006). Tree-ring inferences on water-level fluctuations of Lake Athabasca. *Canadian Water Resources Journal*, *31*, 229-248.

Meko, D.M. (2011). *Validating the Regression Model* [Lecture notes]. Retrieved from: http://www.ltrr.arizona. edu/~dmeko/notes_12.pdf

National Weather Service (2012). *Pacific North American Pattern*. Retrieved from http://www.cpc.ncep.noaa.gov/products/precip/CWlink/pna/pna.shtml

National Weather Service (2005). *Arctic Oscillation*. Retrieved from http://www.cpc.ncep.noaa.gov/products/precip/CWlink/daily_ao_index/ao.shtml

National Weather Service Forecast Office (2009). *20 Years Ago: The December 1989 Arctic Outbreak across the North Country*. Retrieved from http://www.erh.noaa.gov/btv/events/Dec1989/

Nicholls, R.J., Wong, P.P., Burkett, V.R., Codignotto, J.O., Hay, J.E., McLean, R.F., Ragoonaden, S., and Woodroffe, C.D. (2007). Coastal systems and low-lying areas. *Climate Change 2007: Impacts, Adaptation and Vulnerability. Contribution of Working Group II to the Fourth Assessment Report of the Intergovernmental Panel on Climate Change* [Parry, M.L., O.F. Canziani, J.P. Palutikof, P.J. van der Linden and C.E. Hanson, (eds.)], Cambridge University Press, Cambridge, UK, 315-356.

Okeke, F., and Karnieli, A. (2006). Methods for fuzzy classification and accuracy assessment of historical photographs for vegetation change analyses. Part I: Algorithm development. *International Journal of Remote Sensing, 27* (12), 153-176.

Palmer, W.C., (1965). Meteorological Drought. Research Paper, US Weather Bureau, 45, Washington, DC.

Parkes, J.P., Paulson, J., Donlan C.J., and Campbell, K. (2008). Control of North American beavers in Tierra del Fuego: feasibility of eradication and alternative management options. Landcare Research Contract Report: LC0708/084 prepared for: Comite Binacional para la Estrategia de Erradicacion de Castores de Patagonia, Austral.

Parks Canada (2009). *Phenotypic Differences Between the Bison Subspecies*. Retrieved from: http://www.pc.gc.ca/ eng/pn-np/ab/elkisland/natcul/natcul1/b/iii.aspx

Parks Canada (2012). *History of the Herds - Wood Bison*. Retrieved from: http://www.pc.gc.ca/pn-np/ab/elkisland/natcul/ii.aspx

Pisaric, M.F.J., St-Onge, S.M., and Kokelj, S.V. (2009). Tree-ring Reconstruction of Early-growing Season Precipitation from Yellowknife, Northwest Territories, Canada. *Arctic, Antarctic, and Alpine Research, 41* (4), 486–496.

Porter, T.J (2012). White spruce tree-rings from arctic treeline in Old Crow Flats and the Mackenzie Delta, Northwestern Canada: Indicators of past climate change. Unpublished doctoral dissertation, Carleton University, Ottawa, Ontario.

Porter, T. J. and Pisaric, M. F. (2011). Temperature-growth divergence in white spruce forests of Old Crow Flats, Yukon Territory, and adjacent regions of northwestern North America. *Global Change Biology, 17*, 3418-3430.

Prowse, T.D., Furgal, C., Bonsal, B.R., and Edwards, T.W.D. (2009). Climatic Conditions in Northern Canada: Past and Future. *AMBIO: A Journal of the Human Environment*, *38* (5), 257-265.

Quinn, F.H., and Sellinger, C.E. (2006). A reconstruction of Lake Michigan–Huron water levels derived from tree ring chronologies for the period 1600–1961. *Journal of Great Lakes Research*, *32* (1), 29-39.

Rayner, N.A., Brohan, P., Parker, D.E., Folland, C.K., Kennedy, J.J., Vanicek, M.M., Ansell, T., and Tett, S.F.B. (2006) Improved analyses of changes and uncertainties in sea surface temperature measured in situ since the mid-nineteenth century: the HadSST2 data set. *Journal of Climate*, *19* (3), 446-469.

Roach, J.K., Griffith, B., and Verbyla, D. (2013). Landscape influences on climate-related lake shrinkage at high latitudes. *Global Change Biology, 19*, 2276-2284.

Rodionov, S.N., Bond, N.A., and Overland, J.E. (2007). The Aleutian Low, storm tracks, and winter climate variability in the Bering Sea. *Deep Sea Research Part II: Topical Studies in Oceanography, 54* (23), 2560-2577.

Rosell, F., and Parker, H. (1995). *Beaver Management: present practice and Norway's future needs.* Bo, Norway.

Rouse, J.W., Hass, R.H., Schell, J.A., and Deering, D.W. (1973). Monitoring vegetation systems in the Great Plains with ERTS. *Third ERTS Symposium*, NASA SP-351 I, 309-317.

Schlagel, J.D., and Newton, C.M. (1996). A GIS-Based Statistical Method to Analyze Spatial Change. *Photogrammetric Engineering and Remote Sensing, 62* (7), 839-844.

Schulman, E. (1956). Dendroclimatic Changes in Semiarid America. Tucson: University of Arizona Press.

Schweingruber, F.H. (n.d.[a]). *Schweingruber-Bras d'Or Lake-PCG-ITRDB CANA046* [Data file]. Retrieved from http://hurricane.ncdc.noaa.gov/pls/paleox/f?p=519:1:::::P1_STUDY_ID:4353

Schweingruber, F.H. (n.d.[b]). *Schweingruber-Fort Providence-PCGL-ITRDB CANA047* [Data file]. Retrieved from http://hurricane.ncdc.noaa.gov/pls/paleox/f?p=519:1:::::P1_STUDY_ID:4415

Sen, P.K. (1968). Estimates of the regression coefficient based on Kendall's tau. *Journal of the American Statistical Association, 63*, 1379-1389.

Shabbar, A., and Skinner, W. (2004). Summer Drought Patterns in Canada and the Relationship to Global Sea Surface Temperatures. *Journal of Climate, 17*, 2866-2880.

Sheridan, S.C. (2003). North American weather-type frequency and teleconnection indices. *International Journal of Climatology, 23* (1), 27-45.

Smith, D.G. (1994). Glacial Lake McConnell: Paleogeography, age, duration, and associated river deltas, mackenzie river basin, western Canada. *Quaternary Science Reviews, 13* (9), 829-843.

Speer, J.H. (2010). *Fundamentals of Tree-Ring Research*. Tucson: The University of Arizona Press

Spence, C., and Rausch, J. (2005). Autumn synoptic conditions and rainfall in the subarctic Canadian Shield of the Northwest Territories, Canada. *Arctic, Antarctic and Alpine Research, 41* (4), 486-496.

Stokes, M.A., and Smiley, T.L. (1968). An Introduction to Tree-Ring Dating. Chicago: University of Chicago Press.

Strong, W.L., and Gates, C.C. (2009). Wood bison population recovery and forage availability in northwestern Canada. *Journal of Environmental Management, 90*, 434-440.

Tessaro, S.V., Gates, C.C., and Forbes, L.B. (1992). The brucellosis and tuberculosis status of wood bison in the Mackenzie Bison Sanctuary, Northwest Territories, Canada. *The Canadian Journal of Veterinary Research, 57*, 231-235.

Thornthwaite, C.W. (1948). An approach towards a rational classification of climate. *Geographical Review, 38* (1), 55–94.

Trouet, V., and Taylor, A.H. (2009). Multi-century variability in the Pacific North American circulation pattern reconstructed from tree rings. *Climate Dynamics, 35* (6), 953-963.

Turner, K.W., Wolfe, B.B., and Edwards, T.W.D. (2010). Characterizing the role of hydrological processes on lake water balances in the Old Crow Flats, Yukon Territory, Canada, using water isotope tracers. *Journal of Hydrology, 386*, 103-117.

Van, T.T. and Binh, T.T. (2009). Application of remote sensing for shoreline change detection in Cuu Long estuary. *Vietnam National University Journal of Science, 25*, 217-222.

van der Wielen, S. (2012). Report to Environment and Natural Resources, NWT. Unpublished.

Wells, N., Goodard, S., and Hayes, M.J. (2004) A self-calibrating Palmer Drought Severity Index. *Journal of Climate, 17*, 2335-2351.

Wiles, G.C., Krawiec, A.C., and D'Arrigo, R.D. (2009) A 265-year reconstruction of Lake Erie water levels based on North Pacific tree rings. *Geophysical Research Letters, 36* (5), L05705.

Woo, M., and Waddington, J.M. (1990). Effect of Beaver Dams on Subarctic Wetland Hydrology. *Arctic*, *43* (3), 223-230.

World Meteorological Organization (1989). *Calculation of Monthly and Annual 30-Year Standard Normals*. WMO/TD No. 341, WCDP No. 10, Geneva.

Yamaguchi, D.K. (1991) A simple method for cross-dating increment cores from living trees. *Canadian Journal of Forest Research, 20*, 246-250.

Yoshikawa, K., and Hinzman, L.D. (2003). Shrinking thermokarst ponds and groundwater dynamics in discontinuous permafrost near Council, Alaska. *Permafrost Periglacial Processes, 14* (2), 151-160.

Youngblut, D., and Luckman, B. (2008). Maximum June–July temperatures in the southwest Yukon over the last 300 years reconstructed from tree rings. *Dendrochronologia*, *25*, 153-166.

Yue, S., and Wang, C. (2004). The Mann-Kendall Test Modified by Effective Sampling Size to Detect Trend in Serially Correlated Hydrological Series. *Water Resources Management, 18*, 201-218.

Zadeh, L.A. (1965). Fuzzy sets. *Information and Control, 8* (3), 338-353.

Zhang, J., and Foody, G.M. (1998). A fuzzy classification of sub-urban land cover from remotely sensed imagery, *International Journal of Remote Sensing, 19* (14), 2721-2738.

Zhang, Q., Sun, P., Chen, X., and Jiang, T. (2011).Hydrological extremes in the Poyang Lake basin, China: changing properties, causes, and impacts. *Hydrological Processes, 25,* 3121-3130.

Zhu, X., Sun, J., Liu, Z., Liu, Q., and Martin, J.E. (2007). A Synoptic Analysis of the Interannual Variability of Winter Cyclone Activity in the Aleutian Low Region. *Journal of Climate, 20* (8), 1523-1538.

APPENDIX A
1.0 FUZZY MEMBERSHIP RESULTS

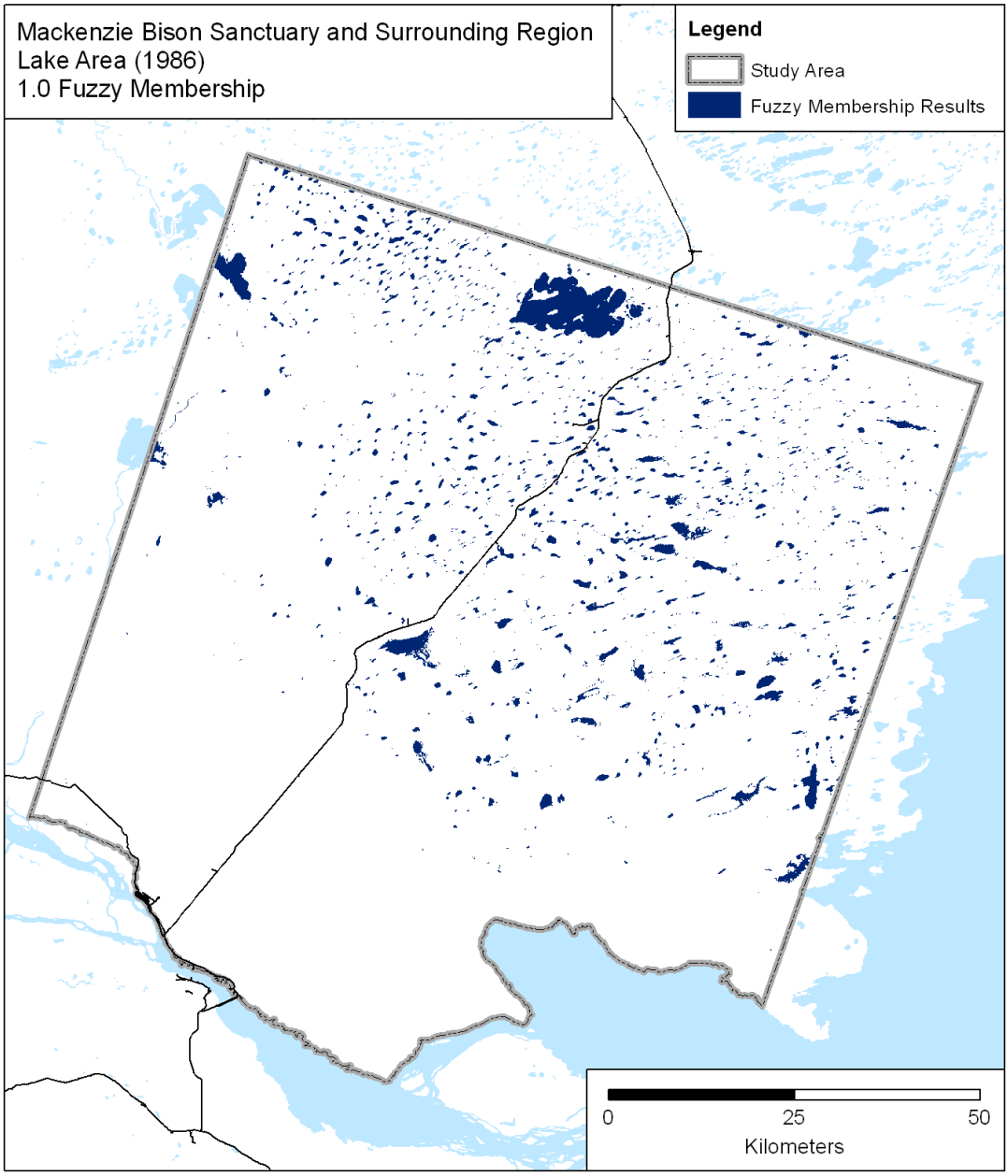

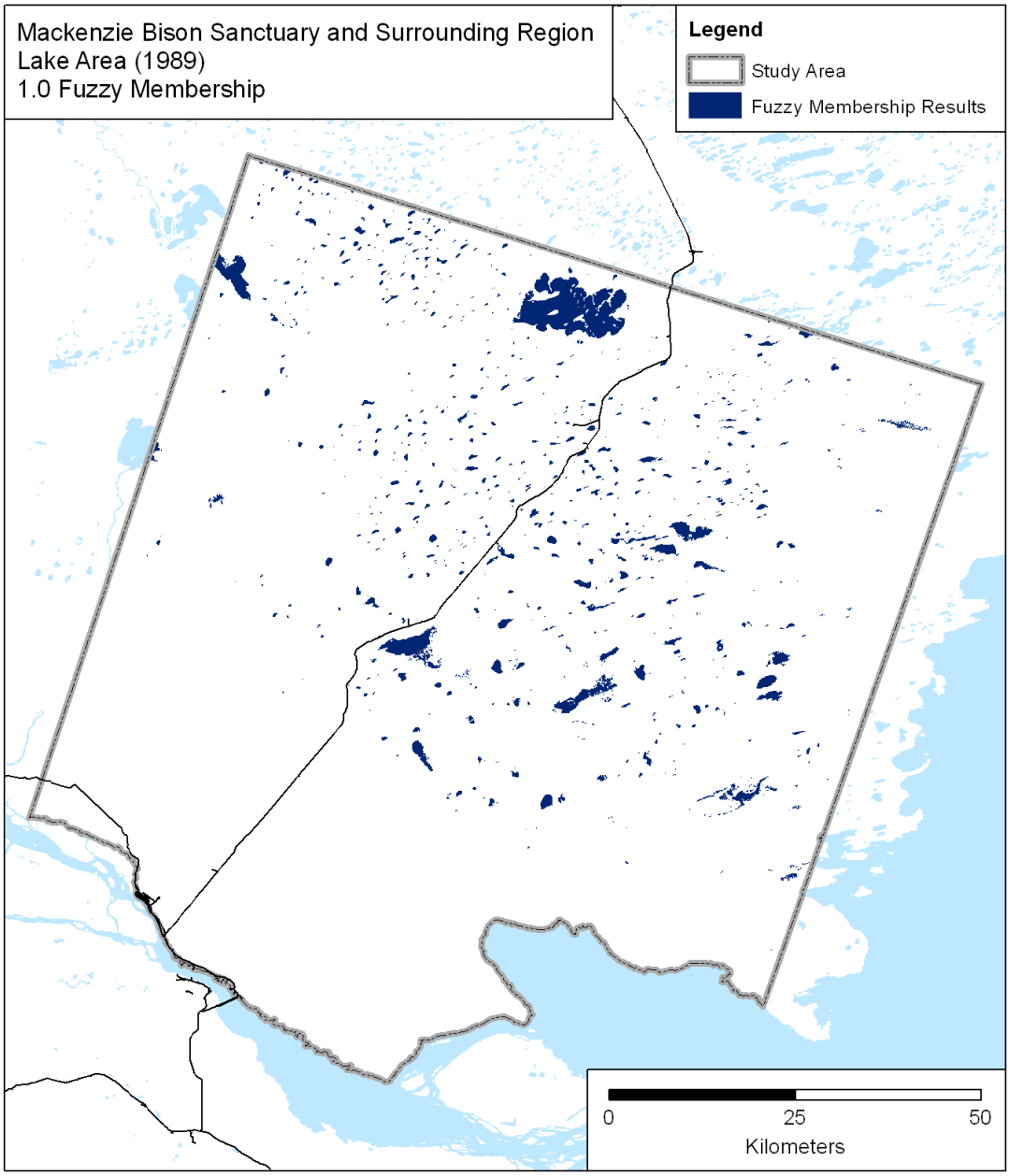
Mackenzie Bison Sanctuary and Surrounding Region
Lake Area (1989)
1.0 Fuzzy Membership
Legend
Study Area
Fuzzy Membership Results
0
25
50
Kilometers

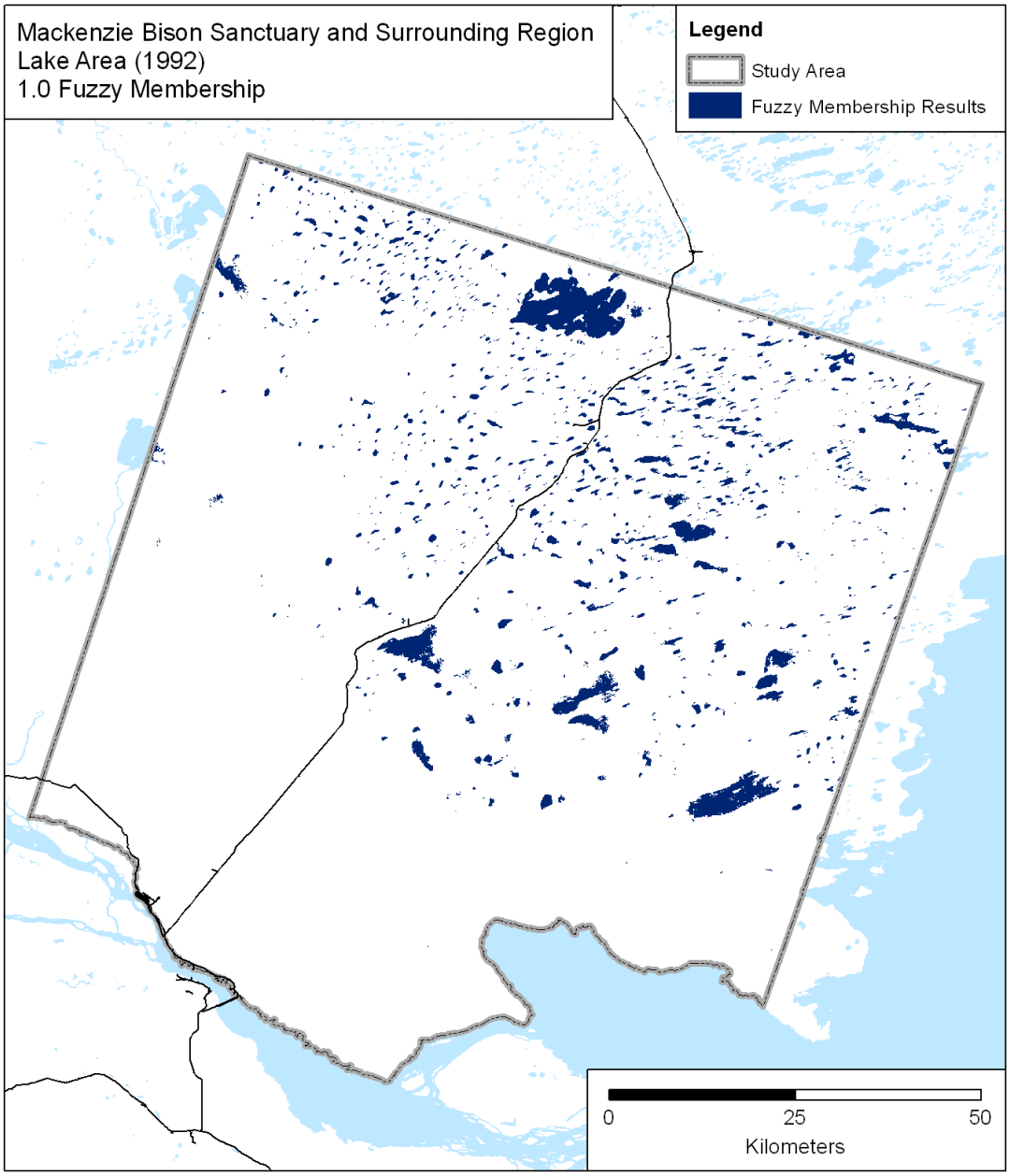
Mackenzie Bison Sanctuary and Surrounding Region
Lake Area (1992)
1.0 Fuzzy Membership
Legend
Study Area
Fuzzy Membership Results
0
25
50
Kilometers

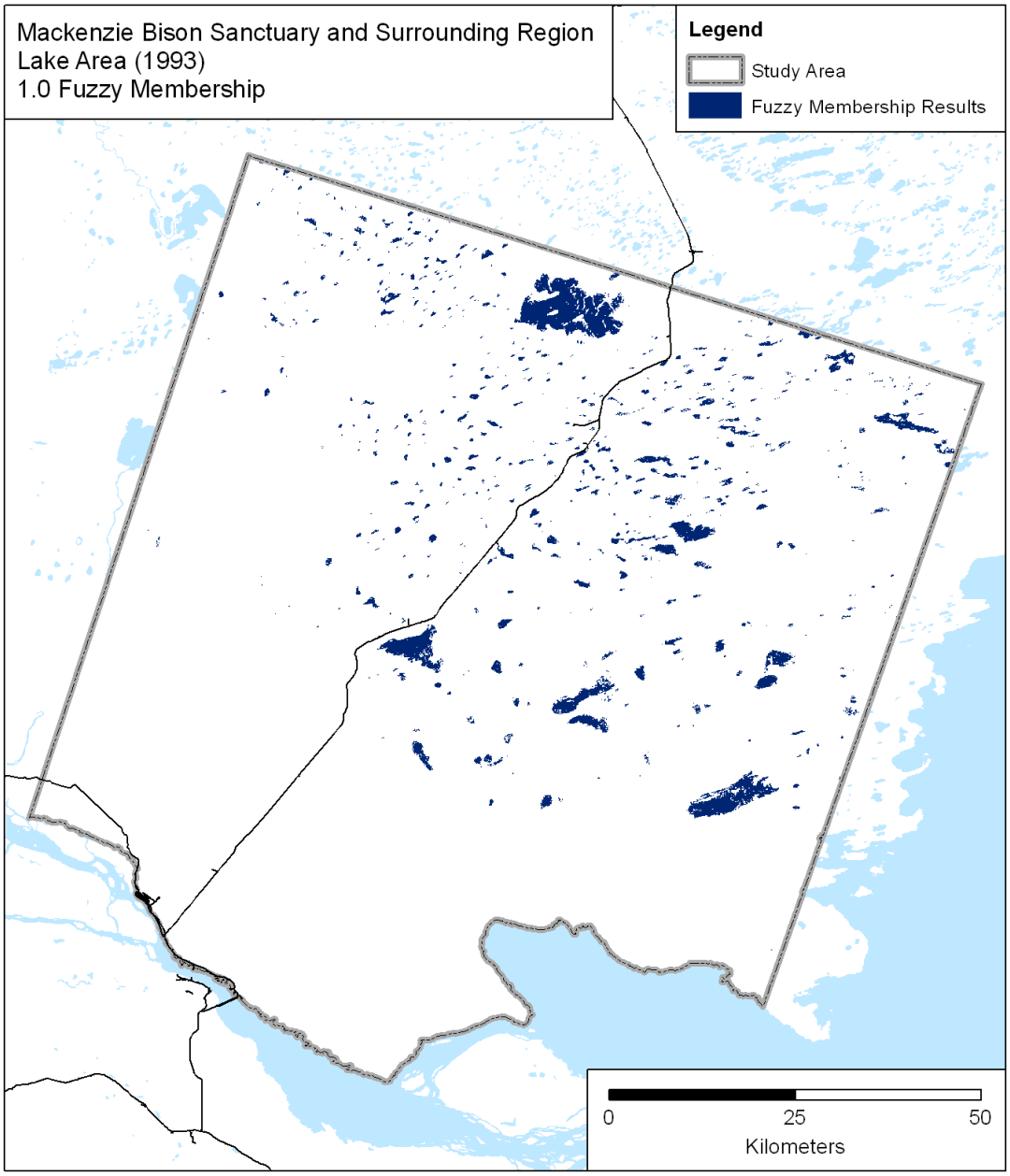
Mackenzie Bison Sanctuary and Surrounding Region
Lake Area (1993)
1.0 Fuzzy Membership
Legend
Study Area
Fuzzy Membership Results
0
25
50
Kilometers

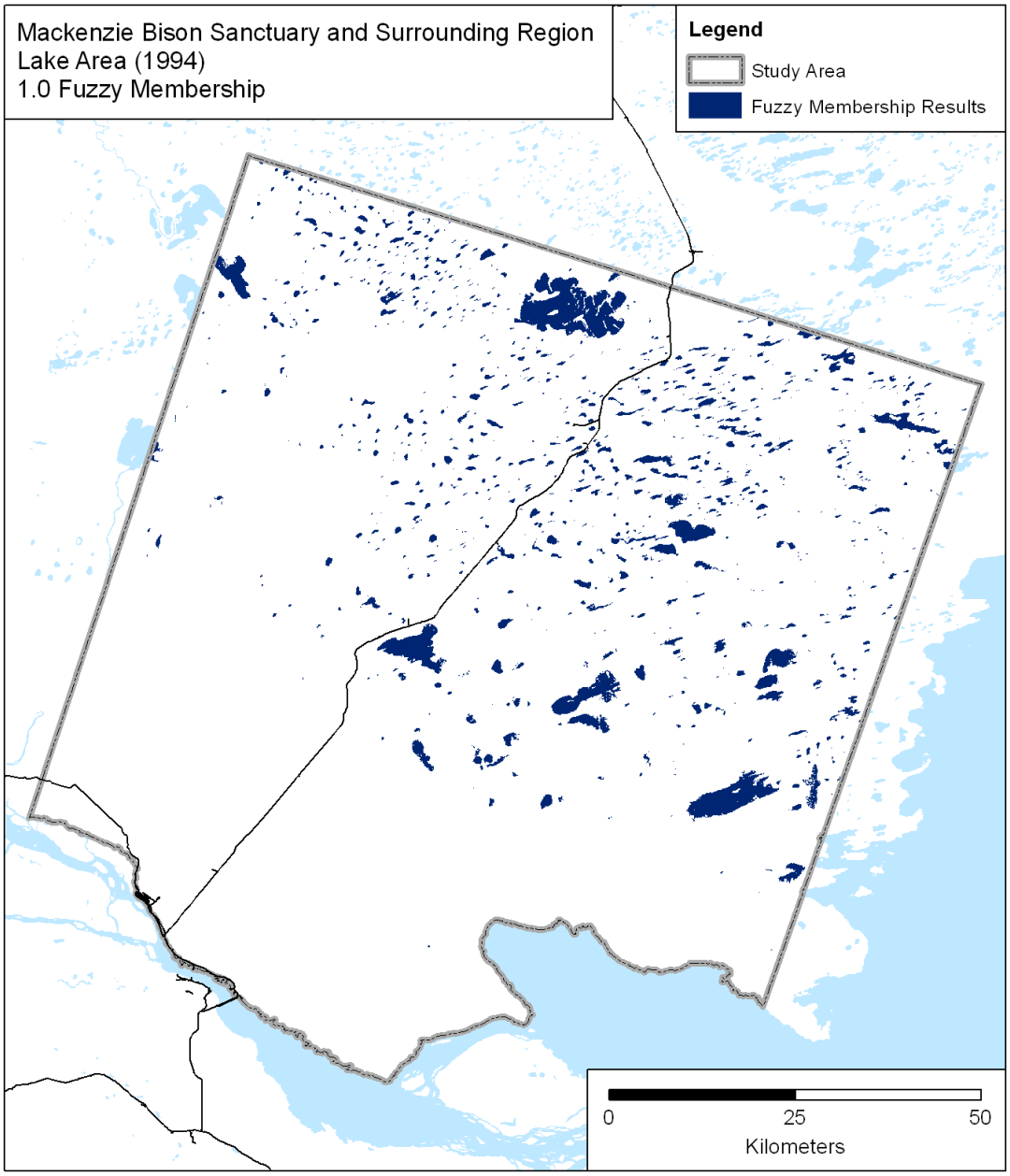
Mackenzie Bison Sanctuary and Surrounding Region
Lake Area (1994)
1.0 Fuzzy Membership
Legend
Study Area
Fuzzy Membership Results
0
25
50
Kilometers

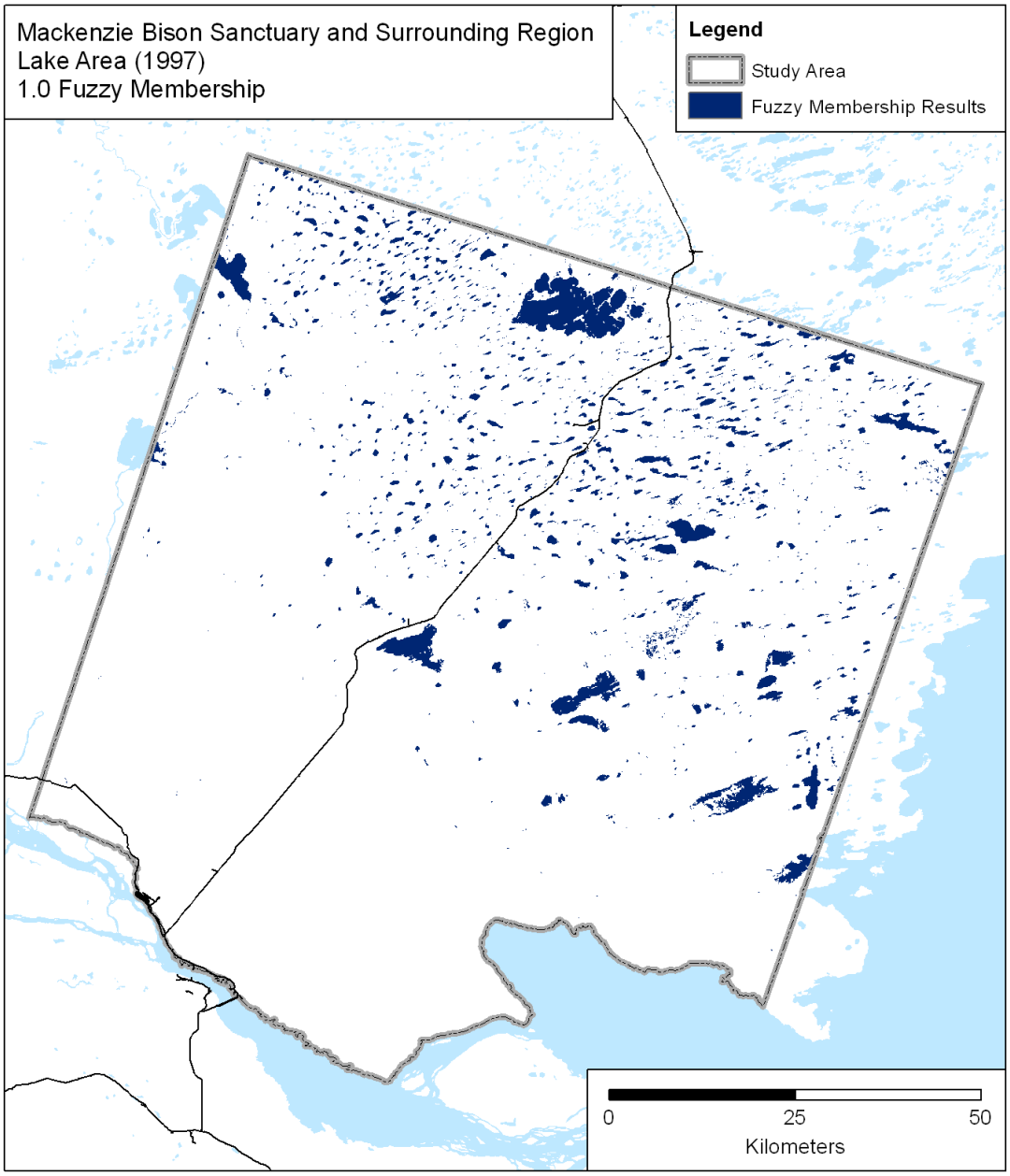
Mackenzie Bison Sanctuary and Surrounding Region
Lake Area (1997)
1.0 Fuzzy Membership
Legend
Study Area
Fuzzy Membership Results
0
25
50
Kilometers

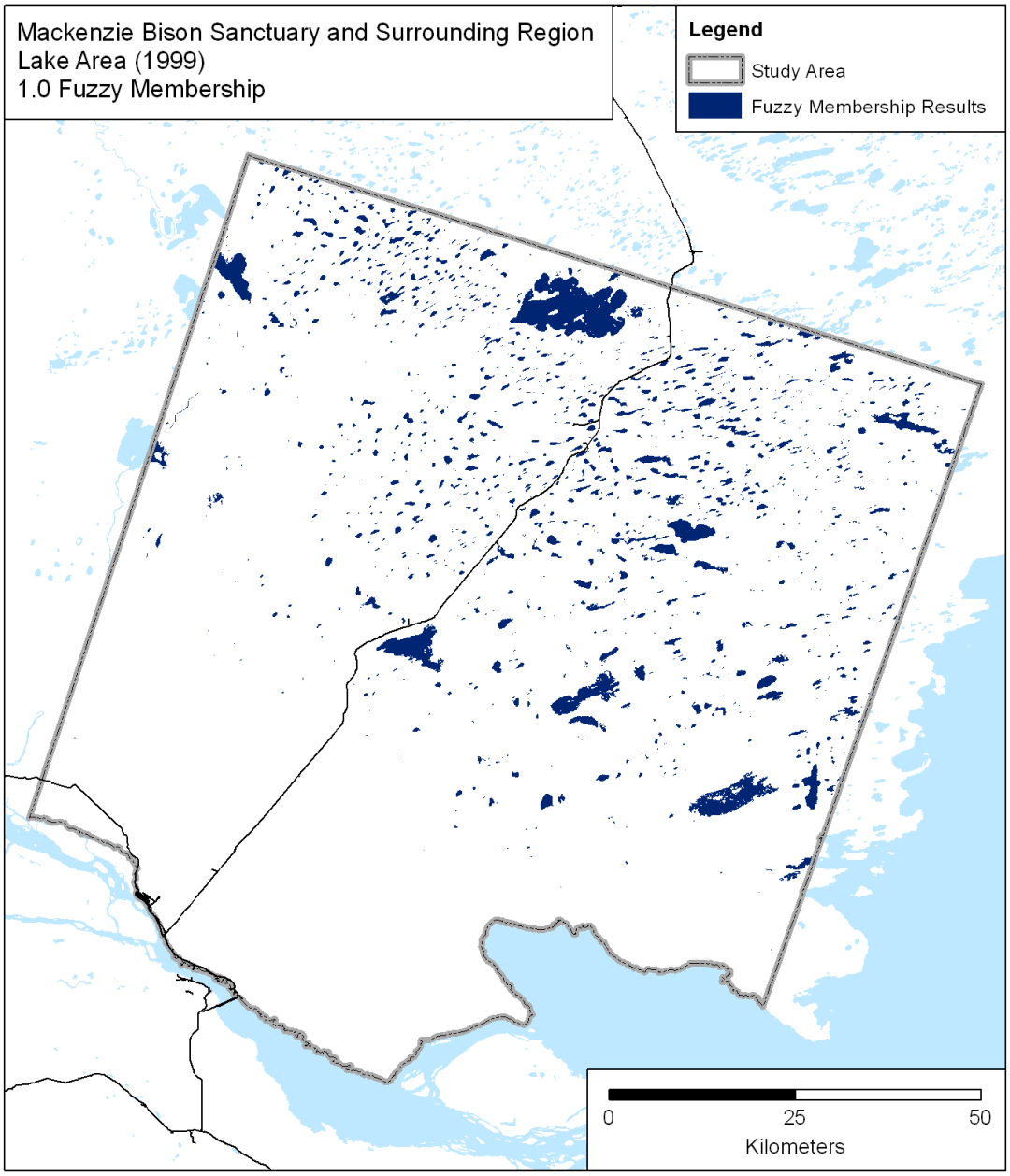
Mackenzie Bison Sanctuary and Surrounding Region
Lake Area (1999)
1.0 Fuzzy Membership
Legend
Study Area
Fuzzy Membership Results
0
25
50
Kilometers

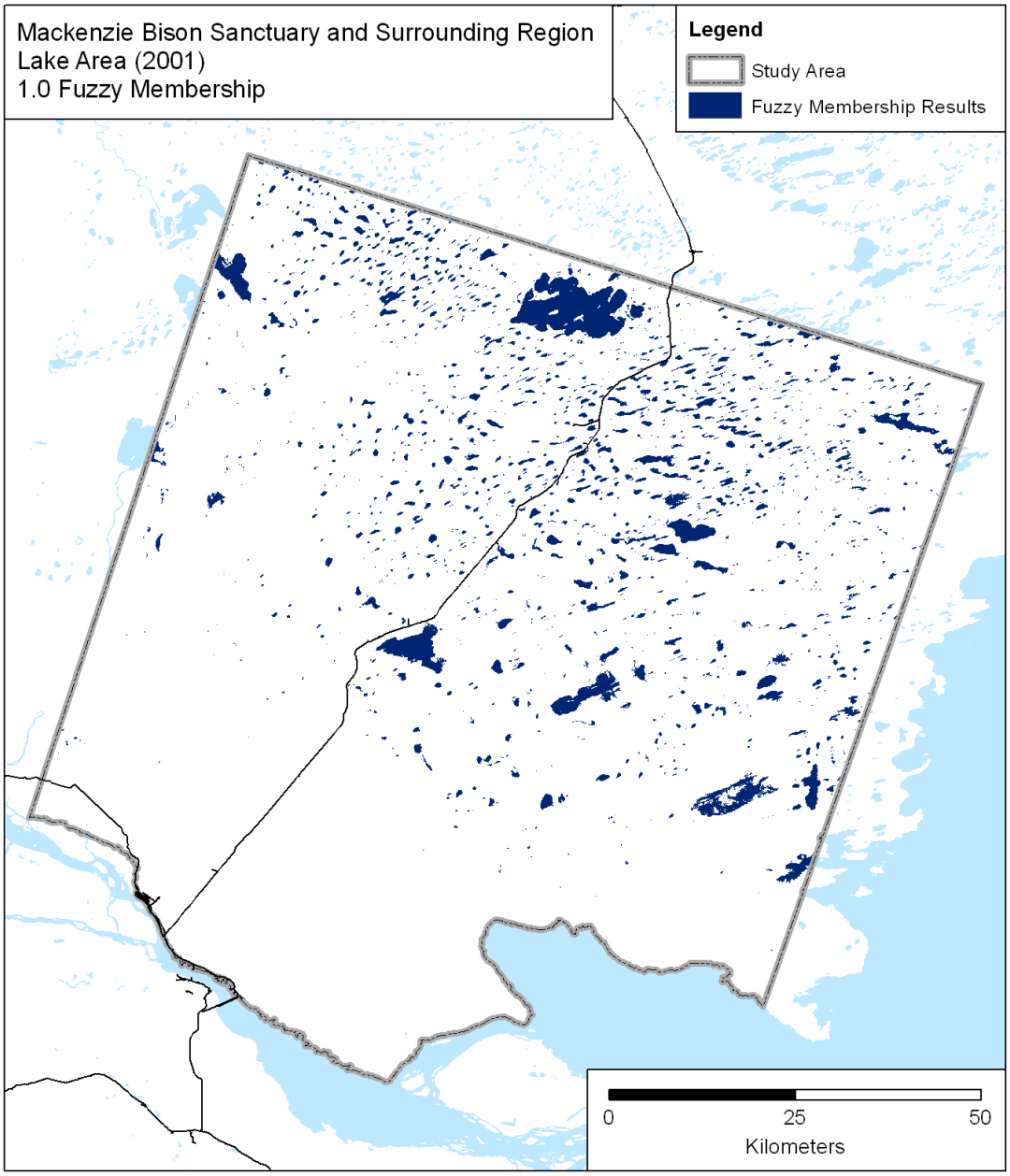
Mackenzie Bison Sanctuary and Surrounding Region
Lake Area (2001)
1.0 Fuzzy Membership
Legend
Study Area
Fuzzy Membership Results
0
25
50
Kilometers

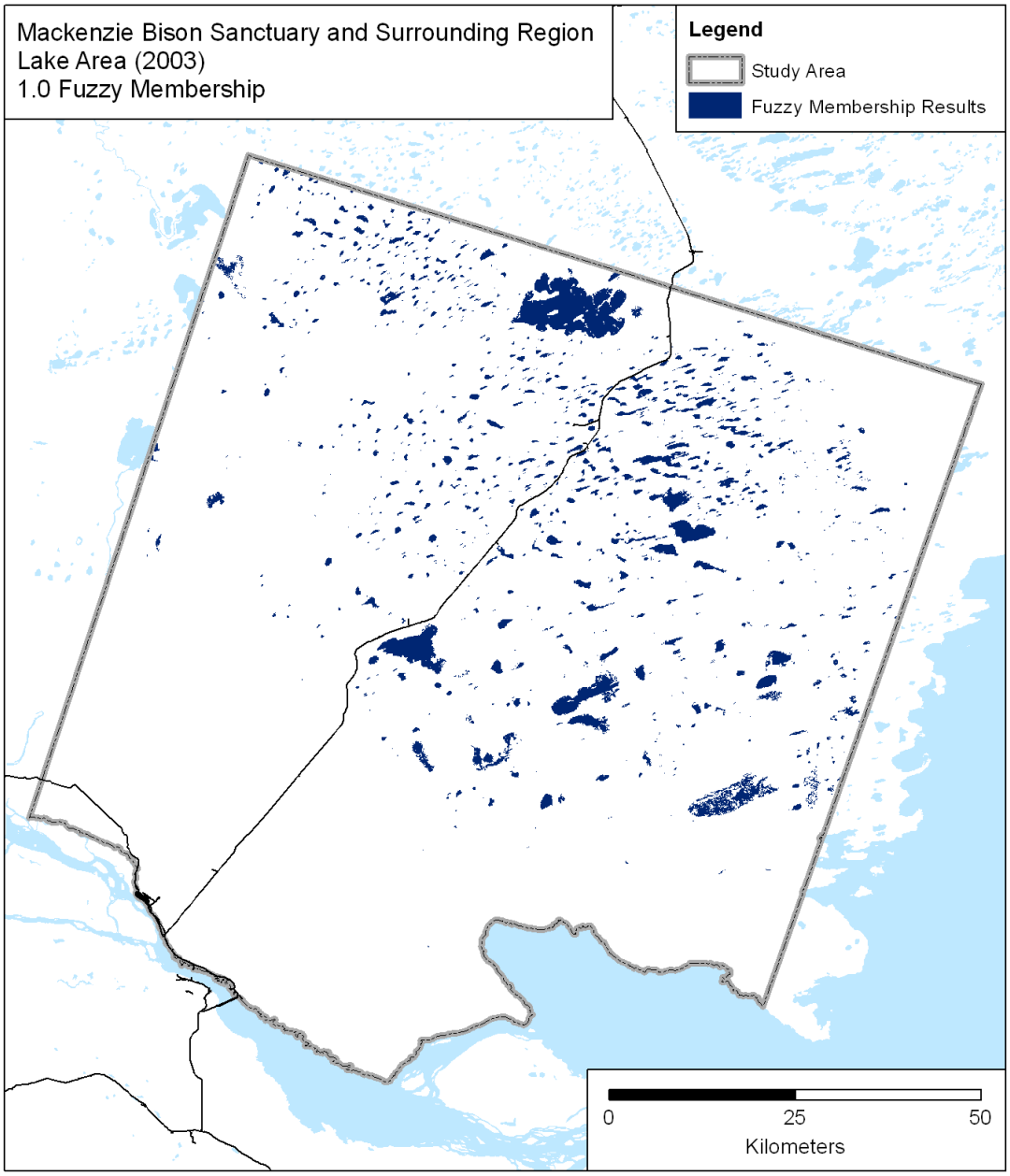
Mackenzie Bison Sanctuary and Surrounding Region
Lake Area (2003)
1.0 Fuzzy Membership
Legend
Study Area
Fuzzy Membership Results
0
25
50
Kilometers

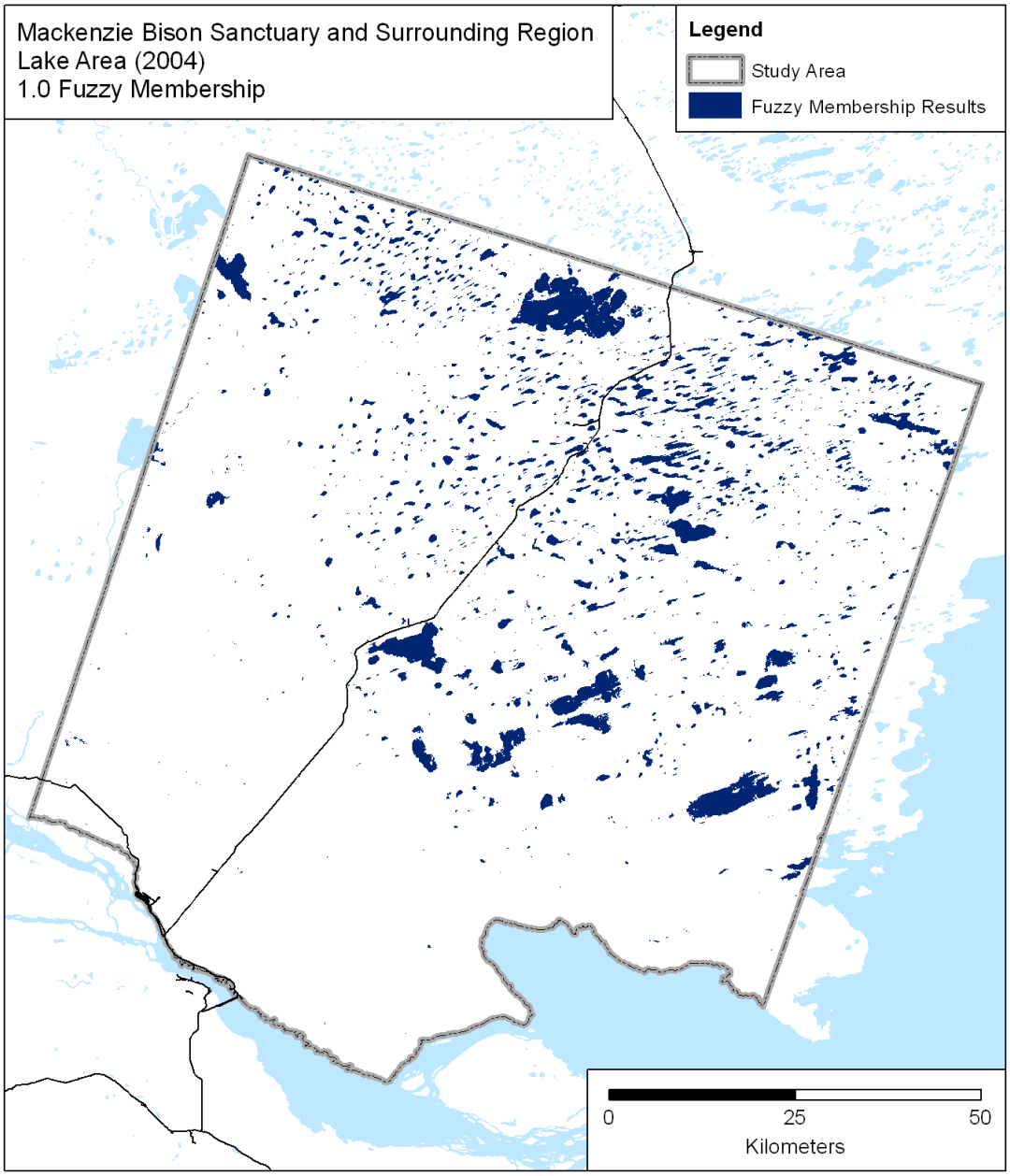
Mackenzie Bison Sanctuary and Surrounding Region
Lake Area (2004)
1.0 Fuzzy Membership
Legend
Study Area
Fuzzy Membership Results
0
25
50
Kilometers

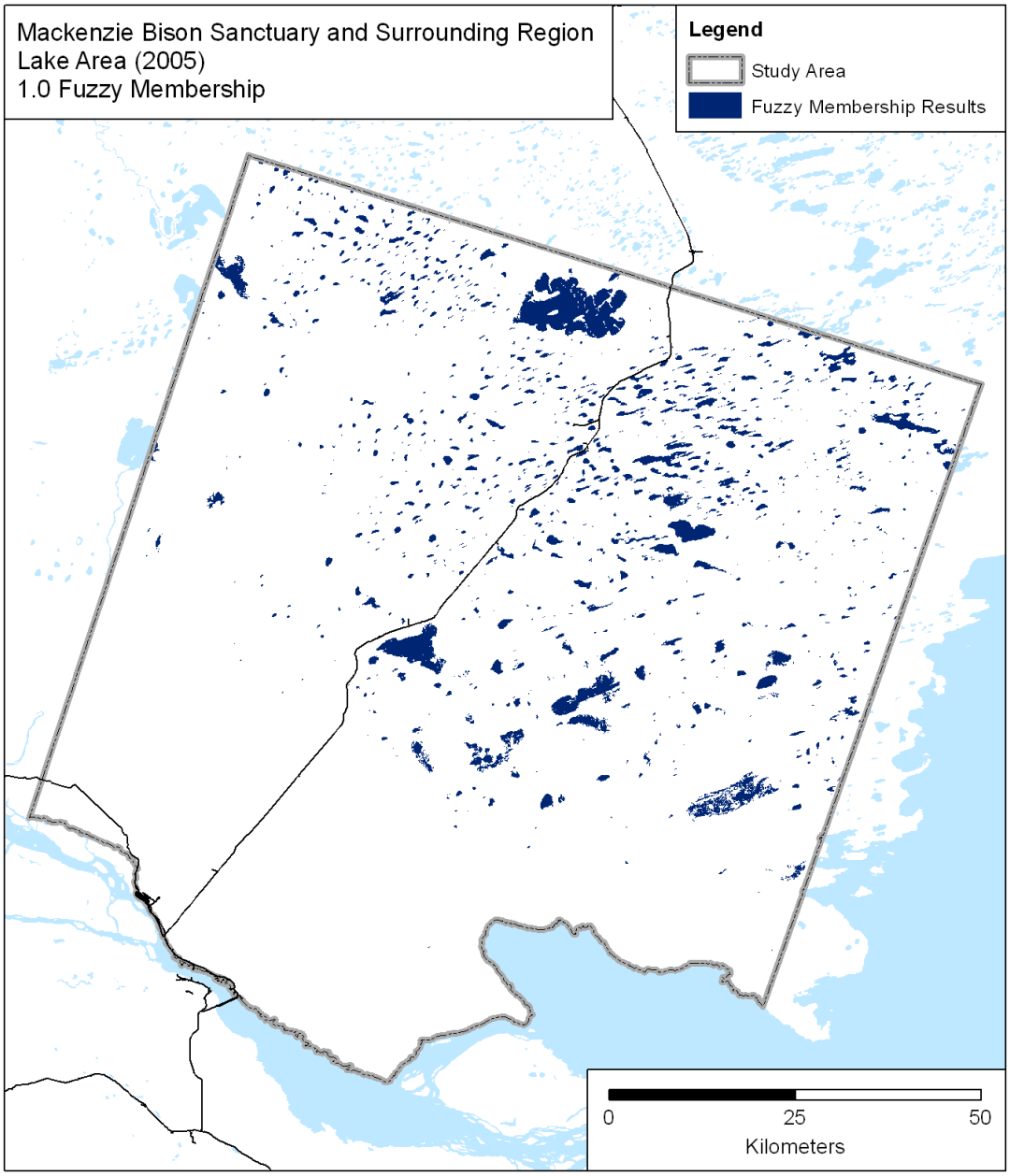
Mackenzie Bison Sanctuary and Surrounding Region
Lake Area (2005)
1.0 Fuzzy Membership
Legend
Study Area
Fuzzy Membership Results
0
25
50
Kilometers

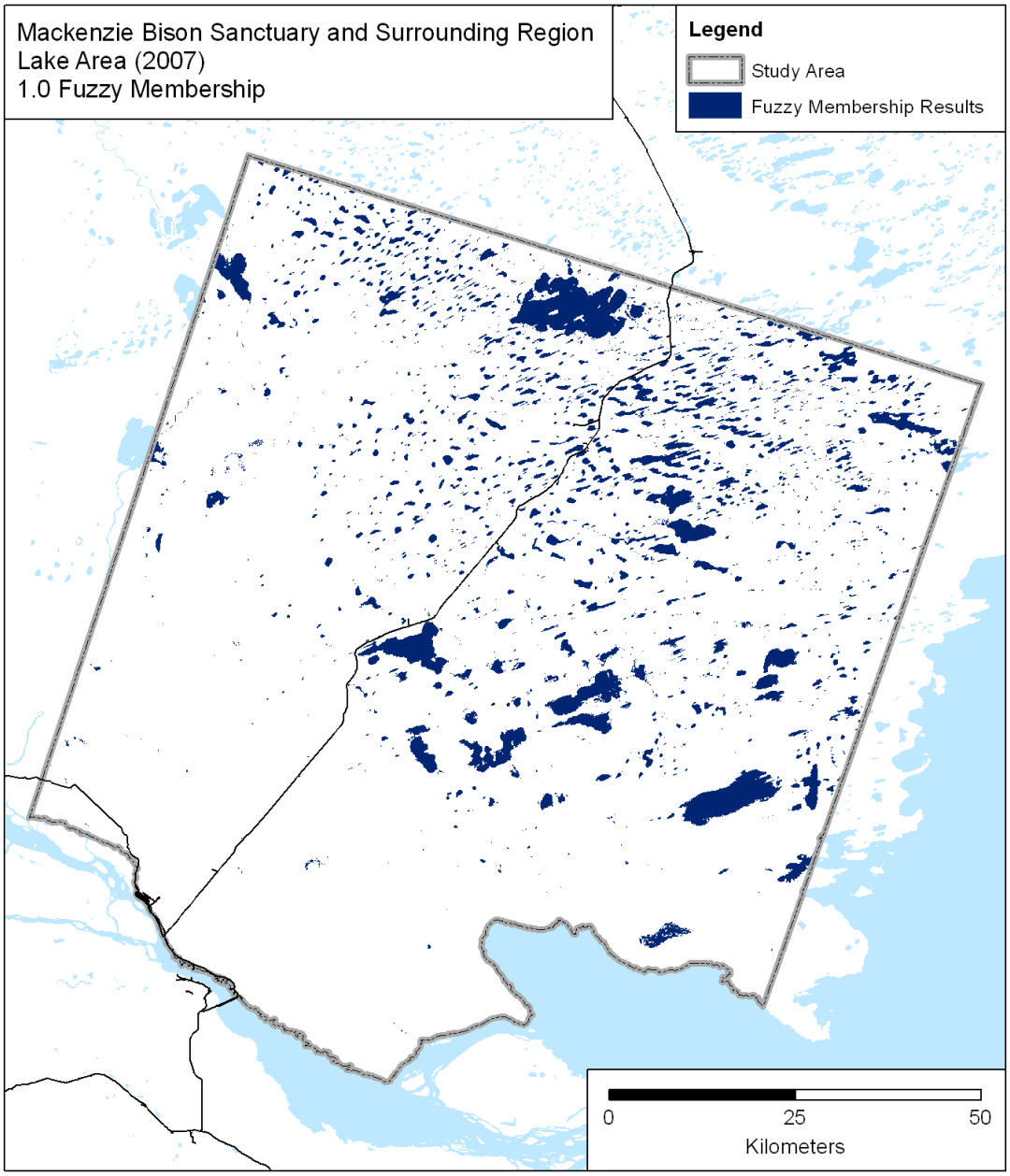
Mackenzie Bison Sanctuary and Surrounding Region
Lake Area (2007)
1.0 Fuzzy Membership
Legend
Study Area
Fuzzy Membership Results
0
25
50
Kilometers

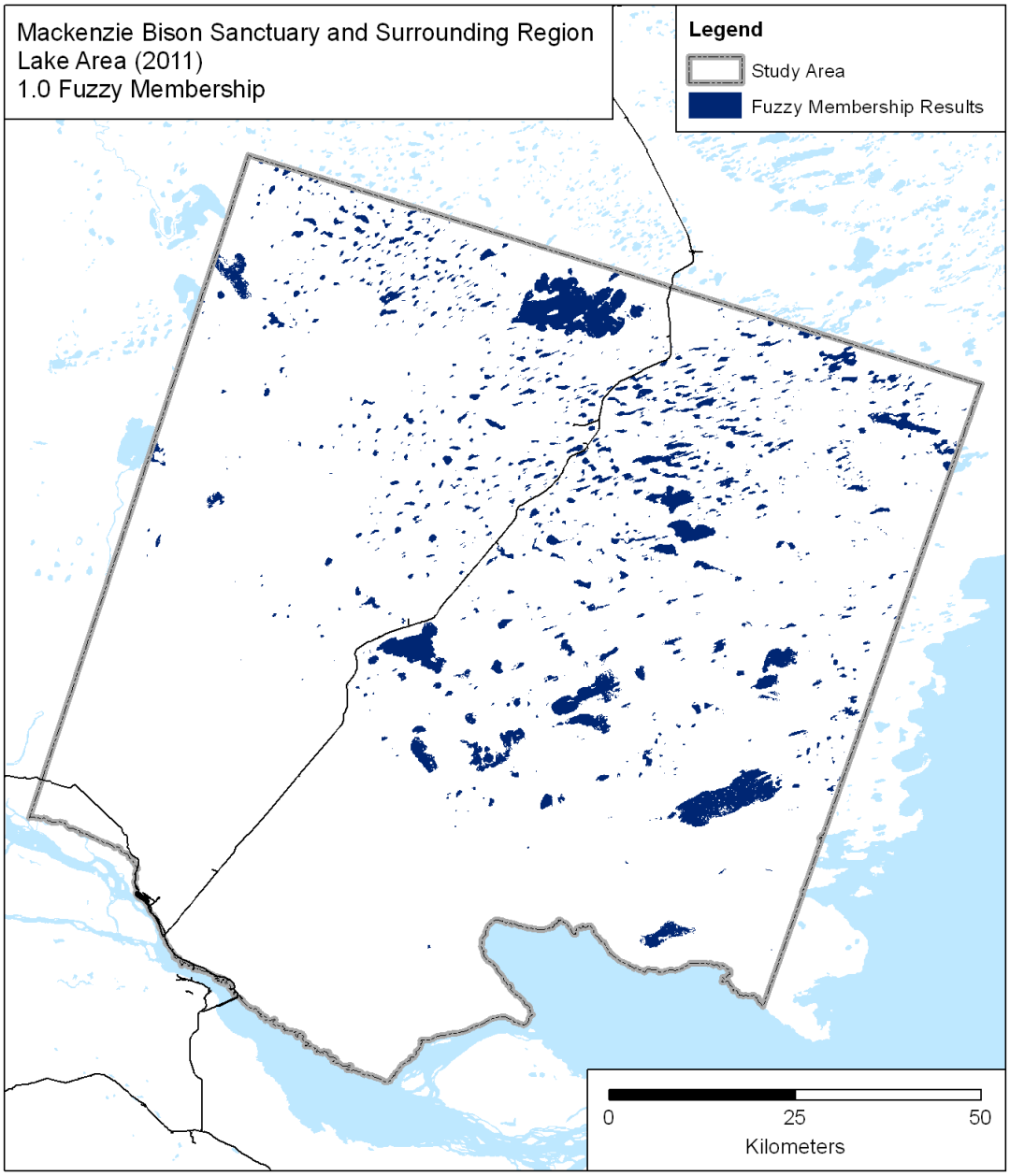
Mackenzie Bison Sanctuary and Surrounding Region
Lake Area (2011)
1.0 Fuzzy Membership
Legend
Study Area
Fuzzy Membership Results
0
25
50
Kilometers

APPENDIX B
≥0.5 FUZZY MEMBERSHIP RESULTS

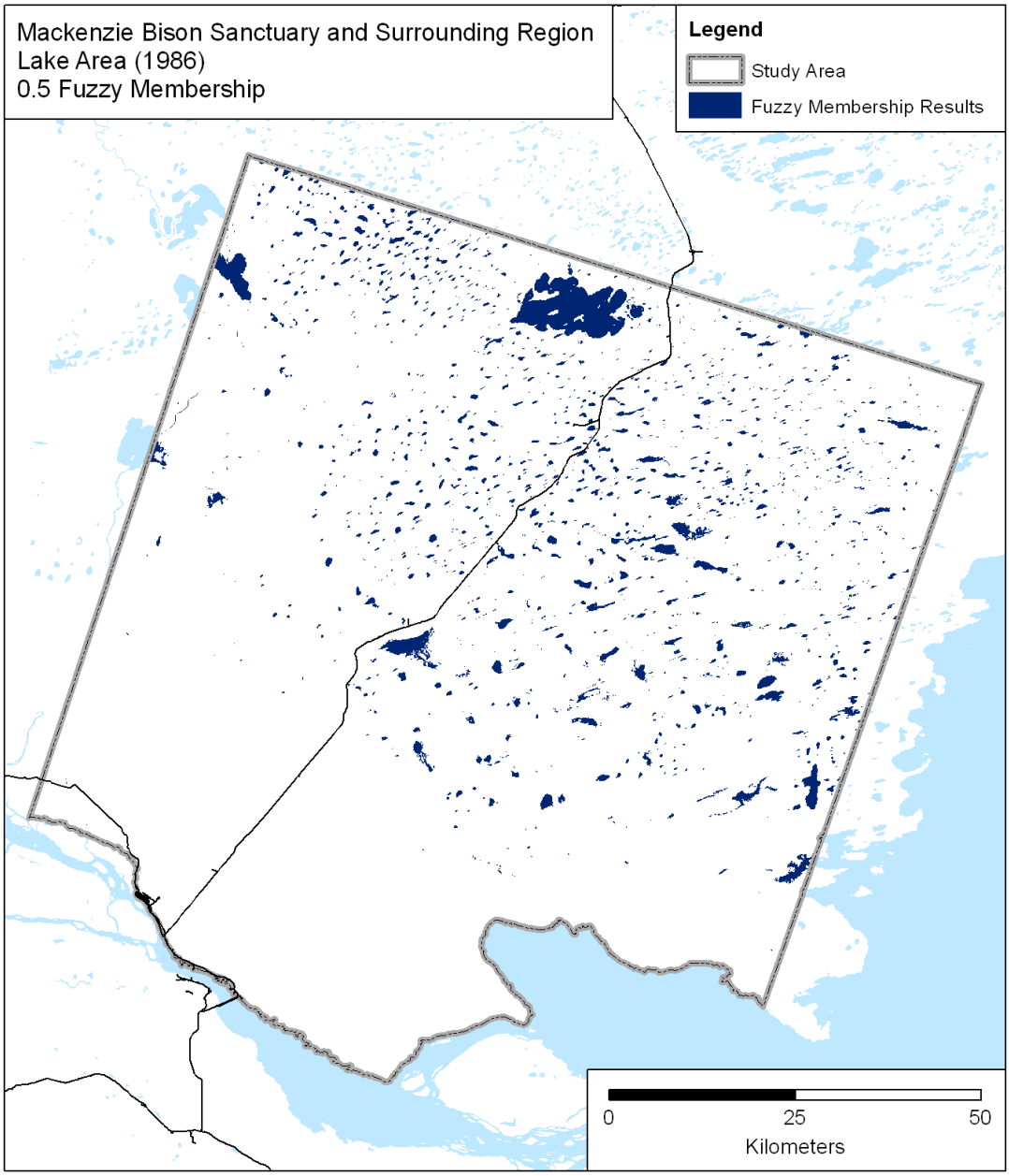

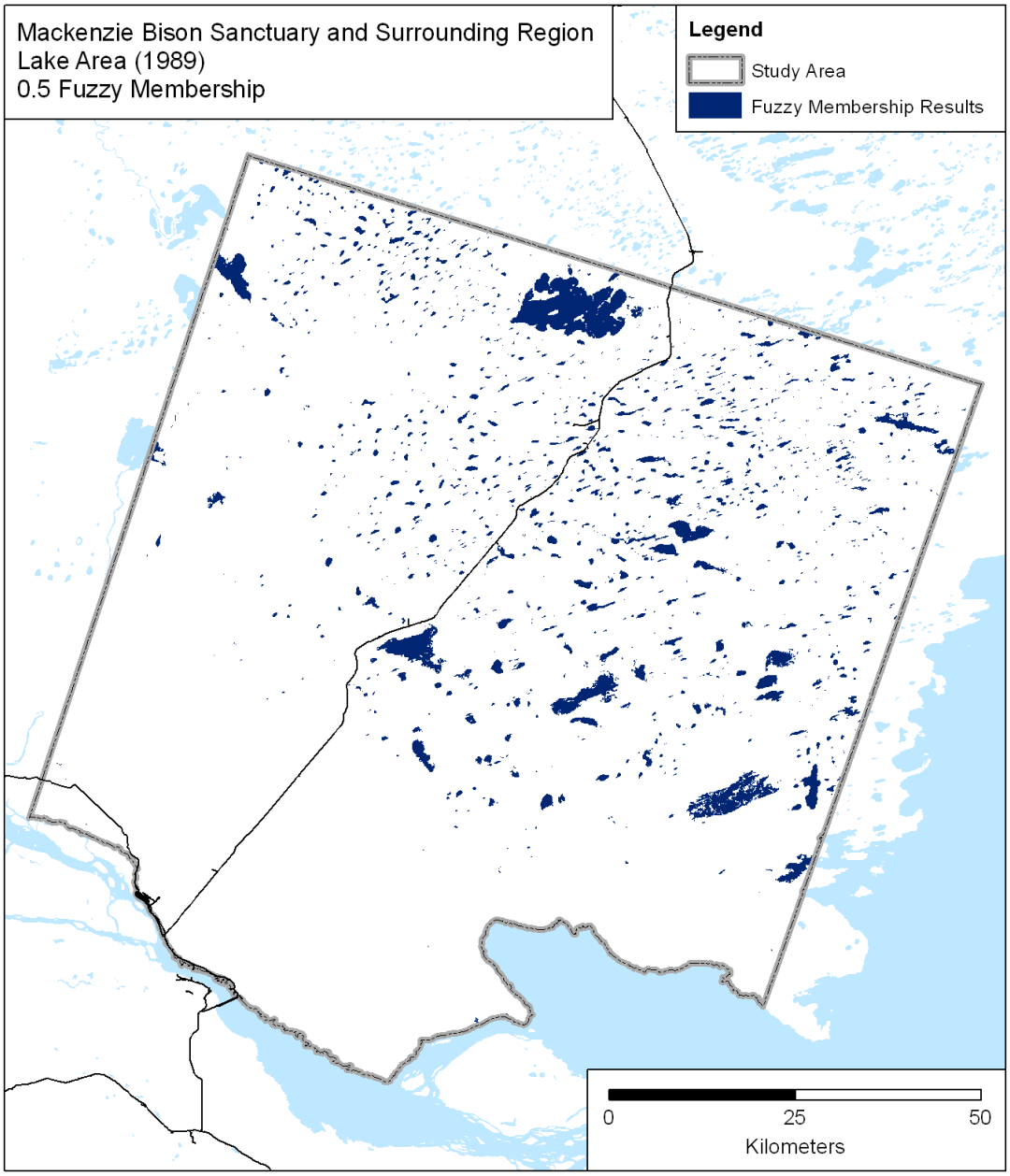
Mackenzie Bison Sanctuary and Surrounding Region
Lake Area (1989)
0.5 Fuzzy Membership
Legend
Study Area
Fuzzy Membership Results
0
25
50
Kilometers

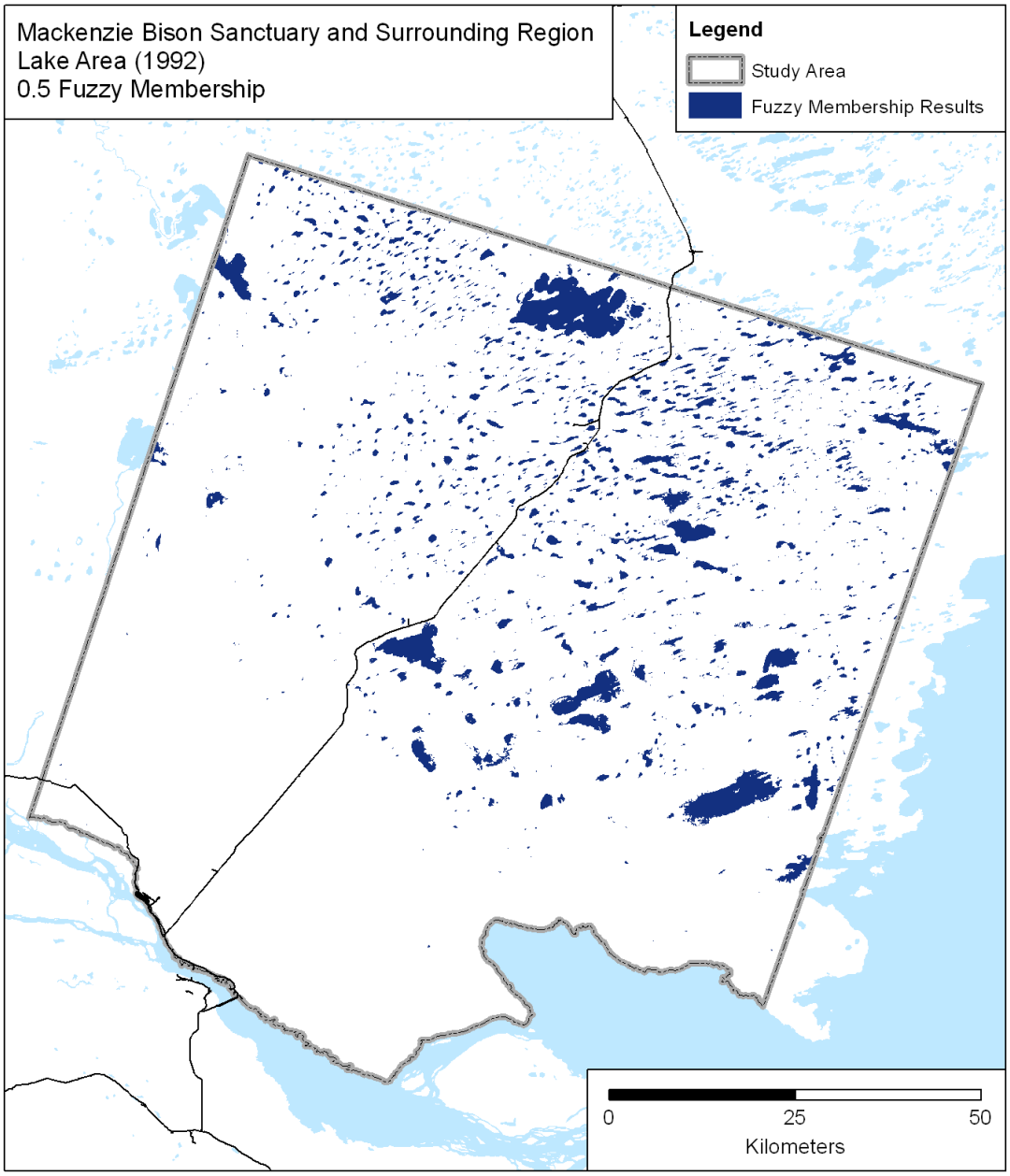
Mackenzie Bison Sanctuary and Surrounding Region
Lake Area (1992)
0.5 Fuzzy Membership
Legend
Study Area
Fuzzy Membership Results
0
25
50
Kilometers

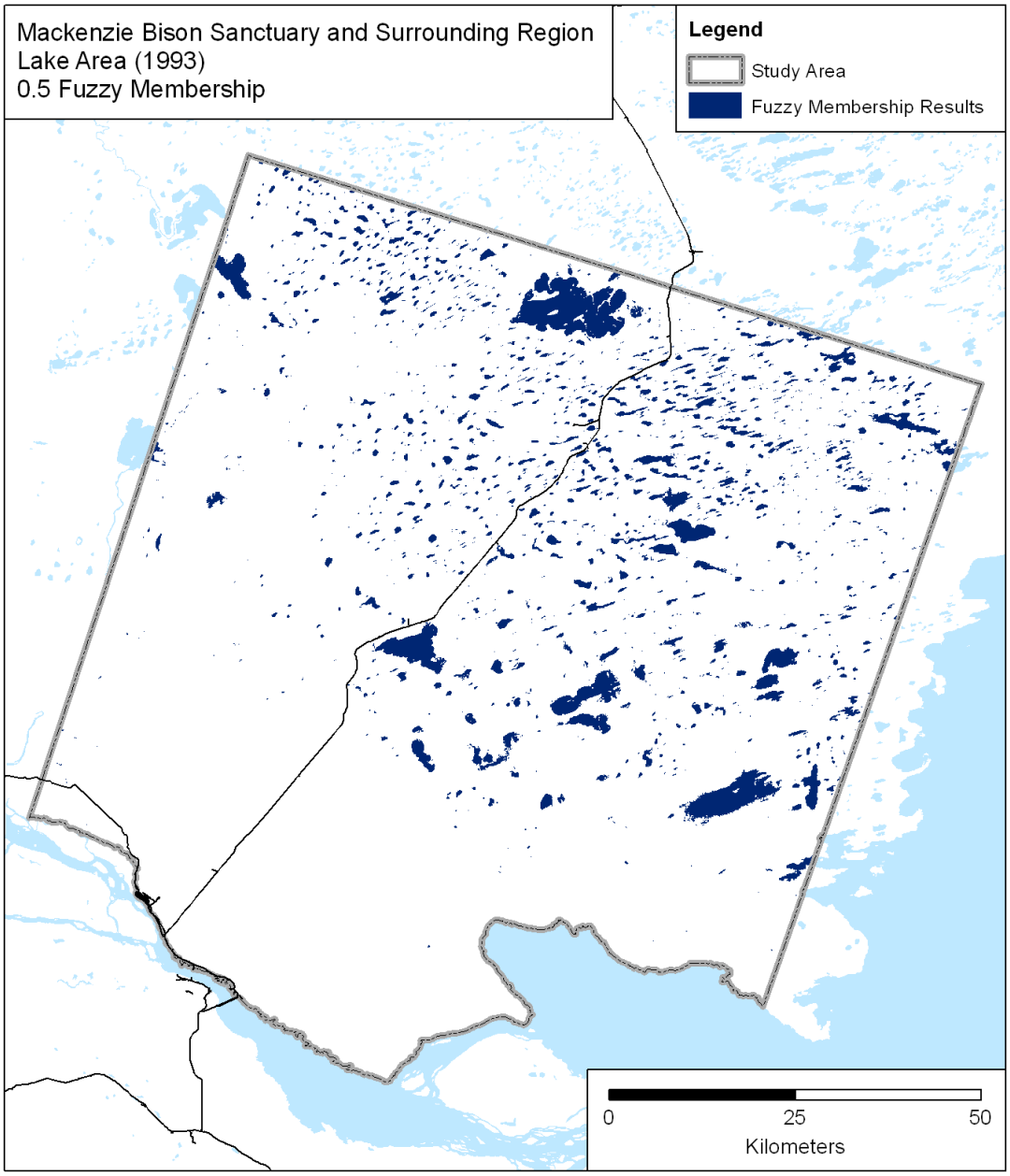
Mackenzie Bison Sanctuary and Surrounding Region
Lake Area (1993)
0.5 Fuzzy Membership
Legend
Study Area
Fuzzy Membership Results
0
25
50
Kilometers

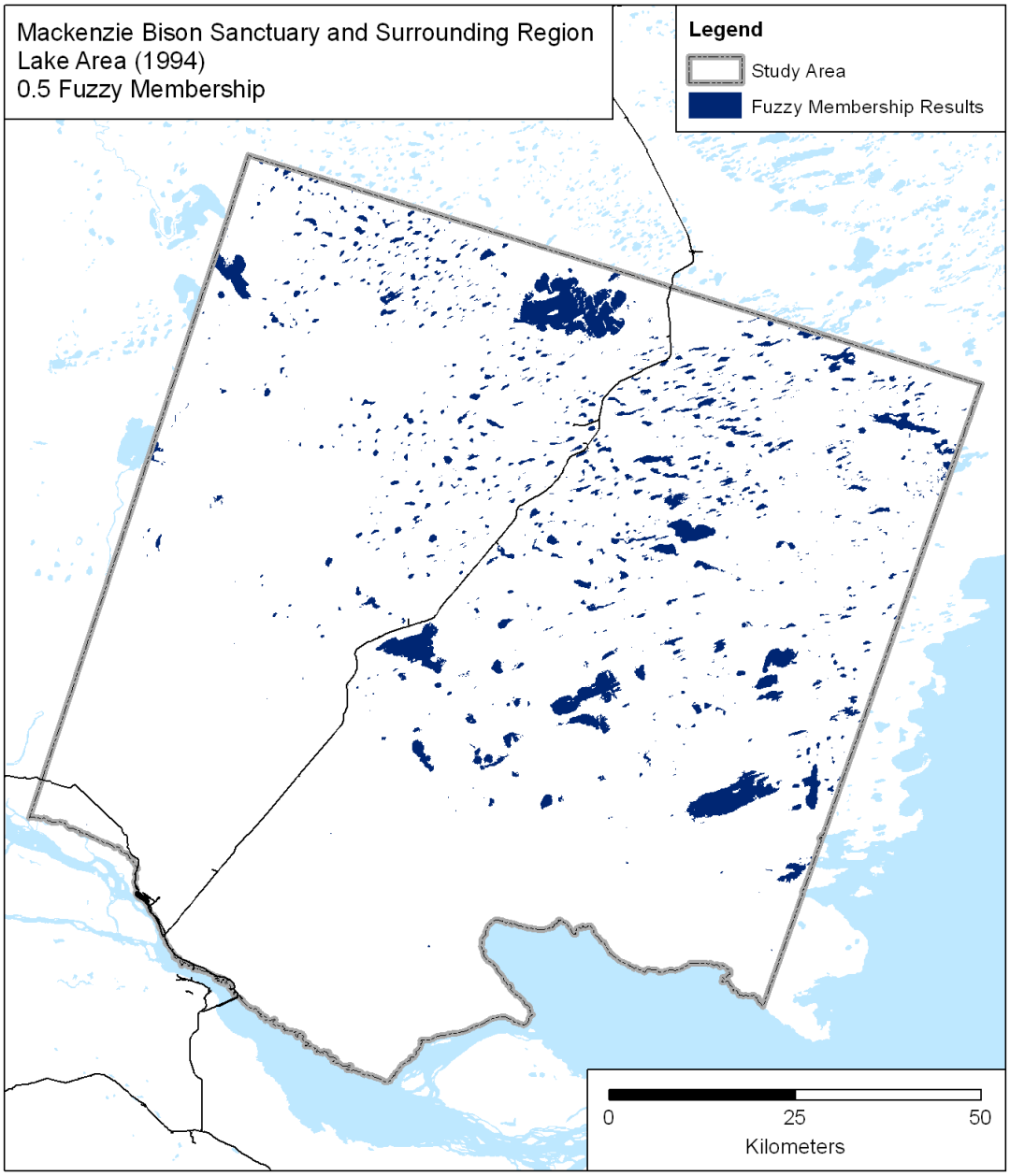
Mackenzie Bison Sanctuary and Surrounding Region
Lake Area (1994)
0.5 Fuzzy Membership
Legend
Study Area
Fuzzy Membership Results
0
25
50
Kilometers

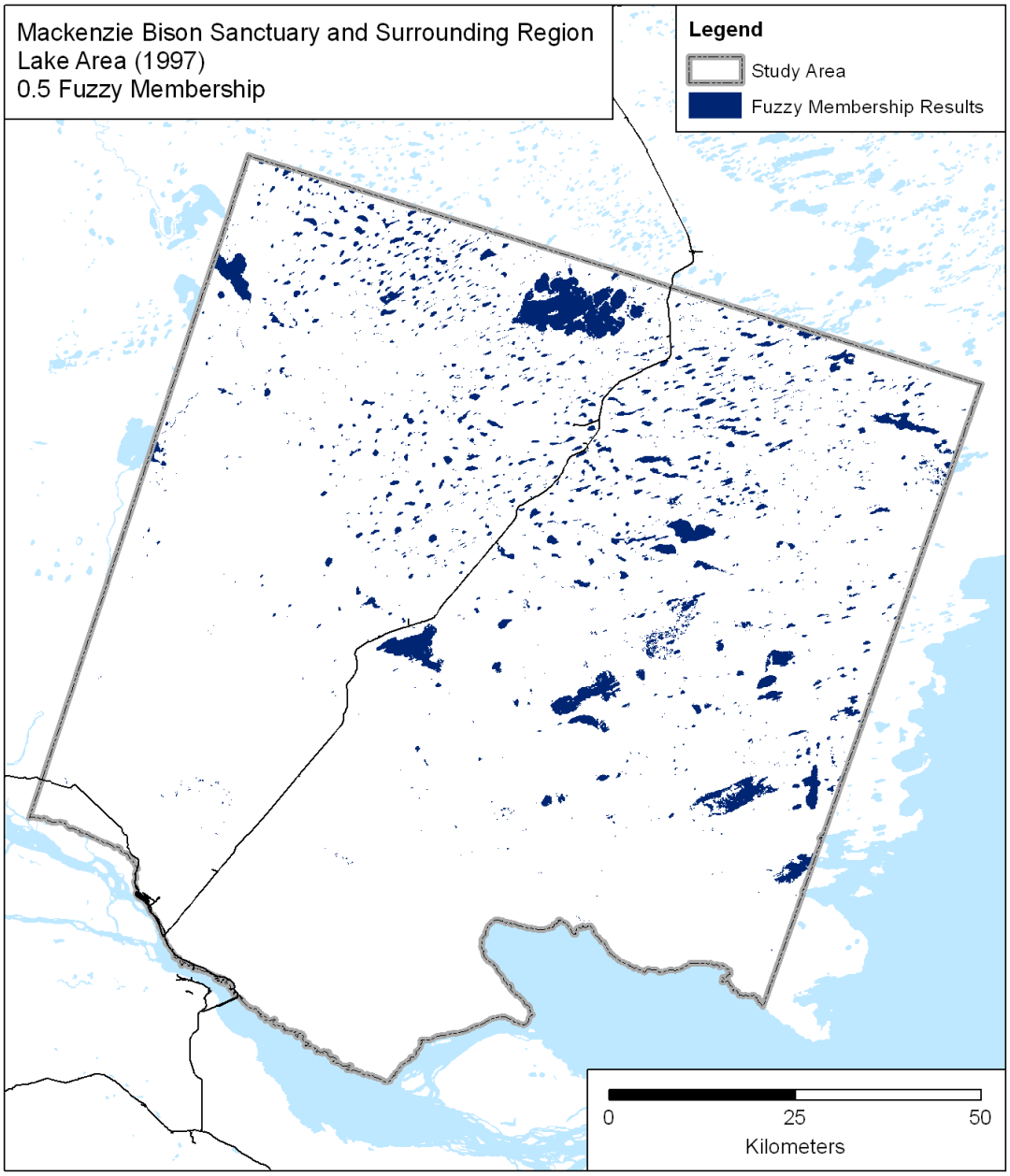
Mackenzie Bison Sanctuary and Surrounding Region
Lake Area (1997)
0.5 Fuzzy Membership
Legend
Study Area
Fuzzy Membership Results
0
25
50
Kilometers

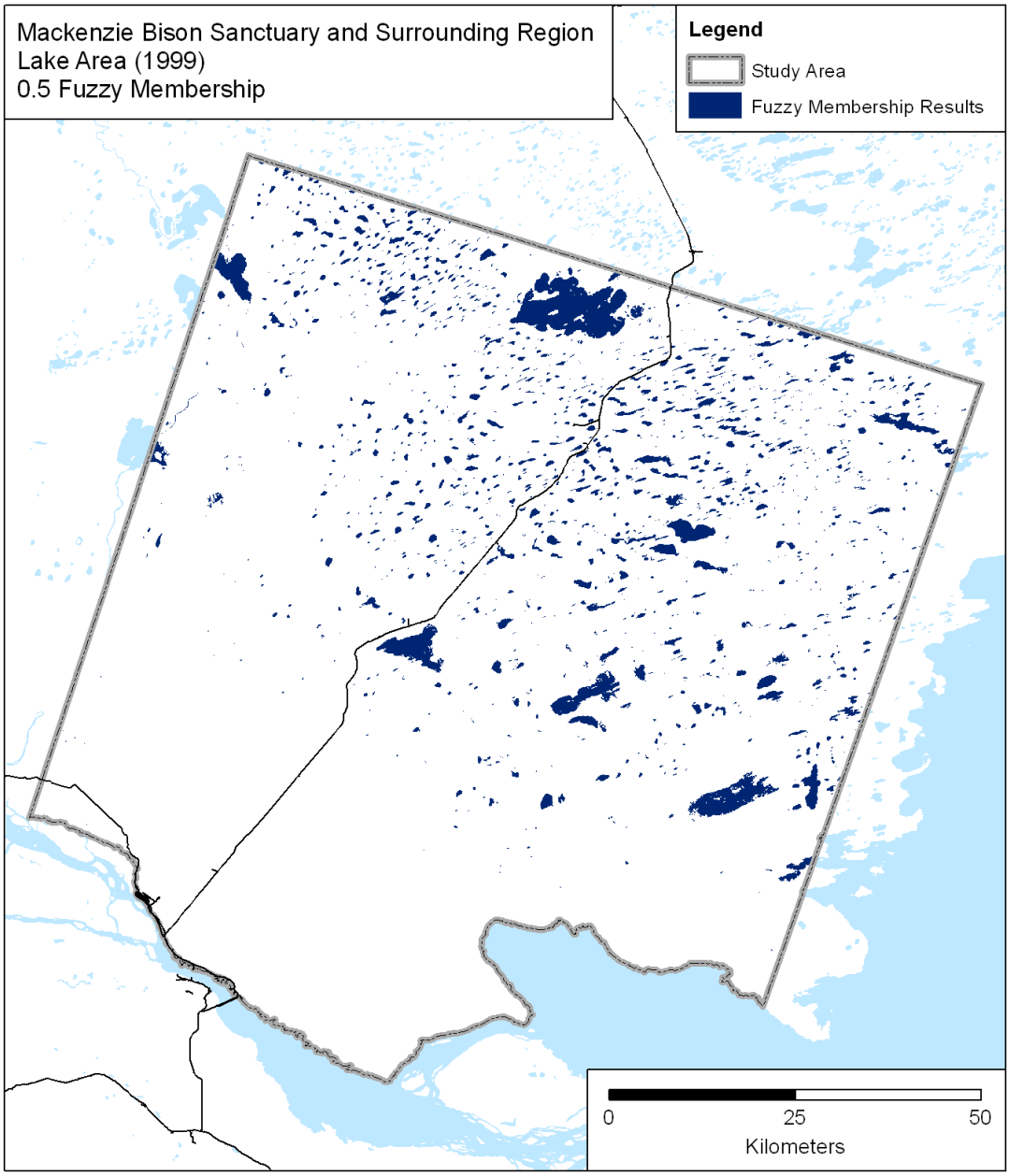
Mackenzie Bison Sanctuary and Surrounding Region
Lake Area (1999)
0.5 Fuzzy Membership
Legend
Study Area
Fuzzy Membership Results
0
25
50
Kilometers

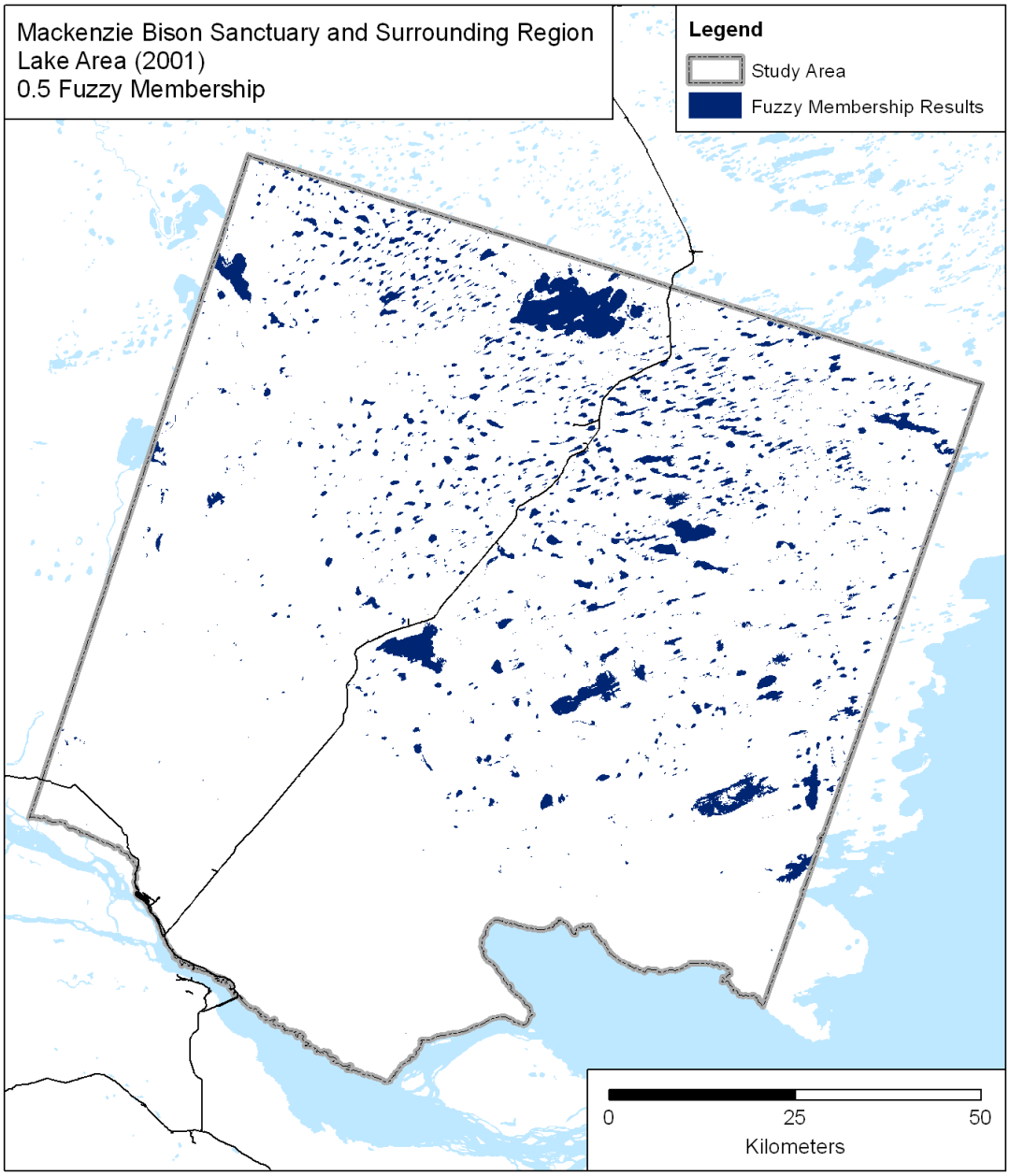
Mackenzie Bison Sanctuary and Surrounding Region
Lake Area (2001)
0.5 Fuzzy Membership
Legend
Study Area
Fuzzy Membership Results
0
25
50
Kilometers

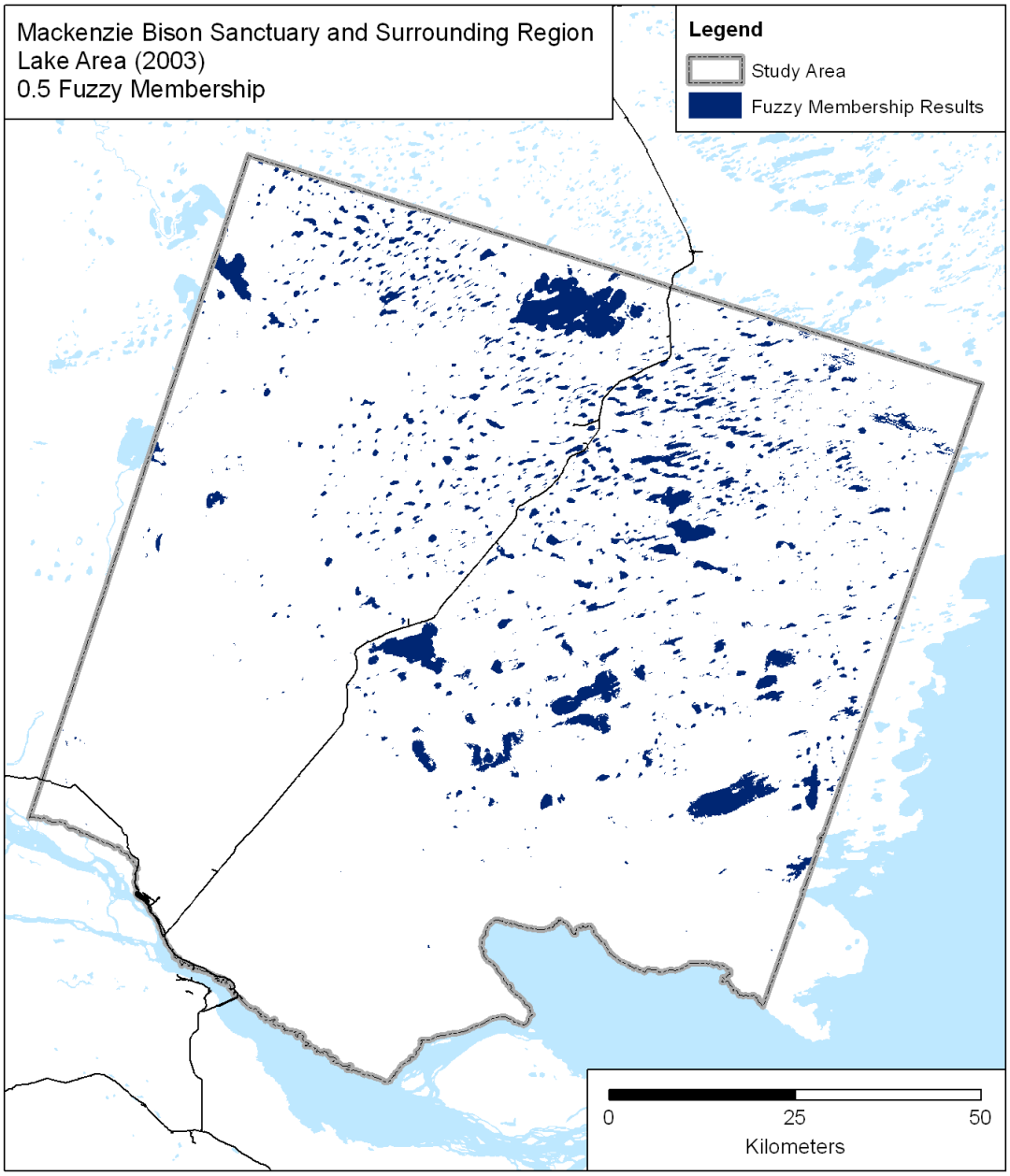
Mackenzie Bison Sanctuary and Surrounding Region
Lake Area (2003)
0.5 Fuzzy Membership
Legend
Study Area
Fuzzy Membership Results
0
25
50
Kilometers

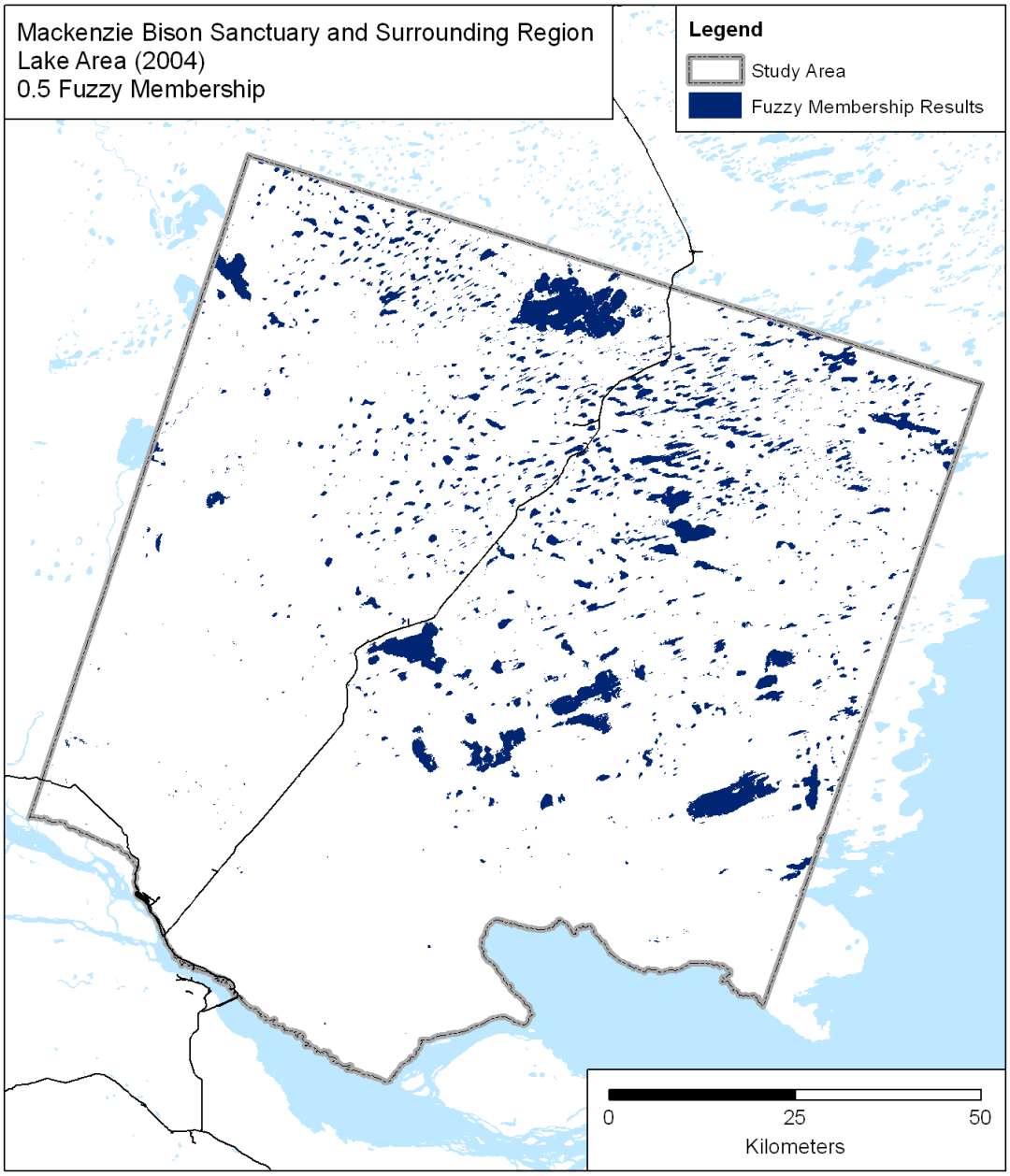
Mackenzie Bison Sanctuary and Surrounding Region
Lake Area (2004)
0.5 Fuzzy Membership
Legend
Study Area
Fuzzy Membership Results
0
25
50
Kilometers

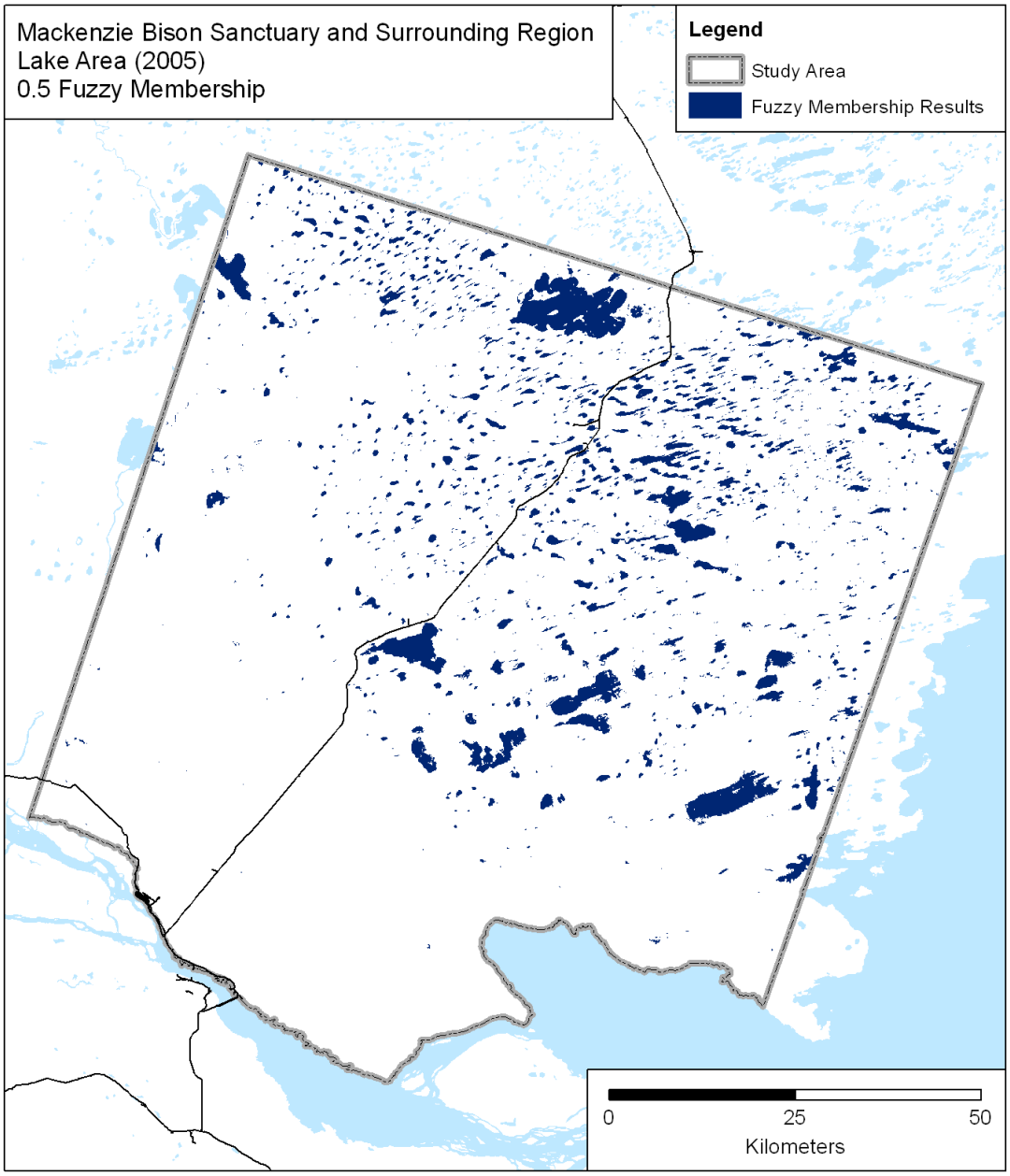
Mackenzie Bison Sanctuary and Surrounding Region
Lake Area (2005)
0.5 Fuzzy Membership
Legend
Study Area
Fuzzy Membership Results
0
25
50
Kilometers

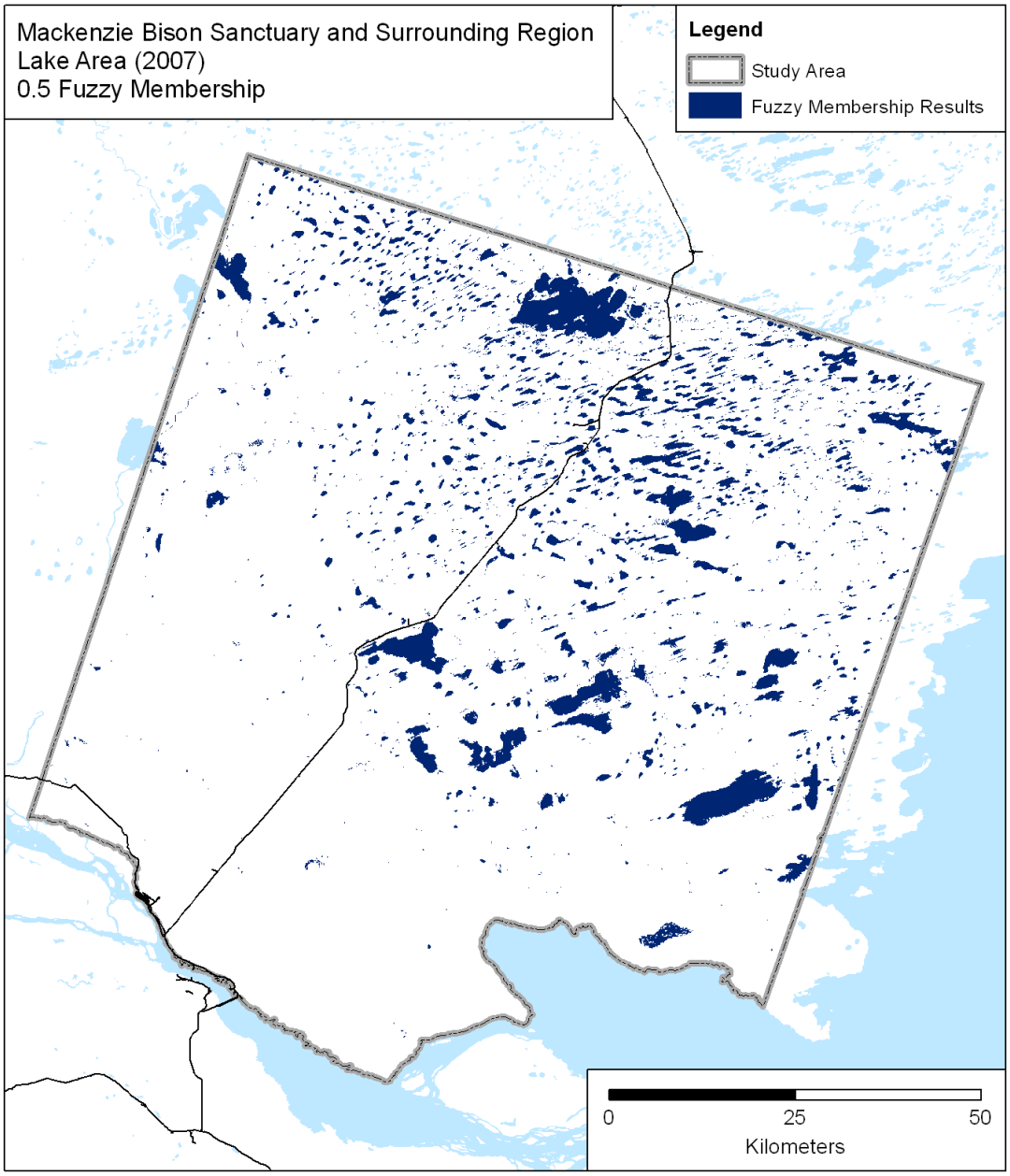
Mackenzie Bison Sanctuary and Surrounding Region
Lake Area (2007)
0.5 Fuzzy Membership
Legend
Study Area
Fuzzy Membership Results
0
25
50
Kilometers

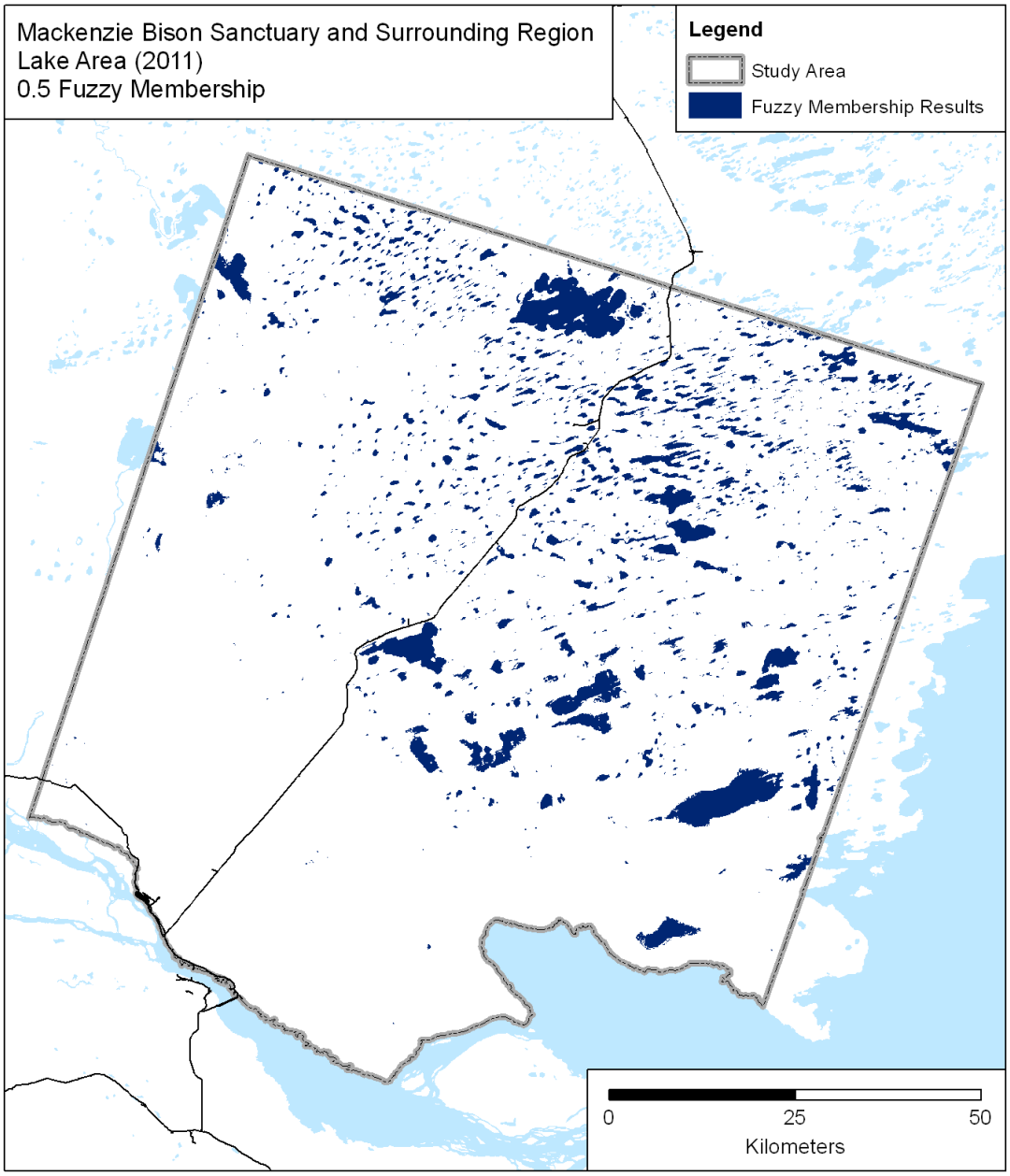
Mackenzie Bison Sanctuary and Surrounding Region
Lake Area (2011)
0.5 Fuzzy Membership
Legend
Study Area
Fuzzy Membership Results
0
25
50
Kilometers

APPENDIX C
≥0.1 FUZZY MEMBERSHIP RESULTS

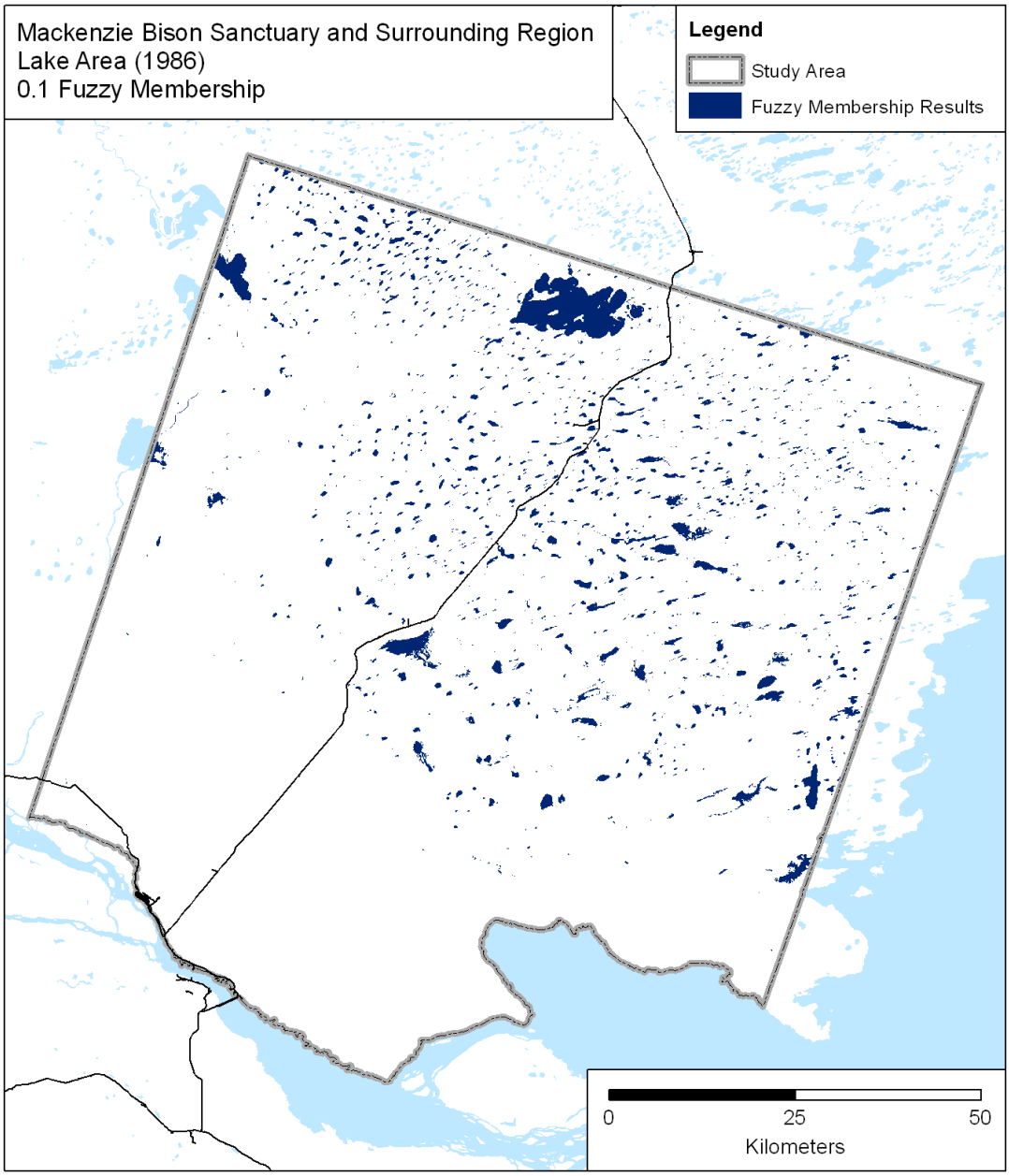

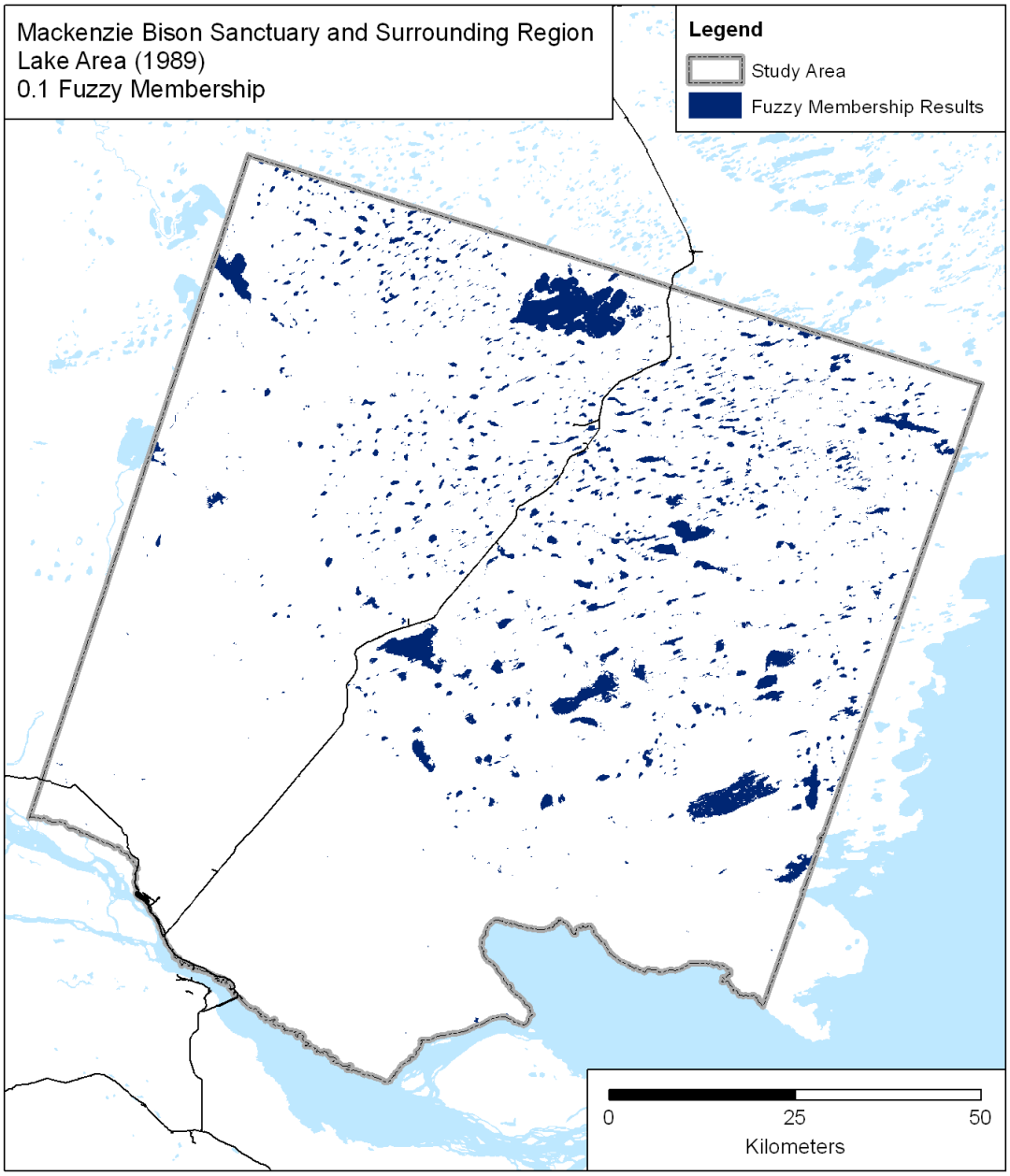
Mackenzie Bison Sanctuary and Surrounding Region
Lake Area (1989)
0.1 Fuzzy Membership
Legend
Study Area
Fuzzy Membership Results
0
25
50
Kilometers

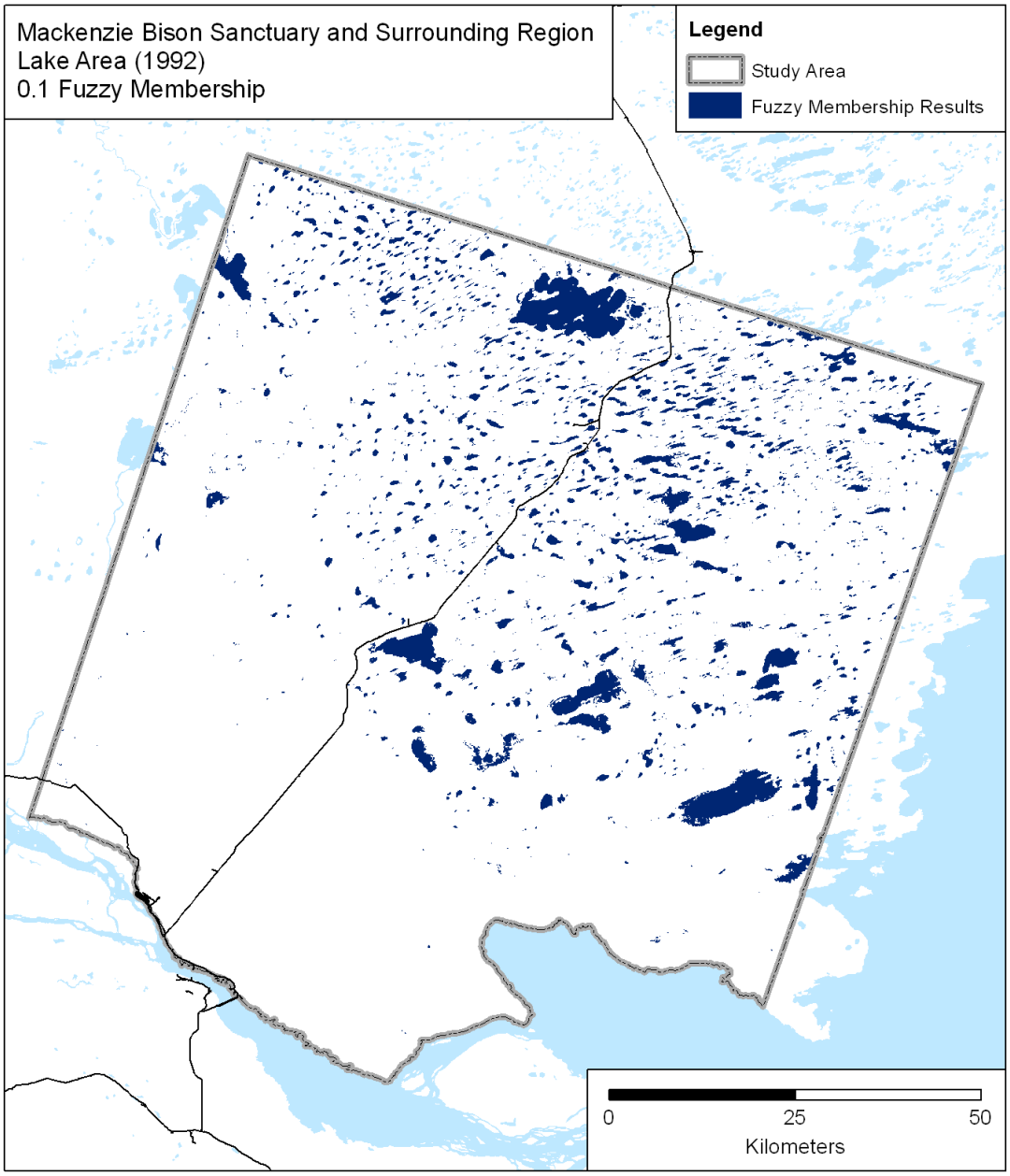
Mackenzie Bison Sanctuary and Surrounding Region
Lake Area (1992)
0.1 Fuzzy Membership
Legend
Study Area
Fuzzy Membership Results
0
25
50
Kilometers

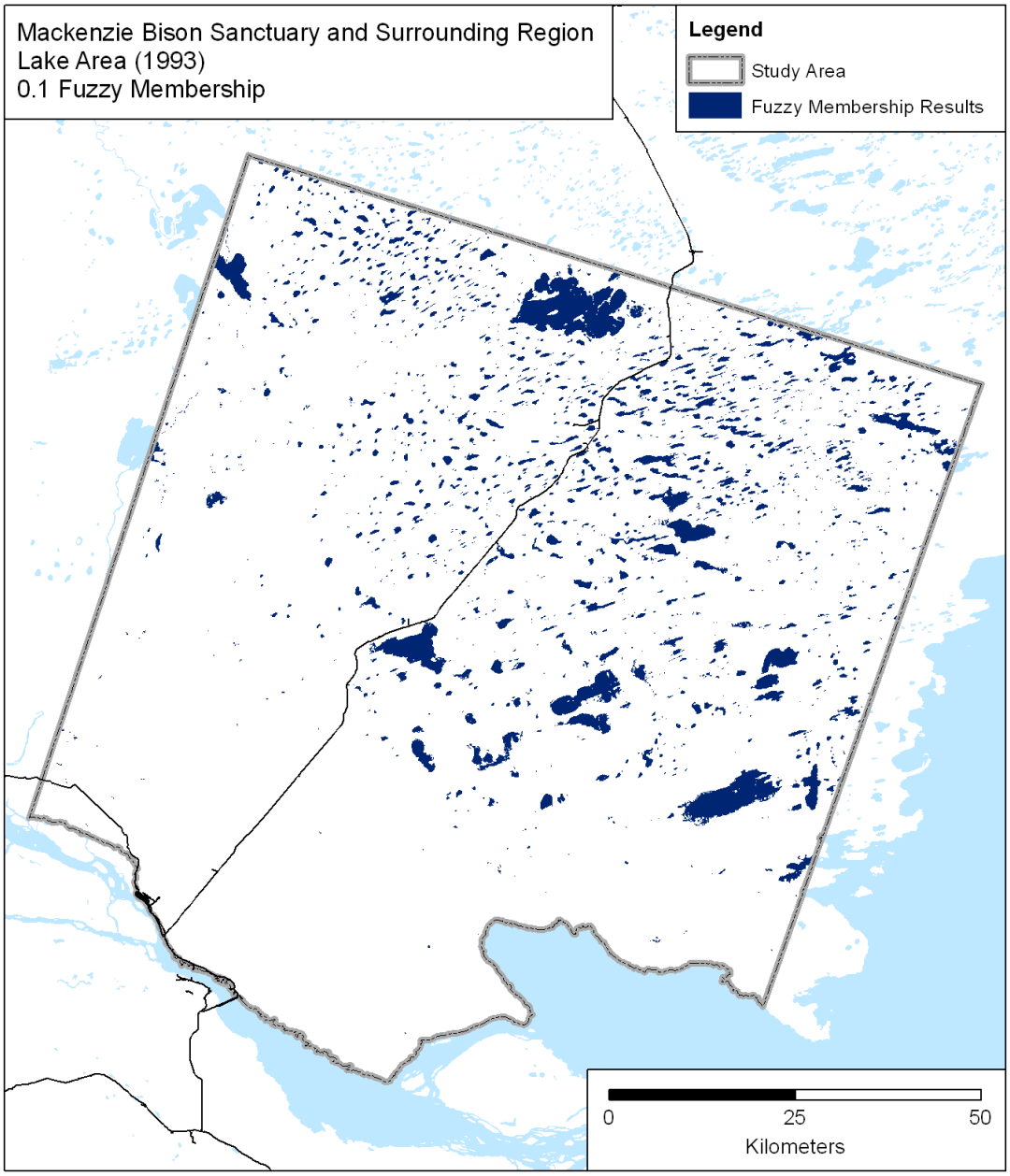
Mackenzie Bison Sanctuary and Surrounding Region
Lake Area (1993)
0.1 Fuzzy Membership
Legend
Study Area
Fuzzy Membership Results
0
25
50
Kilometers

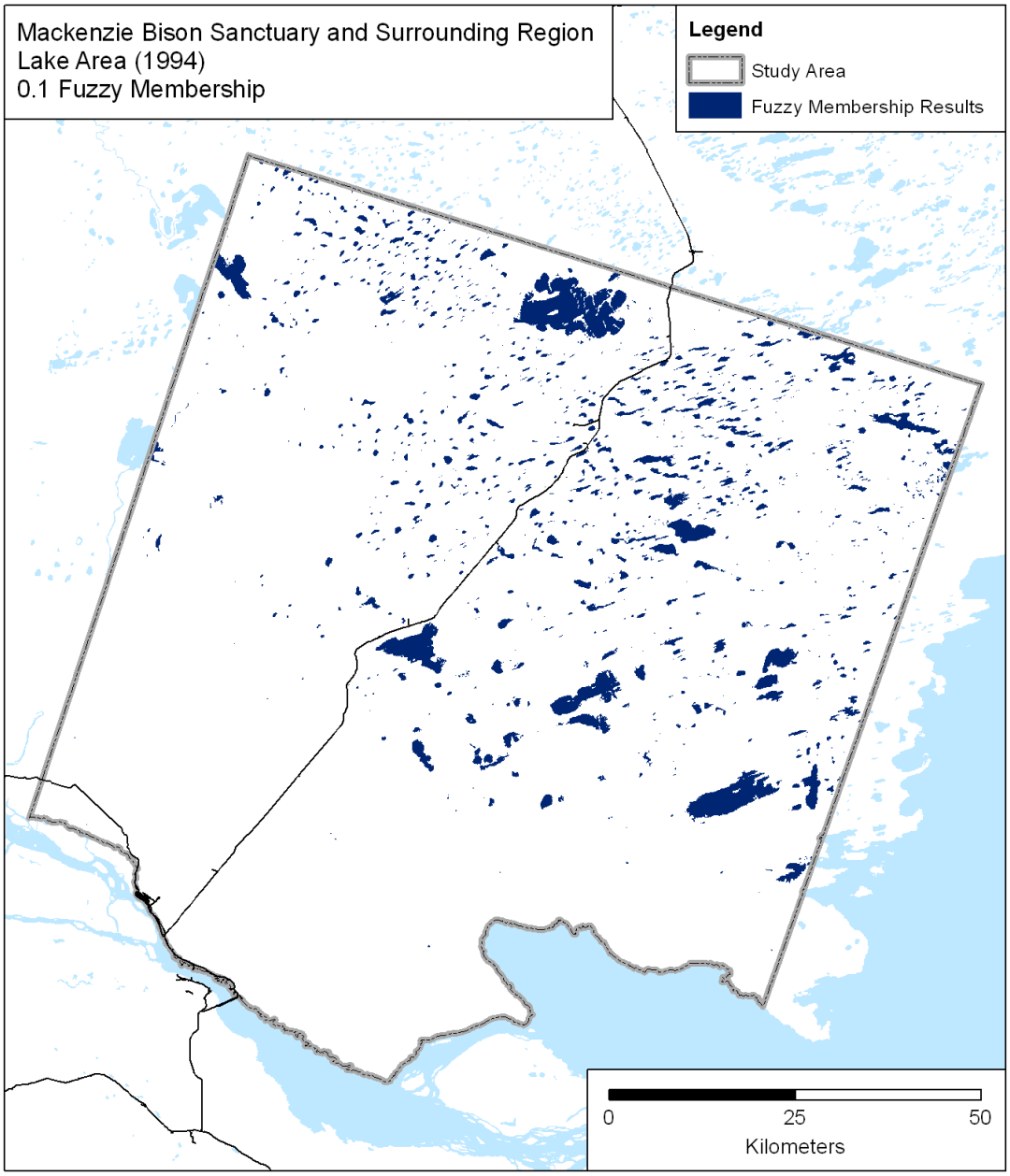
Mackenzie Bison Sanctuary and Surrounding Region
Lake Area (1994)
0.1 Fuzzy Membership
Legend
Study Area
Fuzzy Membership Results
0
25
50
Kilometers

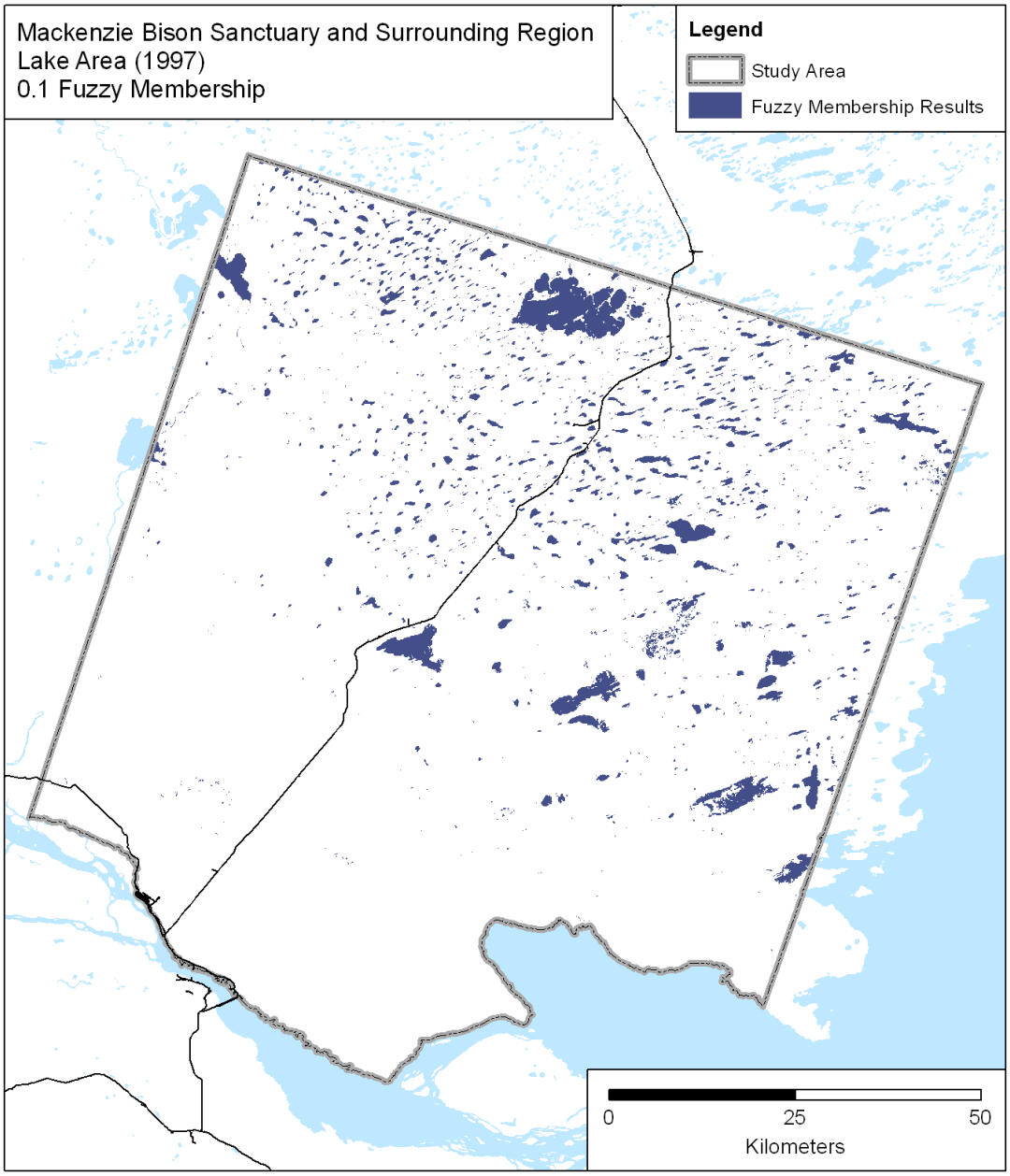
Mackenzie Bison Sanctuary and Surrounding Region
Lake Area (1997)
0.1 Fuzzy Membership
Legend
Study Area
Fuzzy Membership Results
0
25
50
Kilometers

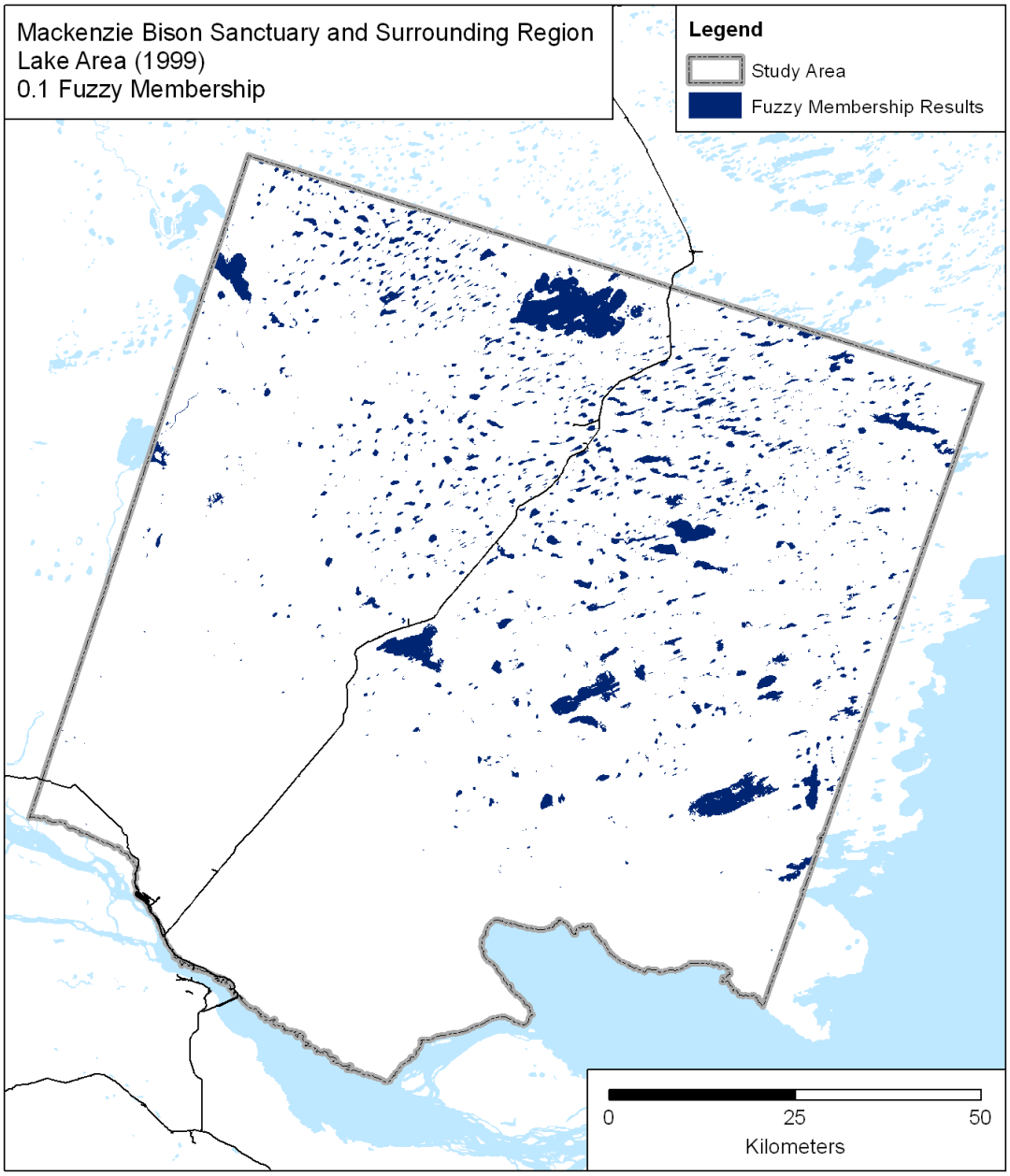
Mackenzie Bison Sanctuary and Surrounding Region
Lake Area (1999)
0.1 Fuzzy Membership
Legend
Study Area
Fuzzy Membership Results
0
25
50
Kilometers

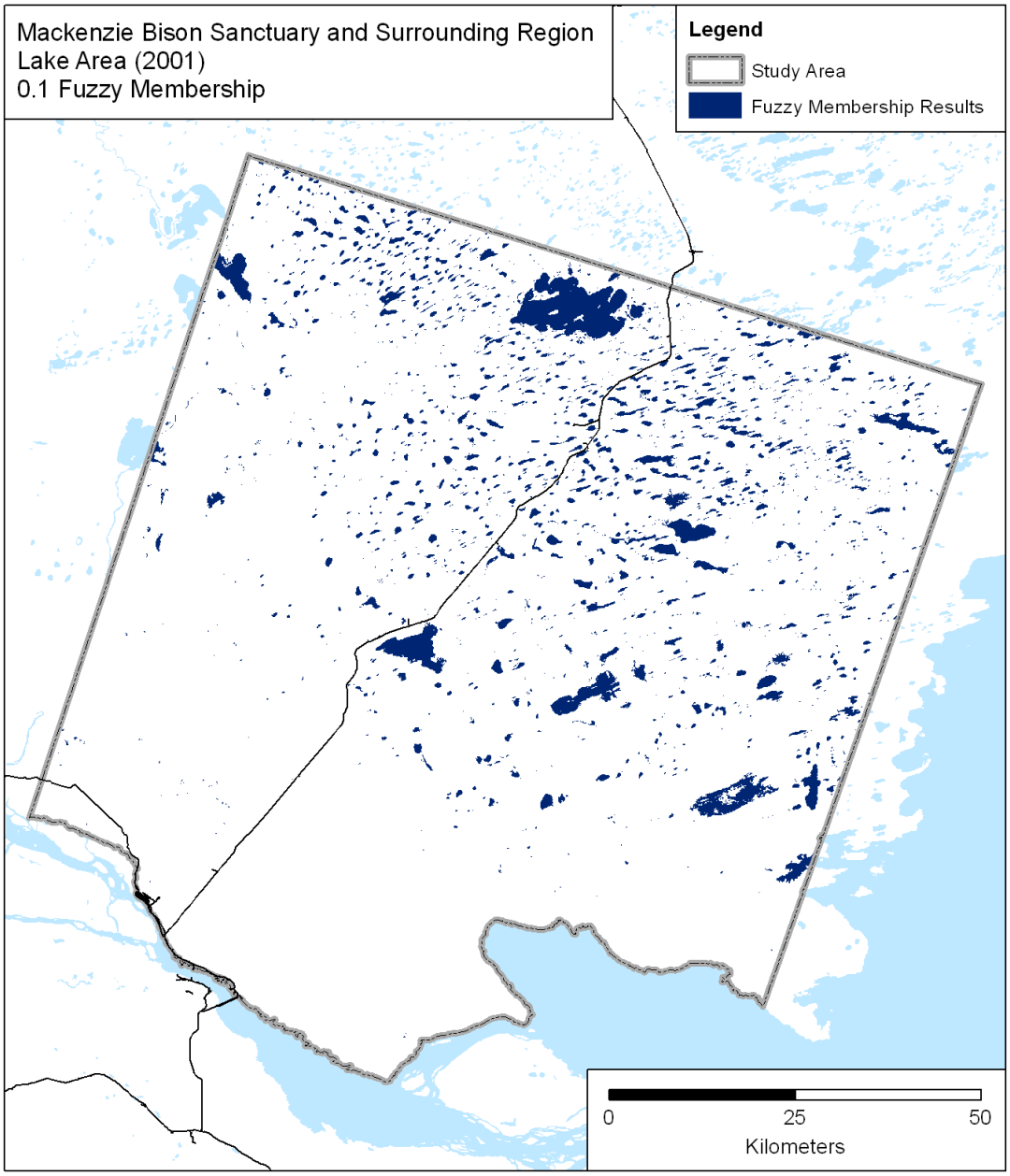
Mackenzie Bison Sanctuary and Surrounding Region
Lake Area (2001)
0.1 Fuzzy Membership
Legend
Study Area
Fuzzy Membership Results
0
25
50
Kilometers

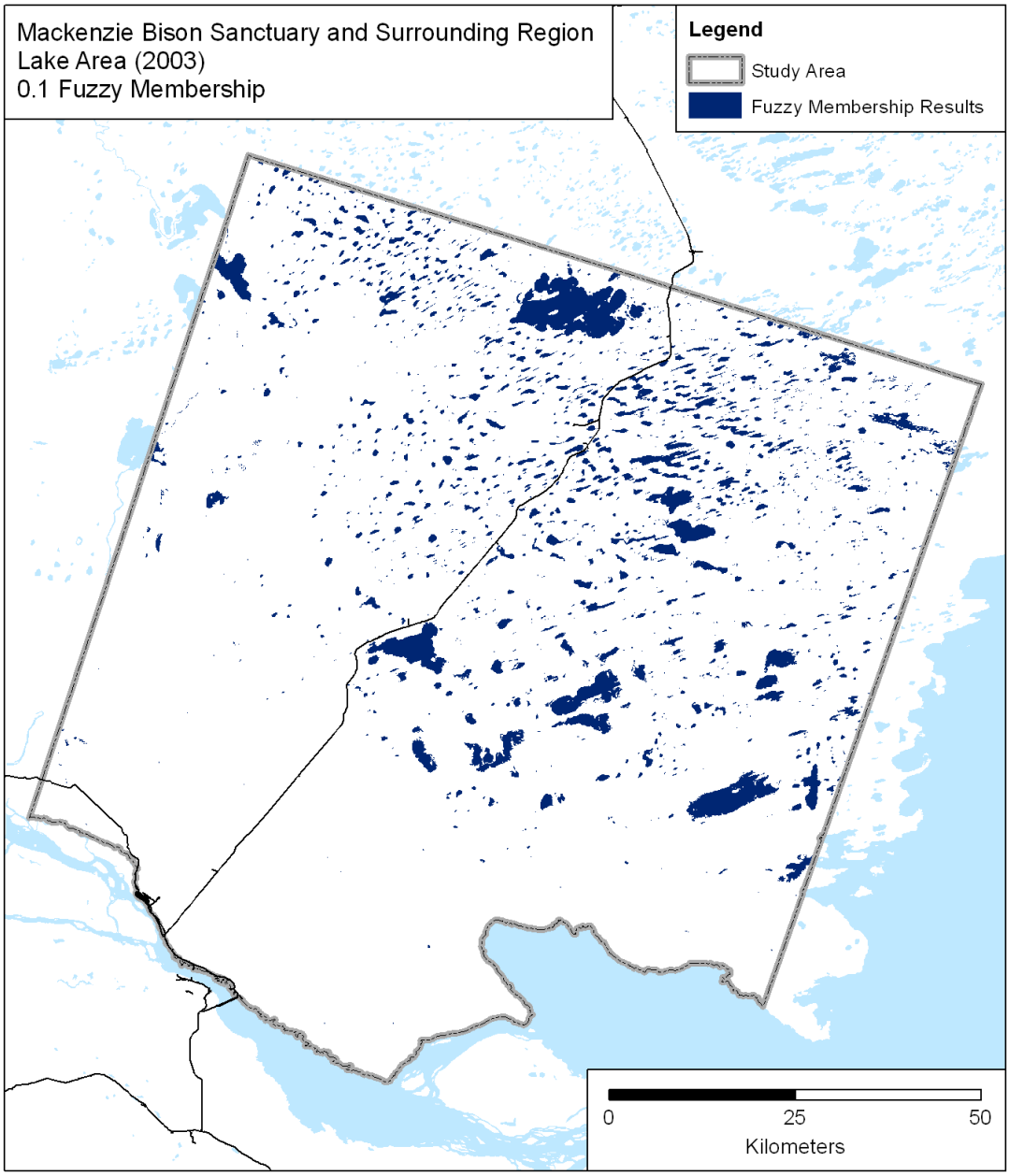
Mackenzie Bison Sanctuary and Surrounding Region
Lake Area (2003)
0.1 Fuzzy Membership
Legend
Study Area
Fuzzy Membership Results
0
25
50
Kilometers

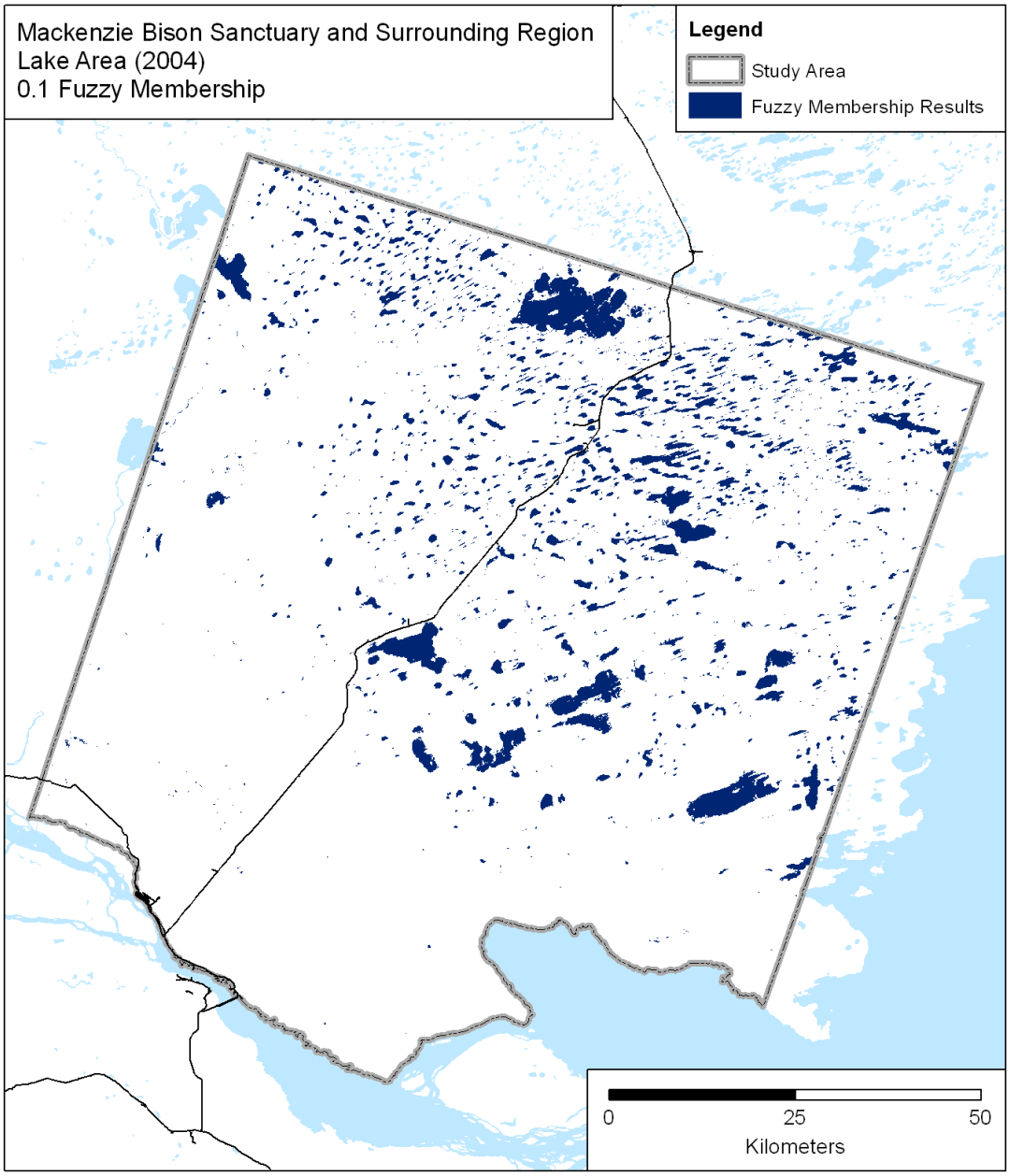
Mackenzie Bison Sanctuary and Surrounding Region
Lake Area (2004)
0.1 Fuzzy Membership
Legend
Study Area
Fuzzy Membership Results
0
25
50
Kilometers

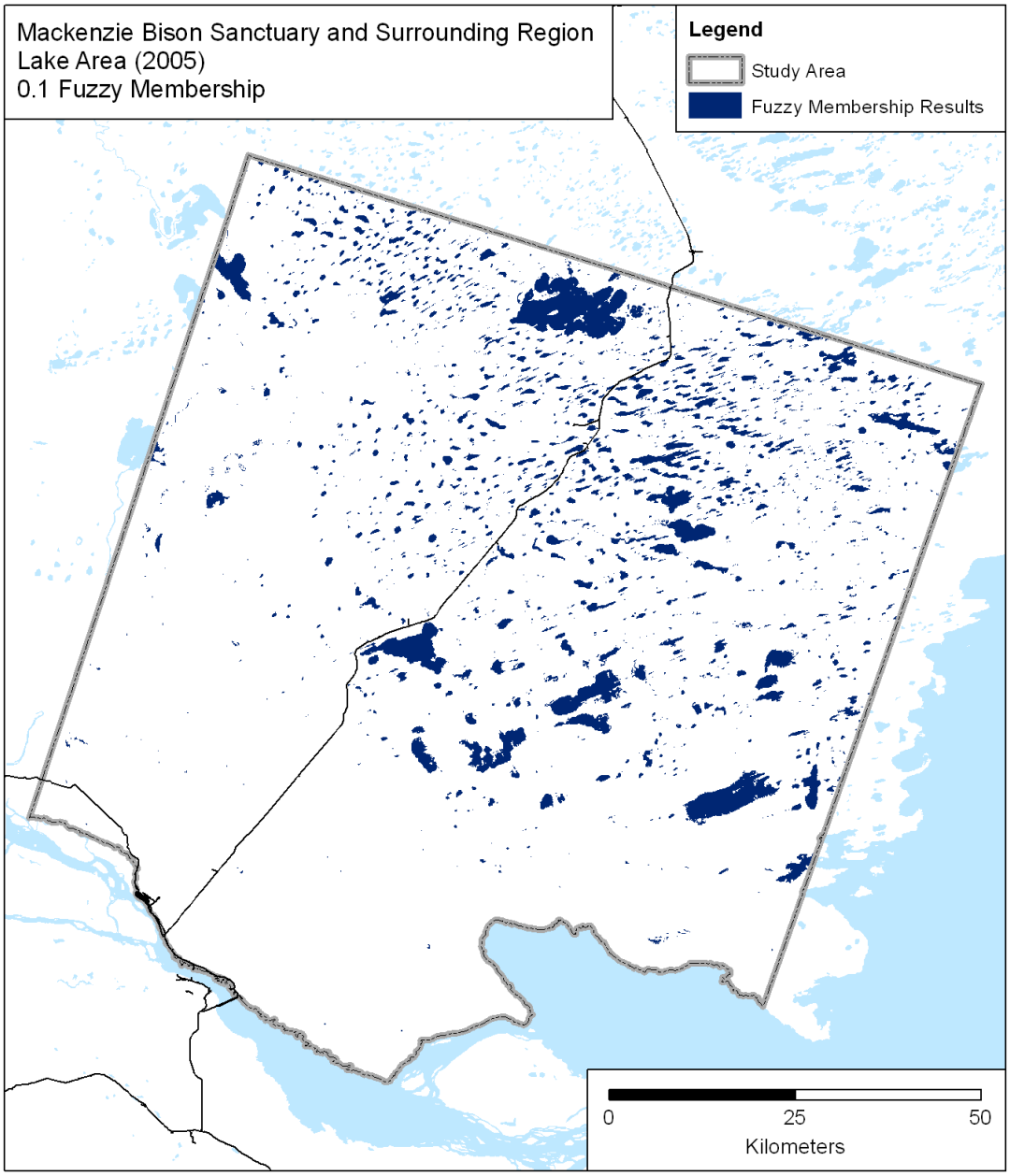
Mackenzie Bison Sanctuary and Surrounding Region
Lake Area (2005)
0.1 Fuzzy Membership
Legend
Study Area
Fuzzy Membership Results
0
25
50
Kilometers

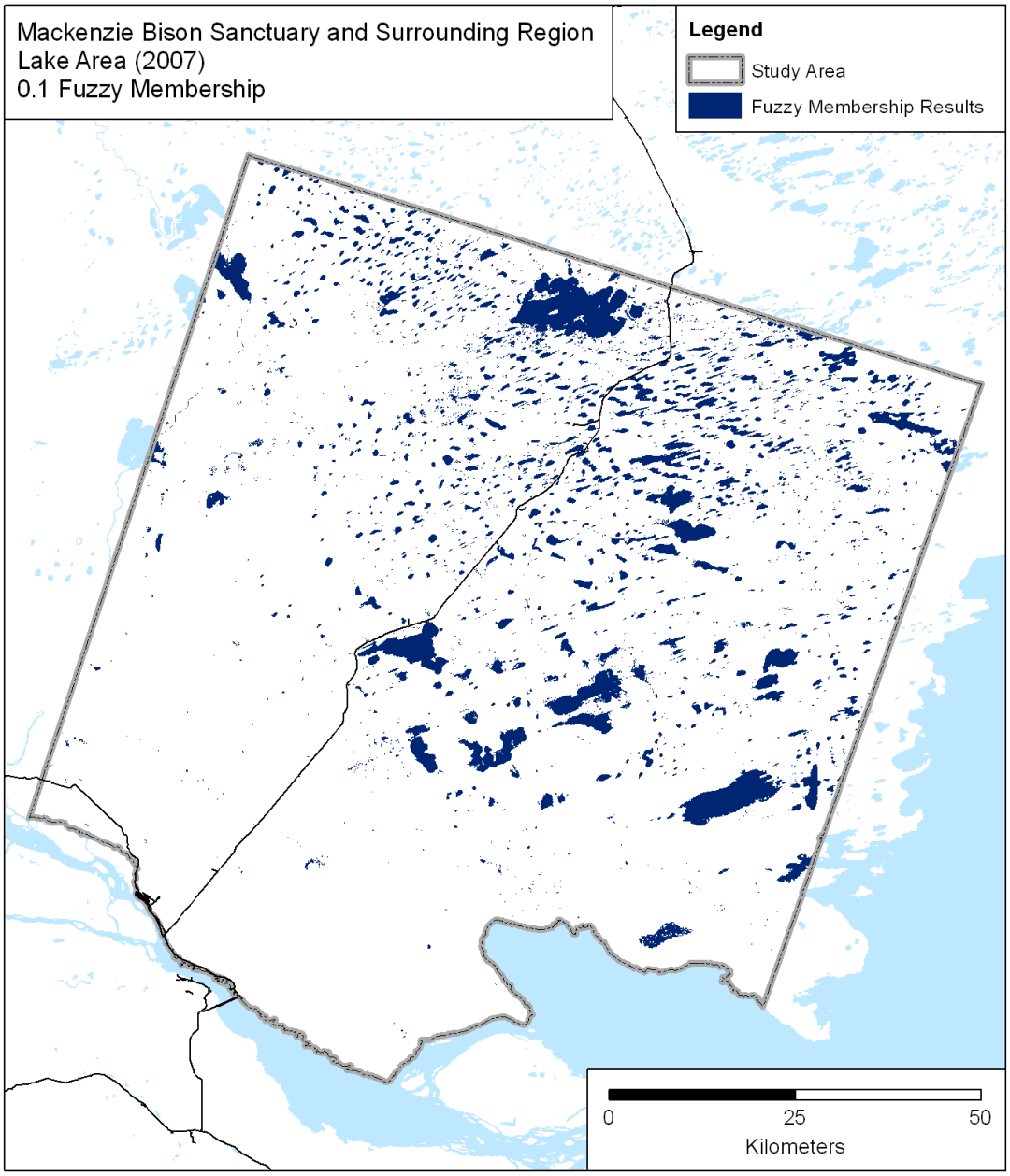
Mackenzie Bison Sanctuary and Surrounding Region
Lake Area (2007)
0.1 Fuzzy Membership
Legend
Study Area
Fuzzy Membership Results
0
25
50
Kilometers

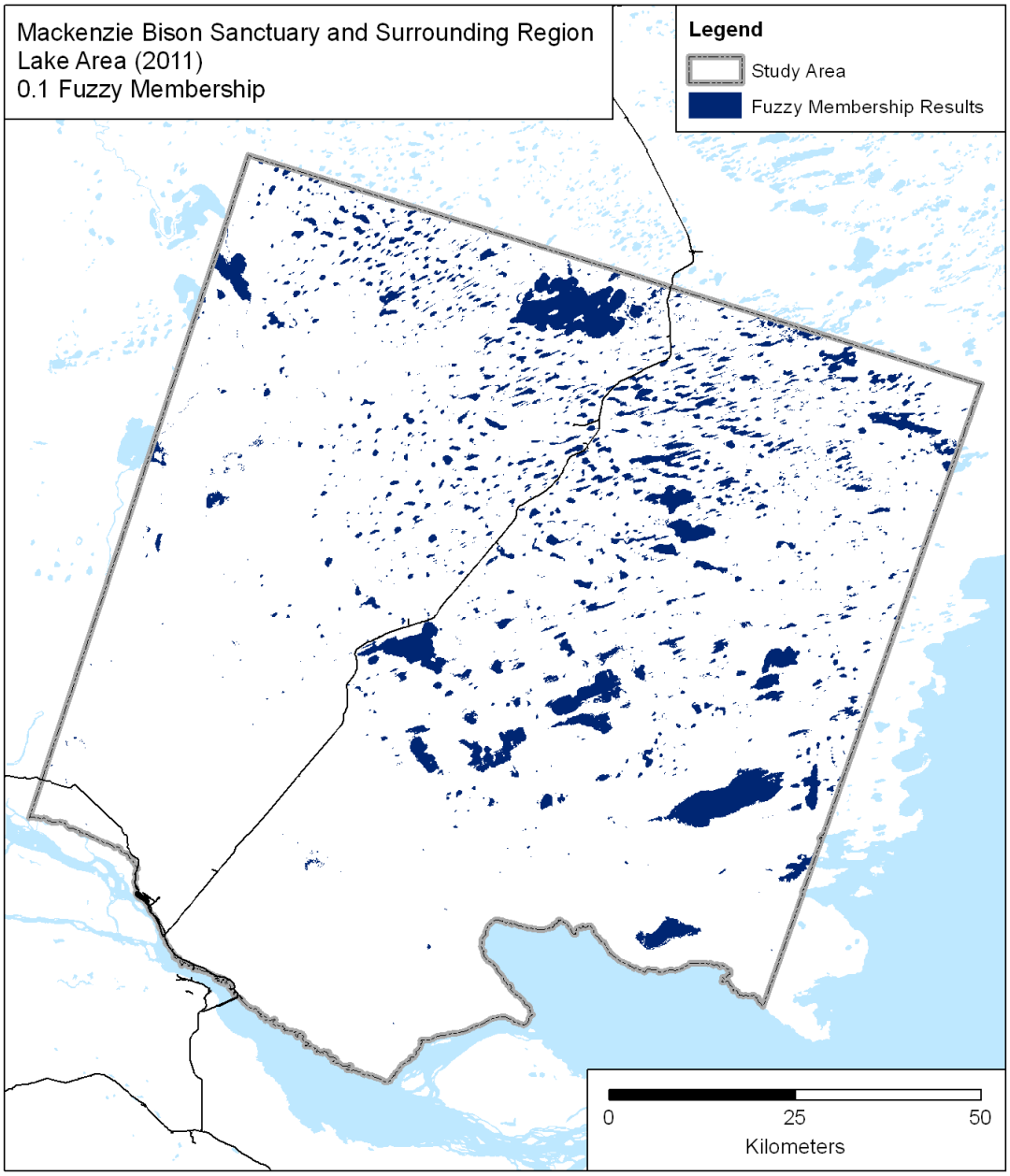
Mackenzie Bison Sanctuary and Surrounding Region
Lake Area (2011)
0.1 Fuzzy Membership
Legend
Study Area
Fuzzy Membership Results
0
25
50
Kilometers

APPENDIX D
SITE CHRONOLOGIES

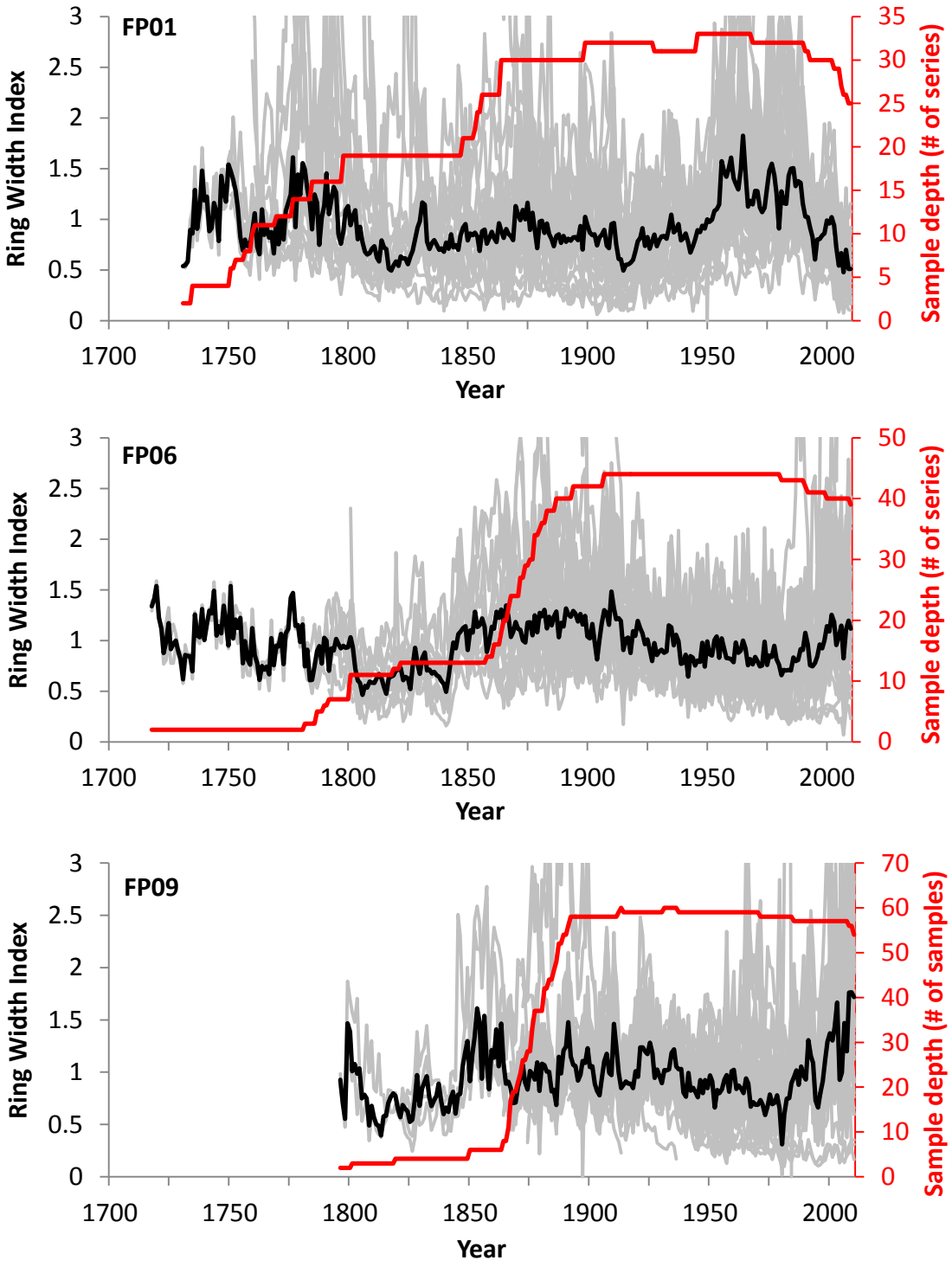

Figure D-1. Standardized ring width indices (grey) and mean site chronologies (black) for white spruce sites based on ARSTAN negative exponential curve standardisation. Sample depth is indicated in red.

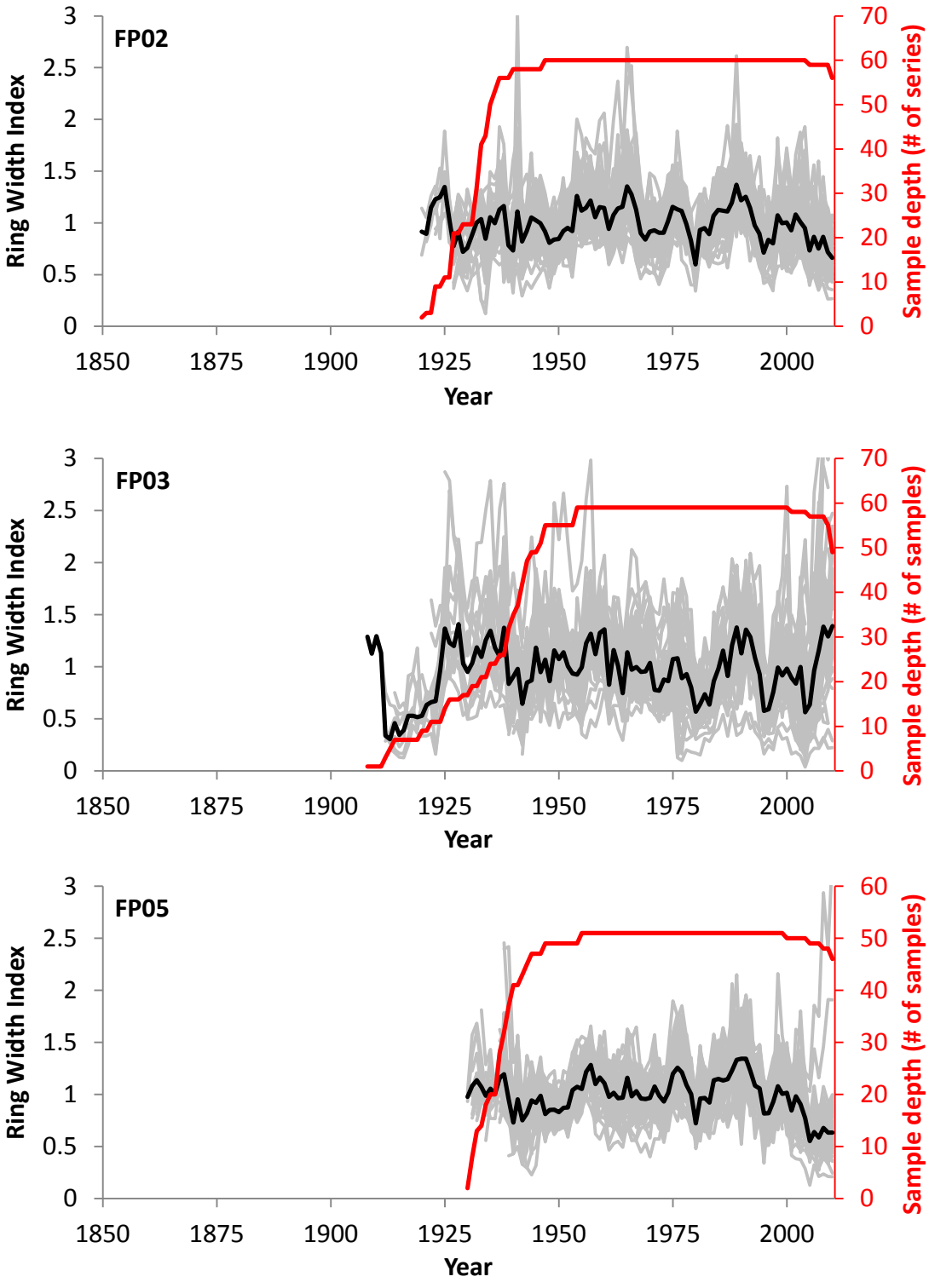

Figure D-1 (Cont'd). Standardized ring width indices (grey) and mean site chronologies (black) for white spruce sites based on ARSTAN negative exponential curve standardisation. Sample depth is indicated in red.

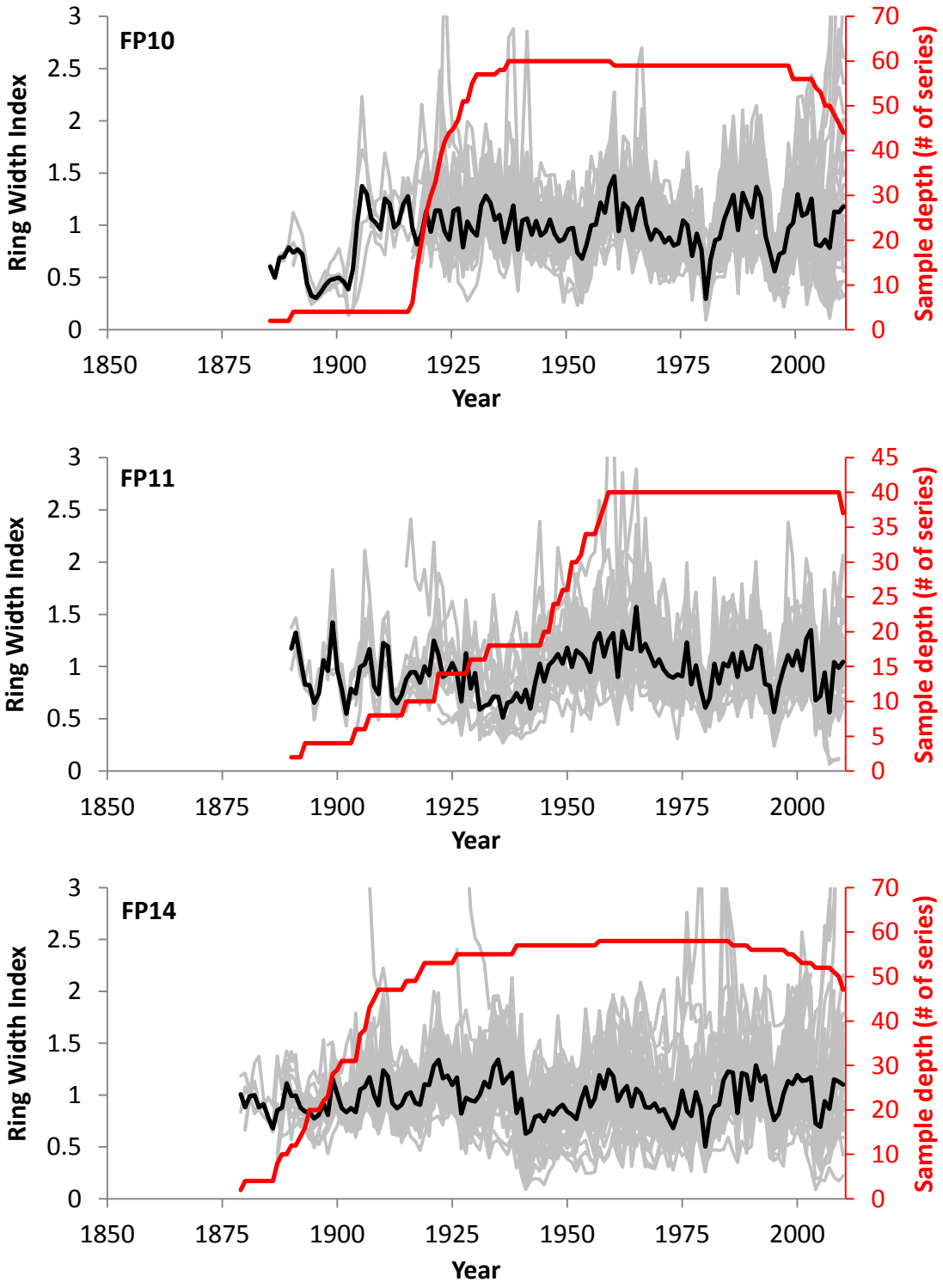

Figure D-1 (Cont'd). Standardized ring width indices (grey) and mean site chronologies (black) for white spruce sites based on ARSTAN negative exponential curve standardisation. Sample depth is indicated in red.

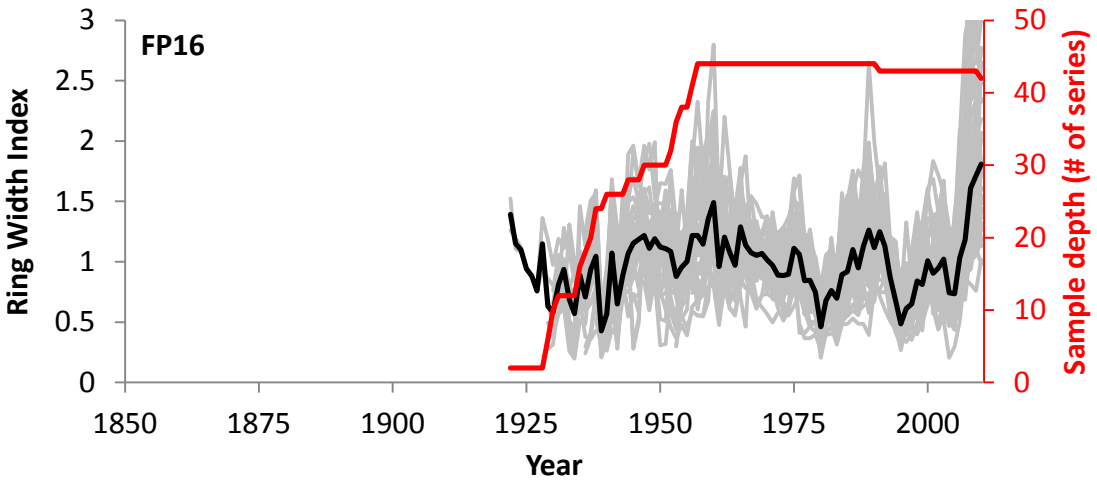

Figure D-1 (Cont'd). Standardized ring width indices (grey) and mean site chronologies (black) for white spruce sites based on ARSTAN negative exponential curve standardisation. Sample depth is indicated in red.

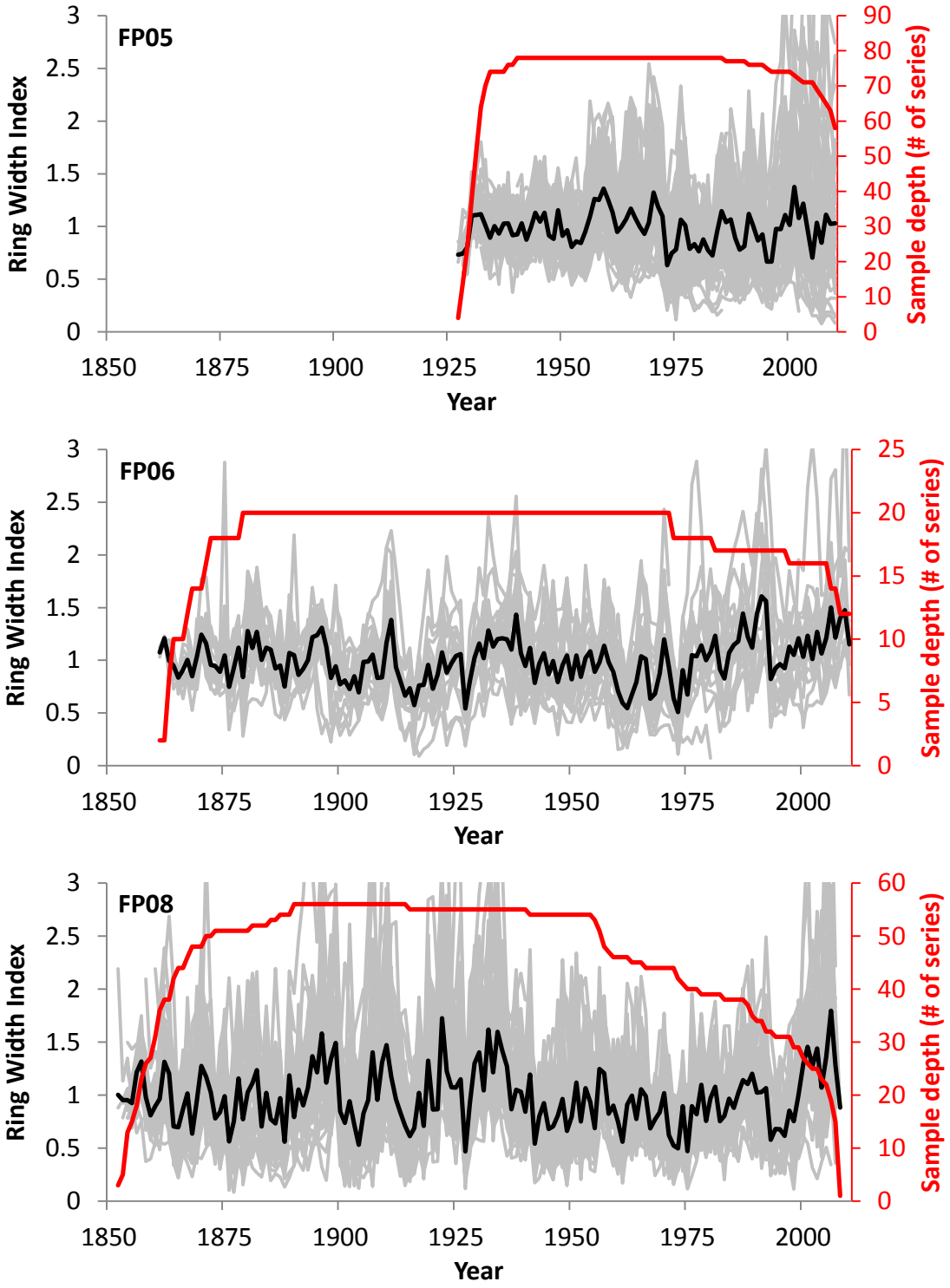

Figure D-2. Standardized ring width indices (grey) and mean site chronologies (black) for jack pine sites based on ARSTAN negative exponential curve standardisation. Sample depth is indicated in red.

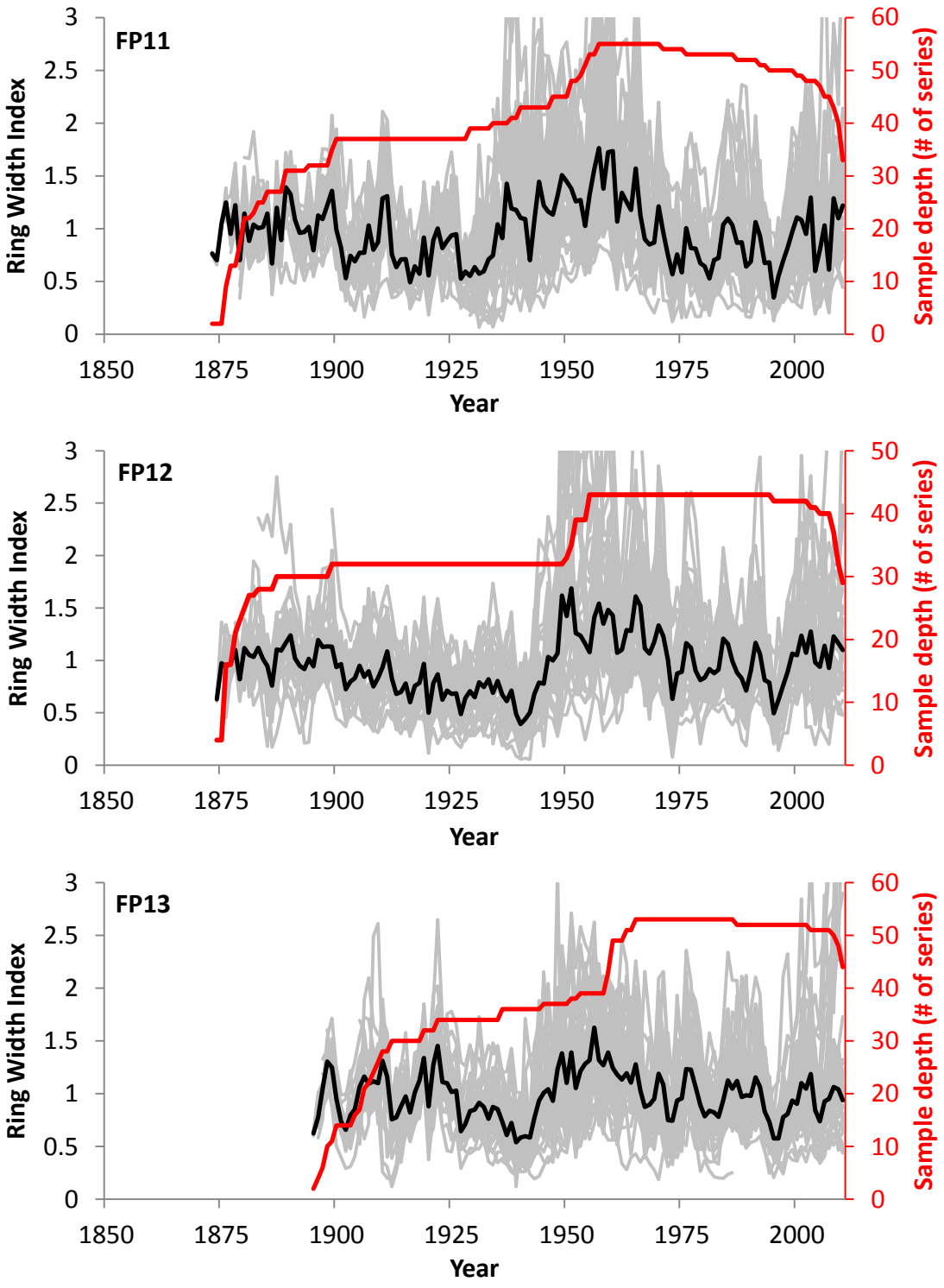

Figure D-2 (Cont'd). Standardized ring width indices (grey) and mean site chronologies (black) for jack pine sites based on ARSTAN negative exponential curve standardisation. Sample depth is indicated in red.

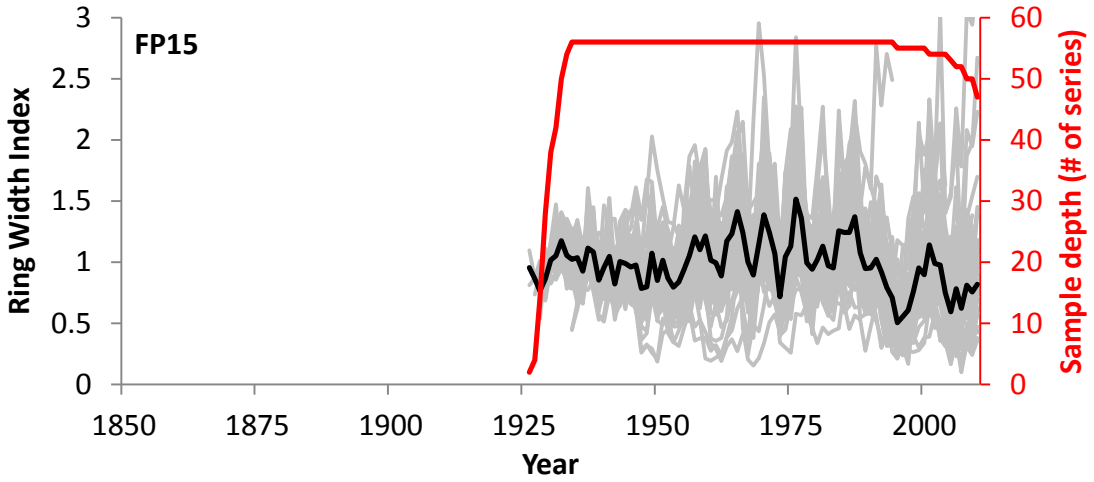

Figure D-2 (Cont'd). Standardized ring width indices (grey) and mean site chronologies (black) for jack pine sites based on ARSTAN negative exponential curve standardisation. Sample depth is indicated in red.